A Report to the World Meteorological Organization on the

Impact and Benefits of AMDAR Temperature, Wind and Moisture Observations in Operational Weather Forecasting

Ralph Alvin Petersen[1,2,3], Lee Cronce[2], Richard Mamrosh[4] and Randy Baker[5]

[1]Performed under contract to the World Meteorological Organization

[2]University of Wisconsin-Madison,
Cooperative Institute for Meteorological Satellite Studies (CIMSS),
Space Science and Engineering Center (SSEC),
1225 West Dayton Street, Madison, WI 53706

[3]Ralph.Petersen@ssec.wisc.edu

[4]National Weather Service (NWS) Forecast Office, Green Bay, WI

[5]United Parcel Service (UPS), Louisville, KY

1 June 2015

Abstract

This report reviews the impact of AMDAR observations on operational NWP forecasts at both regional and global scales that support national and local weather forecast offices across the globe. Over the past three decades, data collected from commercial aircraft have helped reduce flight level wind/temperature forecast errors by nearly 50%. Improvements are largest in 3-48 h forecasts and in regions where the automated reports 1) are most numerous, 2) cover a broad area, and 3) are available at multiple levels, e.g., made during aircraft ascent and descent. Improvements in weather forecasts due to these data have already had major impacts on a variety of aspects of airline operations, ranging from fuel savings from improved wind/temperature forecasts used in flight planning to passenger comfort and safety due to better awareness of en-route and near-terminal weather hazards. Aircraft wind/temperature observations now constitute the 3rd most important data set for global NWP and, in areas of ample reports, have become the single most important data set for use in shorter-term, regional NWP applications. Automated aircraft reports provide the most cost effective data source for improving NWP, being more than five times more cost effective than any other major-impact observing system. They also present an economical alternative for obtaining tropospheric profiles both in areas of diminishing conventional observation and as a supplement to existing data sets, both in time and space.

Although wind and temperature observations provided from commercial aircraft have been shown to improve operational numerical weather prediction (NWP) on global and regional scales, the quality and potential importance of newly available moisture observations are less well recognized. Because moisture changes often occur at much smaller scales than wind and temperature variations, these temporally and spatially frequent moisture observations can have exceptionally large impacts on forecasts of disruptive weather events and could help offset the dwindling number of global moisture observations. Currently, more than 115 aircraft-based Water Vapor Sensing Systems (WVSS-II) provide specific humidity observations en-route and during takeoff/landing, with 112 units operating in the US and 3 in Europe. Results of a series of assessments comparing data from WVSS-II sensors initially installed on twenty-five UPS Boeing 757 aircraft with co-located RAOBs show agreement to within 0.5 g/kg, with minimal biases. Inter-comparisons of observations made amongst nearby aircraft agree to better than 0.2 g/kg. The combined results suggest that the WVSS-II measurements are at least as accurate as water vapor observations from high-quality RAOBs. Information regarding observed spatial and temporal moisture variability could be important in optimizing the use of these observations in future mesoscale assimilation systems. Forecasts of disruptive weather events made by NWS and airline forecasters demonstrate the benefits obtained from combined temperature/moisture/wind profiles acquired during aircraft ascents and descents. Finally, a review of initial NWP impact studies shows that WVSS-II reports obtained throughout the day have greater influence than twice-daily RAOBs on 1-2 day forecasts over the US.

Brief history of automated temperature and wind data collection from commercial aircraft: Data obtained from aircraft have played important roles in meteorological research and operations for over a century (Wendrisch and Brenguier 2013). Although manual meteorological observations have been collected from commercial aircraft since the 1930's, these PIREPS (Pilot REPortS) often provided minimal value, due both to transcription and telecommunication errors and to inaccuracies in aircraft location reports and related wind determinations. The first automated aircraft data acquisition approach was implemented during the Global Atmospheric Research Program (GARP) Atlantic Tropical Experiment (GATE, Julian and Steinberg 1975), when meteorological observations were stored using on-board recording systems. Automated collection and transmission of aircraft observations began during the First GARP Global Experiment (FGGE) experiments in 1978-1979. Although the initial use of these limited AIREPS (AIrcraft REPortS) was restricted primarily to research applications, the number, quality and operational use of these data have expanded substantially in the years since. Critical to this success was the introduction of accurate LORAN (LOng RAnge Navigation, U.S. Coast Guard 1962) and INS (Inertial Navigation Systems, Woodman 2007) instruments that provided reliable aircraft position and earth-relative wind data as routine by-products.

Regular real-time transmission of automated weather observations began using dedicated equipment mounted on commercial aircraft as part of the Aircraft to Satellite DAta Relay (ASDAR) program (Fleming et al. 1979; Sparkman et al. 1981) that remained available after FGGE. More than 20 ASDAR equipped aircraft provided reports during the next 20 years from 8 air carriers around the globe. Although the program provided beneficial information in data-sparse regions, it required that extra equipment be installed and maintained on participating aircraft. The project, however, demonstrated that high-quality wind and temperature observations could be obtained from commercial aircraft, especially near the high kinetic energy regions around the jet stream that can influence predictions of cyclogenesis and storm evolution.

With the development of modern aircraft equipped with flight computers and improved navigation systems, it became apparent that these type of observations could be made much more efficient and affordable by installing ASDAR-like software to collect data from sensors already available on commercial aircraft. The system in the United States (US) was originally known as the Meteorological Data Collection and Reporting System (MDCRS, see Martin et al., 1993). Reports were sent to ground stations using systems available through several available telecommunication service providers, including Aeronautical Radio Incorporated (ARINC) and Société Internationale de Télécommunications Aéronautiques (SITA). The messages included location, temperature and wind reports that were used by individual airlines to monitor aircraft performance and to improve flight planning and systems efficiency. As the LORAN and INS systems used on earlier wide-body aircraft were replaced by Global Positioning System (GPS) location finders on a much broader fleet of aircraft and onboard communications systems were enhanced, the availability of automated aircraft reports increased further. These observations are now part of the broader World Meteorological Organization (WMO) Aircraft Meteorological DAta Relay (AMDAR) program (WMO 2003a, 2014a). (AMDAR observations are obtained from the WMO global AMDAR observing system, which is comprised of those aircraft-based AMDAR observations observing systems, which derive meteorological data from an aircraft platform according to WMO standards and specifications and make it available on the WMO Global Telecommunications System (GTS). The WMO AMDAR observing system is comprised of the national and regional Member AMDAR systems, which are implemented and operated in collaboration with AMDAR partner commercial airlines.)

In the mid-1980s, US airlines approached the Federal Aviation Administration (FAA) with a request to improve the quality of the flight-level wind forecasts used in their flight planning systems. At that time, errors in short-range upper-level wind forecasts from Numerical Weather Prediction (NWP) models over the Northern Hemisphere (NH) ranged between 9 and 10 ms^{-1} (Root Mean Squared Vector [RMSV] wind error). This uncertainty had large negative impacts on airline operating costs, including the need to carry excessively large amounts of extra fuel when tail winds were larger than expected or to make

unplanned refueling stops on long international routes when headwinds were higher than forecast. Further, the airlines needed better quality and vertical/horizontal resolution forecast wind profiles near airports to optimize fuel use, especially during aircraft descent.

To address these and other aviation weather forecasting issues, the FAA established an "Aviation Weather Forecasting Task Force" (NCAR 1986). A principal objective of this effort was to improve flight-level wind and temperature forecasts provided by NWP models through the World Area Forecast Centers (WAFCs) at the UK Meteorological Office (Met Office) and the US National Weather Service (NWS). See WAFC-Washington (2011) for details.

A major outcome of the Task Force was agreements by five US airlines to allow the WAFCs to acquire and use the previously proprietary weather data portions of automated aircraft reports in their real-time operations and NWP systems. In return, the WAFCs made significant efforts to enhance their NWP systems to make better use of these new data. For example, the vertical resolution of the US global NWP system was enhanced in the area near the tropopause and the horizontal resolution of the model and output fields were increased. Development was also begun on a new domestic NWP system designed specifically around the new observations and intended to provide improved very-short-range forecasts of wind and temperatures for use in flight planning and air traffic management systems across the US (Benjamin 1989, Benjamin et al. 1991).

Improvement in global-scale wind forecasts in the two decades after 1984 (Fig. 1) can in part be attributed to use of these new automated aircraft data in improved Data Assimilation (DA) systems. Between 1984 and 2004, average NH wind errors decreased by ~40%, from 10 ms^{-1} to 6 ms^{-1}. More importantly, aircraft were less likely to encounter unexpected areas of excessive head- or tail-winds, as noted in the nearly 45% reduction in wind errors near the jet stream (defined as areas with greater than 40 ms^{-1} wind speeds) from above 13 ms^{-1} to less than 8 ms^{-1}, thereby enhancing airline efficiency and reducing fuel consumption. Although it is difficult to determine the exact contributions of enhancements in observations and DA systems, it should be noted that between 1986 and 2001, a time when few changes were made to the NCEP global DA system, wind forecast errors declined as aircraft observations increased.

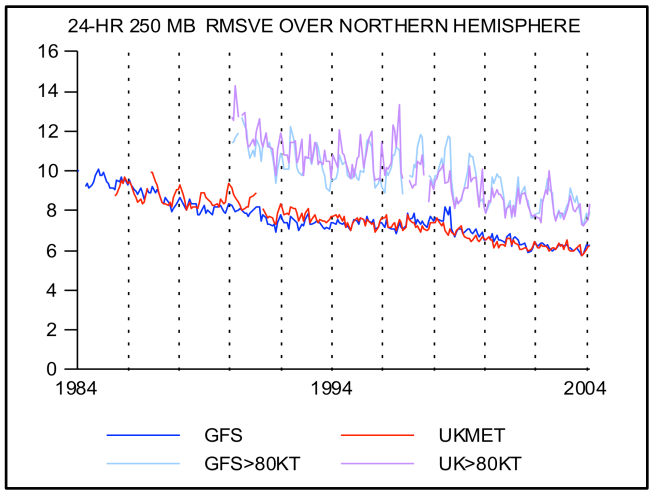

Figure 1: Monthly-average RMSV wind error (ms^{-1}) for 24-h forecasts from World Area Forecasts Centers (WAFCs) and available for distribution 3 hours after 0000 and 1200 UTC for the NH using the US NWS Global Forecast System (GFS) and the UK Met Office (UKMET) global forecast model. Separate plots shown for all wind speeds and for wind speeds greater than 80 knots. Gaps in plots prior to 1992 due to incomplete data archives at NWS.

Since the late 1990s, the AMDAR program has expanded to include more than 3500 aircraft from 39 airlines globally. Ten different national and regional AMDAR programs currently provide more than 680,000 wind and temperature reports daily. The observation intervals range between 5-7 and 1-3 minutes when aircraft are at cruise levels and more frequently during aircraft takeoff and landing, as frequently as every 6 to 20 seconds (See Appendix A for details). High-quality moisture observations are now also available from more than 100 aircraft, primarily over the US.

AMDAR data are routinely available over large portions of the globe, with the highest density of observations over the heavily traveled areas of North America (NA) and Europe (Fig. 2). Oceanic observations are generally limited to upper-tropospheric reports along intercontinental routes. Elsewhere, reports are taken both at cruise levels and during ascent/descent. Although flight level reports are most prevalent, the number of aircraft profiles is increasing steadily, even in some data-sparse regions where AMDAR reports are playing increasingly important roles. The quality of the wind and temperature data has been determined by various

authors to be very high (e.g., Moninger et al. 2003, Benjamin et al. 1999) and is monitored operationally by the National Center for Environmental Prediction (NCEP) as part of WMO data protocols. (Recent statistics are available at htpp://amdar.noaa.gov.)

The first half of this report reviews the impact of AMDAR observations on operational NWP models at weather forecast offices at both regional and global scales. Although much of the discussion of regional NWP impact builds upon a literature review of application of the large number of automated aircraft observations available over the US during the past 2 decades, discussion of recent impacts relies on materials from the Fifth WMO Workshop on the Impact of Various Observing Systems on Numerical Weather Prediction (NWP) conducted as part of the World Weather Watch in Sedona, Arizona in May 2012 (WMO, 2012) and related meetings. An evaluation of the increasingly available AMDAR moisture observations follows later in the paper.

Assessments of AMDAR Temperature and Wind Data Quality: Integral to any operational NWP improvement effort must be a parallel program to monitor the data sets and develop appropriate Quality Control (QC) procedures. A number of schemes have been developed at global NWP centers to assure that erroneous AMDAR data are excluded from operational DA systems (e.g., Ballish and Kumar 2008). Outputs, including lists of aircraft producing questionable reports, are frequently updated and transmitted to other NWP centers and participating airlines so that errors in suspect aircraft instrumentation and communication systems can be corrected. (See Jacobs et al. 2014 for more details regarding candidate data correction procedures.)

A major problem in melding the variety of different data used in modern DA systems is the need to recognize and remove biases contained in each data set (Dee et al., 2009). If this is not done, the biased data reports can reduce the impacts of other data sets. For example, if one large data set has a cold or warm bias compared to all other data sources, those data can have the detrimental effect of cooling (or warming) the entire analysis, even though the data set may contain valuable information about the spatial and temporal temperature variations. The situation can be made even worse if information from a reliable data source available only once or twice per day is countered by biased reports available many times daily. As noted at the recent NOAA Aircraft Data Workshop (see WMO 2014b), however, the availability of multiple reports in proximity is also valuable for cross-validation and QC.

Although numerous studies have shown that AMDAR data have very small random errors, Ballish and Kumar (2008) identified that individual AMDAR temperature reports can have systematic warm biases of as much as 1° C when compared with analysis background fields and can fluctuate by altitude, phase of flight (i.e., ascent, cruise, and descent) and aircraft type. In general, the magnitudes of the biases increase with altitude, ranging from values of a few tenths of a degree near the surface to as much as 1° C at flight levels and may be in part produced by combinations of hysteresis effects in the onboard

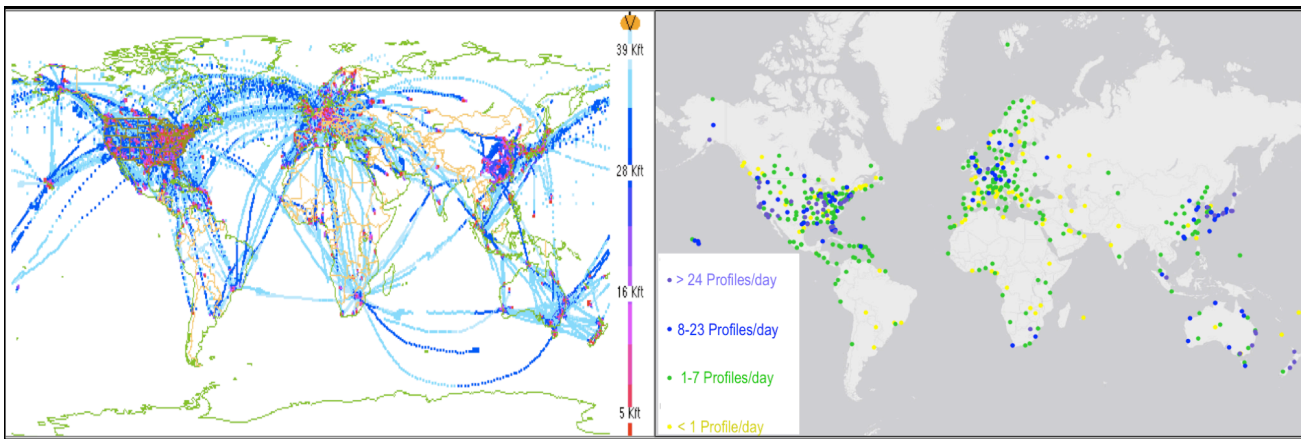

Figure 2: Sample distribution of all automated wind and temperature observations available over a 24 hour period ending 2300 UTC 31 January 2014 from all commercial aircraft (left) and daily average takeoffs and/or landings week of 26 January 2014 (right). Colors represent altitude of reports (left) and report frequencies (right). Plots based on www.amdar.noaa.gov and Lockett 2015.

sensors (especially during ascent and to lesser degree descent), dynamic heating within the sensor at high speeds (at cruise levels) and truncations by the on-board data processing systems (which vary between aircraft). The biases also can fluctuate between seasons (with slightly larger values noted in summer) and aircraft type (e.g., three different Boeing 737 models had biases that ranged from 0.8 to 1.2^{o}C). A scheme designed by Isaksen (2011) to correct these biases and implemented at the European Centre for Medium Range Weather Forecasts (ECMWF) has improved upper-level temperature analyses and fits with stratospheric satellite measurements, especially near and above the tropopause. Other NWP centers are planning to implement similar bias correction schemes in the near future, some of which include relationships between aircraft ascent/descent rates and vertical variations in biases (Zhu et al. 2015).

Review of the impact of AMDAR observations on short-range regional forecasts: Although data impact tests generally focus initially on the global and longer-time scales and then later on regional scales, the availability of large volumes of automated aircraft observations taken throughout the day (called asynoptic observations) over the US provided the opportunity to develop a succession of short-range DA and NWP models tailored specifically to use these unique data sets. The first of these was the Rapid Update Cycle (RUC), developed by the National Oceanic and Atmospheric Administration (NOAA) at the Earth Systems Research Laboratory (ESRL) and run hourly at NCEP, provides the focus of the following discussion. The evolution of the model and the importance of various asynoptic and synoptic data sets to the quality of short-range RUC forecasts are described in a series of papers by Benjamin et al. (1991, 2004). Results of short-range impact tests using other analysis and forecast systems can be found in Cardinali et al. 2003, Cardinali et al. 2004, Gao et al. 2012, Huang et al. 2013, Laroche et al. 2010 and Lupu et al. 2011.

In an early attempt to quantify the impact of aircraft observations, Benjamin et al. 1991 compared results including MDCRS data in an 80km resolution developmental version of the RUC against equivalent twice-daily forecasts from the NWS's then-operational Nested Grid Model (NGM) that relied primarily on rawinsonde observations (RAOBs) for upper-air information. Aircraft temperature and wind reports at this time were typically collected only at regular 7 to 10 minutes intervals over the US, mostly at cruise levels near the jet stream. The continual insertion of aircraft data had positive impact on short-range forecasts throughout the day. By 2100 UTC, the inclusion of nine hours of MCDRS reports available since the previous RAOB reports reduced errors in forecasts of 250 hPa winds over 40 ms^{-1} by approximately 10% when compared to 12-h NGM forecasts valid at the same time. This in turn lowered flight duration estimate errors along several major US flight routes by 30%, thereby offering airlines a means of refining fuel use estimates.

In 2000, Schwartz and Benjamin examined the effect of model resolution and physics on the utility of MDCRS observations. For these tests, a 60 km version of the RUC was compared to a 40 km version of the RUC-2, which included more sophisticated surface physics, improved orography and higher vertical resolution. The RUC-2 performed better at all forecast ranges, with the largest impacts noted at the shortest forecast ranges. Improvements above 300 hPa and below 700 hPa were attributed primarily to increased vertical model resolution and improved boundary layer parameterizations, while the reduced improvements at mid-levels was likely related to the paucity of ascent and descent reports available at the time.

Recognizing the need to obtain profiles during aircraft ascent and descent, the NWS and Federal Aviation Administration (FAA) worked with participating US airlines in the late 1990's to increase observing frequencies to approximately every 10 hPa in the lowest 100 hPa during takeoff and every 50 hPa until an aircraft finished its climb-out (typically near 400 hPa), with a higher vertical reporting rate used again during descent. (See Appendix A for details.) To quantify the impact of these higher-frequency wind and temperature profiles, Petersen et al. (2004) conducted a limited series of tests using the then operational 20 km resolution RUC-2. For three weeks in June 2002, operational runs of the RUC-2 using all AMDAR data were compared to experimental runs in which all aircraft wind and temperature reports below 350 hPa were removed. Unlike some of the global data denial tests to be discussed later, no thinning or averaging of the aircraft data was done.

Comparisons of analyses and 3-, 6-, 9- or 12-h forecasts from both systems to RAOBs over the Contiguous US (CONUS) at 0000 and 1200 UTC are shown in Fig. 3. The asynoptic ascent/descent temperature and wind aircraft profiles had positive impacts on wind analyses at all levels at the 0000 and 1200 UTC synoptic times. Although improvements were noted at all levels, impacts below 300 hPa were 3-4 times greater than at upper levels where abundant cruise-level data was retained in both tests.

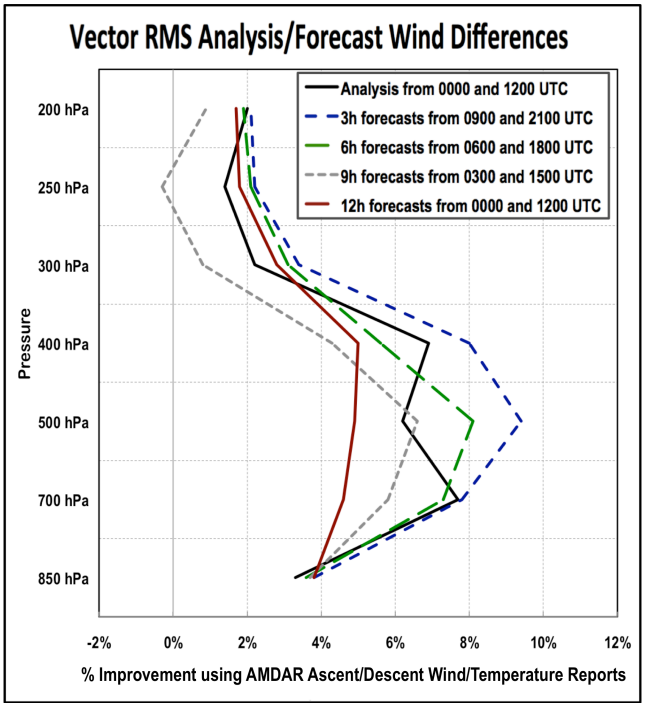

Figure 3: Improvement in 850 to 200 hPa RMSV wind errors (%) in RUC-2 analyses and 3-, 6-, 9- and 12-h forecasts between tests that included and excluded automated aircraft reports made during ascent/descent below 300 hPa. Tests preformed using a 20 km version of the model and data from a 3-week period in June 2002. All validations made over the CONUS used 0000 and 1200 UTC RAOB observations as comparison standard.

Improvements at these synoptic analysis times, when RAOBs typically dominated analyses over the US, were the combined result of both the additional aircraft ascent/descent reports available at these times and enhancements in the analysis background fields resulting from the inclusion of those reports during the previous 12 hours. The latter effect is especially apparent above 350 hPa, where the amount of data available to both tests was unchanged.

The impacts of analysis improvements on 12-h forecasts were also positive across all variables. Wind forecast improvements at and above 300 hPa were comparable to the initial analysis differences. Below 300 hPa, the impacts of the ascent/descent data on the forecasts were smaller than in the analyses, but still averaged about 4%, more than double the improvement found at upper-levels where cruise-level observations dominated. Inclusion of aircraft ascent/descent data in the mid-troposphere also improved most 3- to 9-h forecasts by 5 to 9%, with the largest error reductions in the shortest forecast ranges when AMDAR data dominated both the initial condition and analysis background fields. These improvements were equivalent to doubling the model resolution, which would have required a 10-fold increase in computing resources (see Benjamin et al., 2002). The smaller changes in the 9-h forecasts from 0300 and 1500 UTC above 400 hPa and slight degradation near 250 hPa may be the residual effect of the assimilation system adjusting to biased cruise-level aircraft temperature reports in the periods immediately after RAOB data were used.

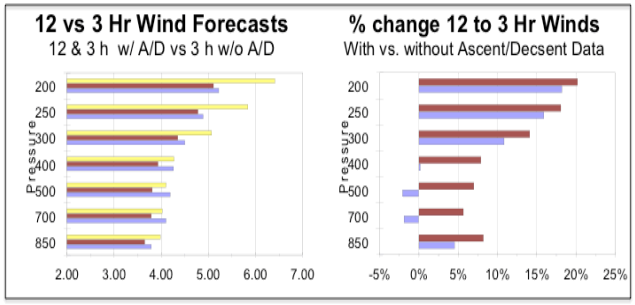

Figure 4: Left - Comparison of RMSV wind errors between 12-h RUC forecast using all available data (yellow) and updated 3-h RUC forecasts with (red) and without (blue) aircraft ascent/descent data, all valid at 0000 and 1200 UTC from tests in Fig. 3. Right - Normalized differences in improvements (%) between 3- and 12-h forecasts made with/without ascent/descent data.

The cumulative impact of AMDAR observations received throughout the day was determined by comparing forecasts made with/without ascent/descent data from successive hourly RUC analysis updates between 0000 and 0900 UTC and 1200 and 2100 UTC with 12 h forecasts from 0000 and 1200 UTC. Improvements using all AMDAR data collected during the updating interval ranged from 0.2 and 1.2 ms^{-1} across all levels (Fig. 4), equivalent to improvements of about 5% at lower levels to 20% aloft. The larger error reduction aloft is likely a combination of the inherent presence of larger errors (and therefore larger margin for improvement) near the jet stream and improvements in the underlying thermal structures supporting the vertical wind structures provided by the ascent/descent temperature data. Forecasts using only upper-level aircraft reports showed slightly

smaller improvements aloft and degradations in the middle troposphere, illustrating both the quality of the full-tropospheric aircraft data and the importance of using them frequently within NWP data assimilation systems.

Figure 5 summarizes the overall impact of automated aircraft wind and temperature profiles on regional analyses and very-short-range forecasts valid at 0000 and 1200 UTC. AMDAR reports have positive impacts at all times and for all parameters, including indirect improvements in moisture forecasts. Improvements were greatest for the 3- and 6-h ranges when the largest cumulative amount of asynoptic data had been assimilated. The especially large temperature improvements reflected not only the availability of thermal data in the aircraft reports, but also the use of more accurate wind and temperature fields in advection calculations employed in determining analysis background fields. Because no new humidity data were included in these tests, the enhancements in the humidity fields must similarly be attributed to improved advection computations.

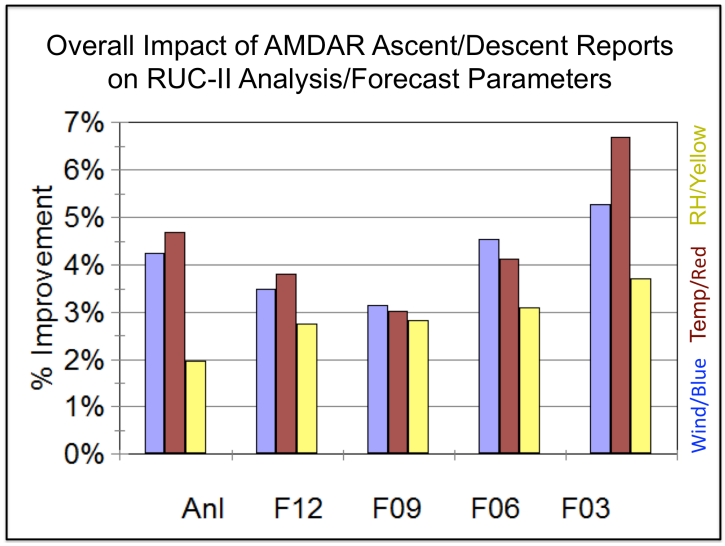

Figure 5: Vertically averaged, normalized difference (%) in RMSV wind errors between RUC analyses and 12- 9-, 6- and 3-hour forecasts of wind (blue), temperature (red) and relative humidity (yellow) made with and without aircraft ascent/descent reports, all valid at 0000 and 1200 UTC. Same model and validations used as in Fig. 3.

The slightly reduced impact of the aircraft data in the 0000 and 1200 UTC analyses (relative to the 3-h forecasts) was again likely due to conflicts and redundancies between the biased AMDAR reports and RAOB profiles at these times.

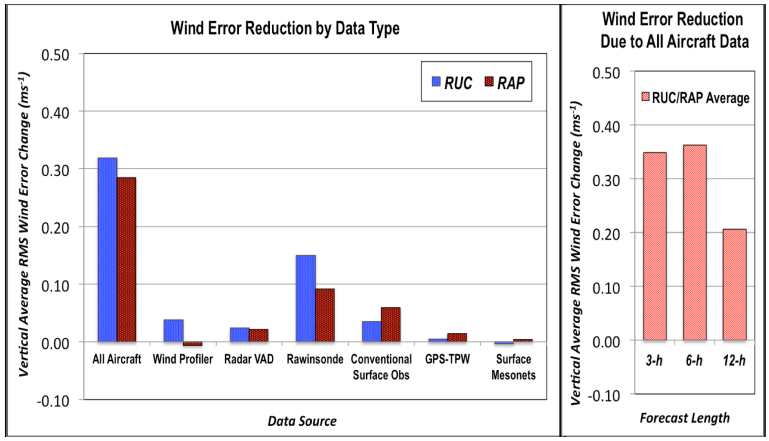

Figure 6: Left: Impact of various data sources on 3-, 6- and 12-h RUC and Rapid Refresh (RAP) wind forecasts averaged over between 850 and 150 hPa, expressed in improvement in RMSV wind error (ms^{-1}). Results for RUC for multi-week periods in Fall 2006 and RAP results for Spring 2011. Right: Impact of aircraft observations by forecast length. (Adapted from Benjamin et al. 2010, 2014).

More recent tests have documented the increasing influence of aircraft reports in short-range forecasts over the US where automated aircraft data abound. "Data Denial" tests were conducted using 13-km versions of both the last operational version of the Isentropic-hybrid coordinate RUC and its successor, the sigma-coordinate Rapid Refresh (RAP) Model, which includes advanced DA systems and enhanced NWP physics (Benjamin et al. 2010, 2012, 2014). Results from the "Control Run" analysis and forecasts using all data sources were compared with reruns in which different sources of data were removed individually, with differences in forecast errors between the Control Run and various tests used as a measure of the impact of each data source (Fig. 6). It should be noted that for these tests, aircraft reports included not only AMDAR reports available on the GTS, but other sources. Most notably, 10-15% of the observations were from Tropospheric Airborne Meteorological DAta Reporting (TAMDAR, see Daniels et al. 2006, Moninger et al. 2007 and Gao et al., 2012) equipped aircraft, generally made below 500 hPa and near airports not usually served by AMDAR aircraft.

Overall, aircraft data dominated as the single most important data set over the CONUS for both the analyses and forecasts out to at least 12 h. This was especially apparent in shorter-range forecasts and in the cold season when baroclinic processes dominate the mid-latitudes (not shown). The next most

important data sets were RAOB and surface observations. Only for 12-h forecasts during winter did RAOB reports show comparable impact to AMDAR data. Automated aircraft observations continued to show their largest impacts at shorter forecast ranges and during the daytime and early evening hours when observations are most abundant. These results provide evidence that collaborations between US airlines and the NWS to promote improved access to and use of AMDAR wind and temperature reports has benefited both the data providers and other users of the products issued by NWP centers and forecasters using these data.

Review of the impact of AMDAR observations on global forecasts: As with regional NWP systems, the impact of aircraft observations in global systems results from a combination of enhancements in the global AMDAR coverage and improvements in the analysis systems. Global DA systems must integrate the in-situ aircraft with a huge number of different types of observations, the vast majority of which are satellite-based and provide critical information over the oceans globally. Within this mix of data, automated aircraft reports are unique in that they are the only non-surface, globally-distributed asynoptic data set that directly measures both temperature (mass), wind (momentum) and, in some cases, moisture. RAOBs provide these same types of observations, but only at synoptic times and are generally not available over oceans. All other data systems need to infer one of these variables from the others based upon a variety of different assumption and constraints within the DA systems. In addition, because AMDAR observations tend to be concentrated near the jet stream level, they can be particularly useful in defining the sources of kinetic energy that drive many weather systems, especially in data sparse regions. It is worth noting that in-situ AMDAR measurements not only provide independent observations in the same places observed by satellite data to improve their value, but also supply additional horizontal and vertical detail.

Since the volume of automated aircraft reports began increasing in the late 1980s, a number of major advances have also occurred in operational DA systems, led to a large degree by the need to make better use of the increasing number of higher-resolution satellite observations that are available (see progression from using techniques that allowed the satellite data to be treated in their native form (i.e., as radiances, rather than converting them to the NWP parameters of temperature, wind and moisture) to implementing procedures that use more data throughout longer assimilation periods. Had additional resources been put toward improving the availability and use of aircraft observations in DA systems in the past, it is likely that the impacts of satellite systems would have been improved even further. In order to ascertain the relative importance of the different data sets, a variety of Global Observing Systems Experiments (OSEs) have been conducted during the past 2 decades. The following brief synopsis of earlier impacts of AMDAR data will focus on EMCWF results, followed by a review of more recent findings from a broader set of global NWP centers.

One of the longer global studies by Kelly et al. (2004) used the ECMWF global analysis and forecast system [T-159 (~120 km) 4D-Var analysis and T-511 (~40km) forecast model] with data from August-September 2002 and December 2002-January 2003. Fifteen airlines provided AMDAR data internationally during the period, less than half the number of current participants, and some data thinning was done (see Andersson et al. 2005 for details). Although the importance of satellite data collected throughout the day from multiple spacecraft on medium-range 500 hPa forecasts increased notably in the improved version of 4D-Var implemented in 2004 (Kelly and Thépaut 2007), AMDAR temperature and wind observations had greater impact at shorter forecast ranges and in the upper troposphere, as discussed next.

Using data provided by Kelly et al. (2004), Petersen (2004) performed a more detailed analysis of the specific impact of AMDAR observations in the ECMWF global forecast system on shorter-range global (12- to 48-h) temperature and wind predictions for the NH and the more-aircraft-data rich NA area (Fig. 7). In contrast to the regional tests described earlier that used both en-route and vertical profile reports over the US, most oceanic AMDAR reports used in these tests only provided cruise-level data. When evaluated over the full NH, AMDAR data had positive impact on forecasts out to at least 48 hours.

When evaluagted over the full NH, AMDAR data had positive impacts on all forecasts out to at least 48

hours. The impacts were largest in the first day, with average 12-h errors temperature and wind errors reduced by 14 and 8% respectively. The improvements were most pronounced near the primary flight levels between 200 and 300 hPa and extending downward to 500 hPa. Above the levels where AMDAR reports are available, improvements in both parameters were smaller (3-6% and 2-5% at 100 hPa). In general, the reports had greater relative influence on temperature forecasts than wind forecasts (especially in the first forecast day).

Over NA, where more AMDAR data were available both at flight levels and during aircraft ascents/descents, the impacts were larger than over the entire NH at all levels below 100 hPa and extended over a longer range of forecast times. During the first day, 12-h temperature forecasts between 200 and 300 hPa improved by nearly 23% and wind forecast errors were reduced by 12-14%. Improvements in 200-300 hPa temperature and wind forecasts continued through two days. Relative improvements were again larger for temperature than for winds.

The impacts of AMDAR data on wind forecasts over other portions of the globe are depicted in Fig. 8.

Although AMDAR reports available then were concentrated in the NH, the data benefited most regions of the globe, including the tropics and the Southern Hemisphere (SH). The largest forecast improvements occurred at cruise levels in the tropics and in the regions that had the highest data concentrations at the time of this study, particularly over the US, Europe, and oceanic flight routes in the NH, as well as in the area around Indonesia. Similar improvements should be expected in other areas as data availability increases in the future.

On average, forecasts for the NH (right-most panels in Fig. 8) improved by more than 0.25 ms^{-1} between 200 and 300 hPa. From the North Pacific into Europe (top panels), average improvements ranged from 0.3 to nearly 0.5 ms^{-1} for 12-h forecasts. In individual events, improvements were notably larger, often exceeding 5 ms^{-1}. For longer forecast periods, impacts decreased by 25 to 75% at different levels and locations. Similar improvements and trends were also noted in temperature forecasts for these same levels for each region (not shown). Enhancements in global forecasts such as these not only allow aviation users to adjust flight plans to reduce fuel use and optimize efficiency (NCAR 1986) but also benefit medium-range NWP systems by improving background fields used in data assimilation systems.

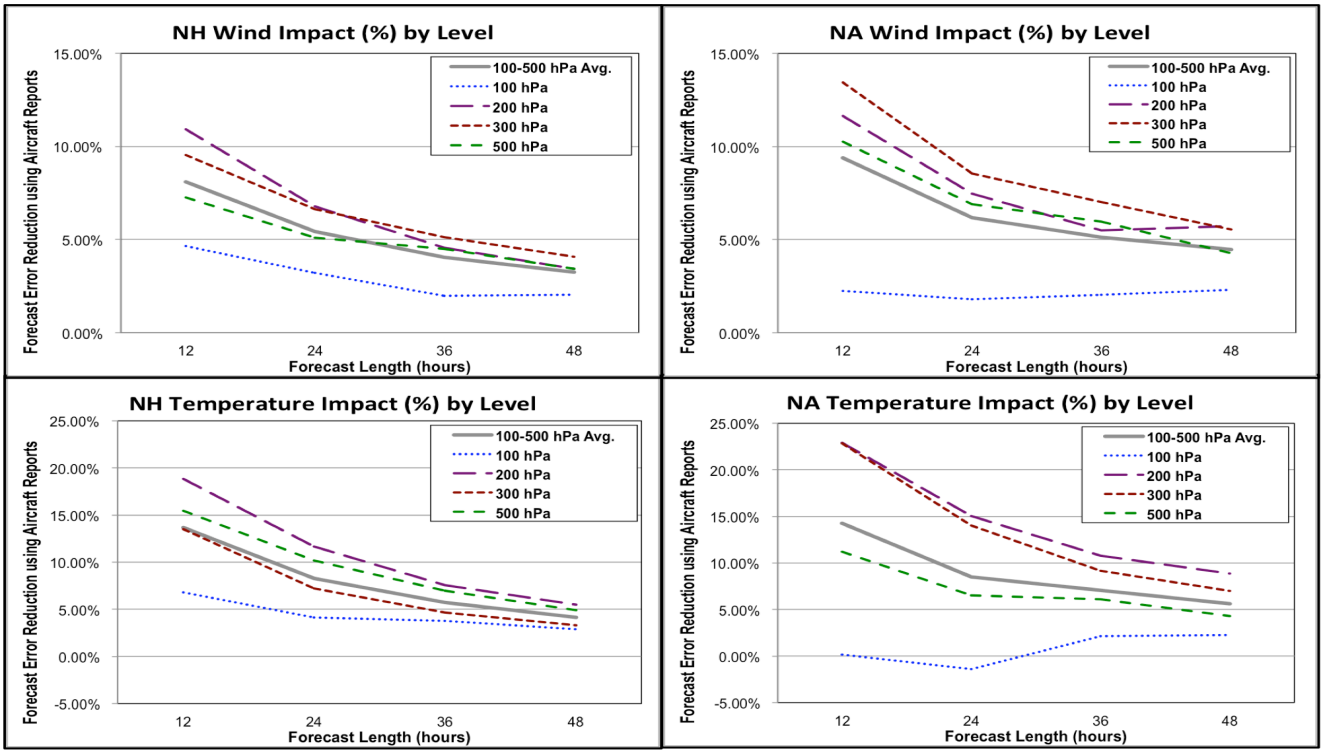

Figure 3: Impact of AMDAR Wind (top) and Temperature (bottom) observations on 12-, 24-, 36- and 48-h ECMWF forecasts at 100, 200, 300, 500 hPa and for 100-500 hPa layer average over NH (left) and NA (right), calculated as % error reduction using aircraft data. Based on data provided by ECMWF Kelly (2004) from experiments conducted with data from August-September 2002 and December 2002-January 2003.

Recent tests of the impact of AMDAR observations – Since 1996, the WMO has sponsored a series of quadrennial scientific meetings to understand and assess the impact of various observing systems on NWP skill. The following summarizes results from the fifth such meeting held in Sedona, Arizona in May 2012 (WMO 2012). Participants included representatives of all major global and regional DA and NWP centers, as well as experts in various observing systems and forecast applications. During the past several years, more advanced techniques have been developed to increase understanding and assess the relative impact of various observing systems using sophisticated DA systems. Although the number of satellite observations available to DA systems has increased dramatically, typically fewer than 5% of the available radiance data are used (Derber and Collard 2011). By contrast, only about 5% of AMDAR-equipped aircraft are excluded through rejection lists at any one time (Pauley et al. 2014). Automated aircraft observations now represent the largest non-satellite data source in most global NWP systems, an indicator of their quality and increasing importance, and supply nearly 35% of the impact of all 'conventional' observations globally and 60% over the US (Isakson, 2014).

Figure 9 shows the average impact of various observations obtained by compositing independent results from five participating DA centers using similar data combinations, including the UK Met Office, NCEP, ECMWF, Meteo France and the NASA Global Modeling and Assimilation Office (GMAO). It should be noted that variations in results amongst centers are expected due to a number of factors, different data selection criteria and DA techniques, including varying ability to maximize benefits from hyper-spectral IR satellite observations.

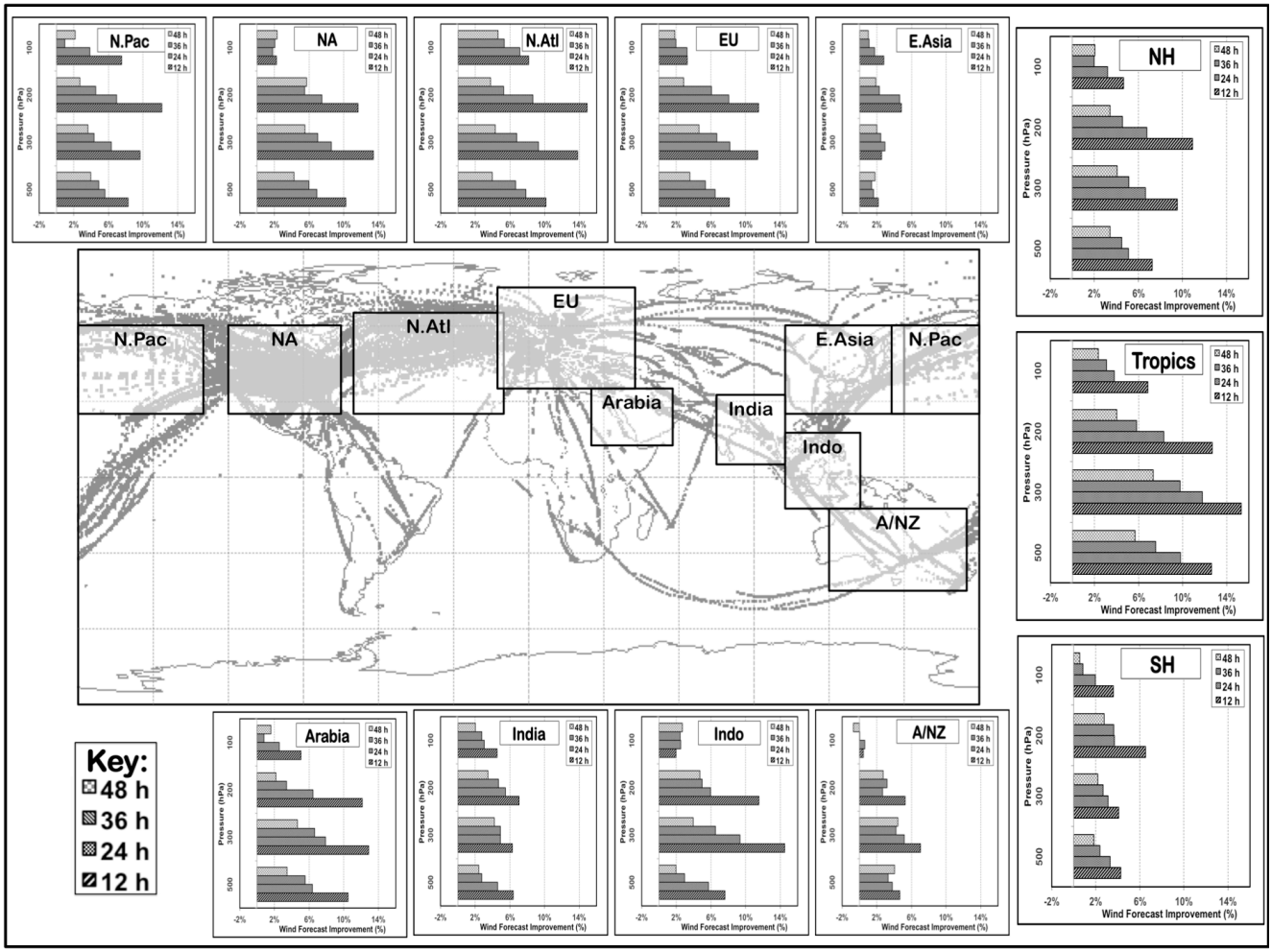

Figure 4: Improvement in RMSV wind errors (ms^{-1}) at 500, 300, 200 and 100 hPa in 12-, 24-, 36- and 48-h ECMWF forecasts for different areas of the globe when including AMDAR reports in ECMWF global DA and forecast system. Verification areas are overlaid on plot of typical 6-hr aircraft data distribution at time of study. Based on data provided by ECMWF Kelly (2004) from experiments conducted with data from August-September 2002 and December 2002-January 2003.

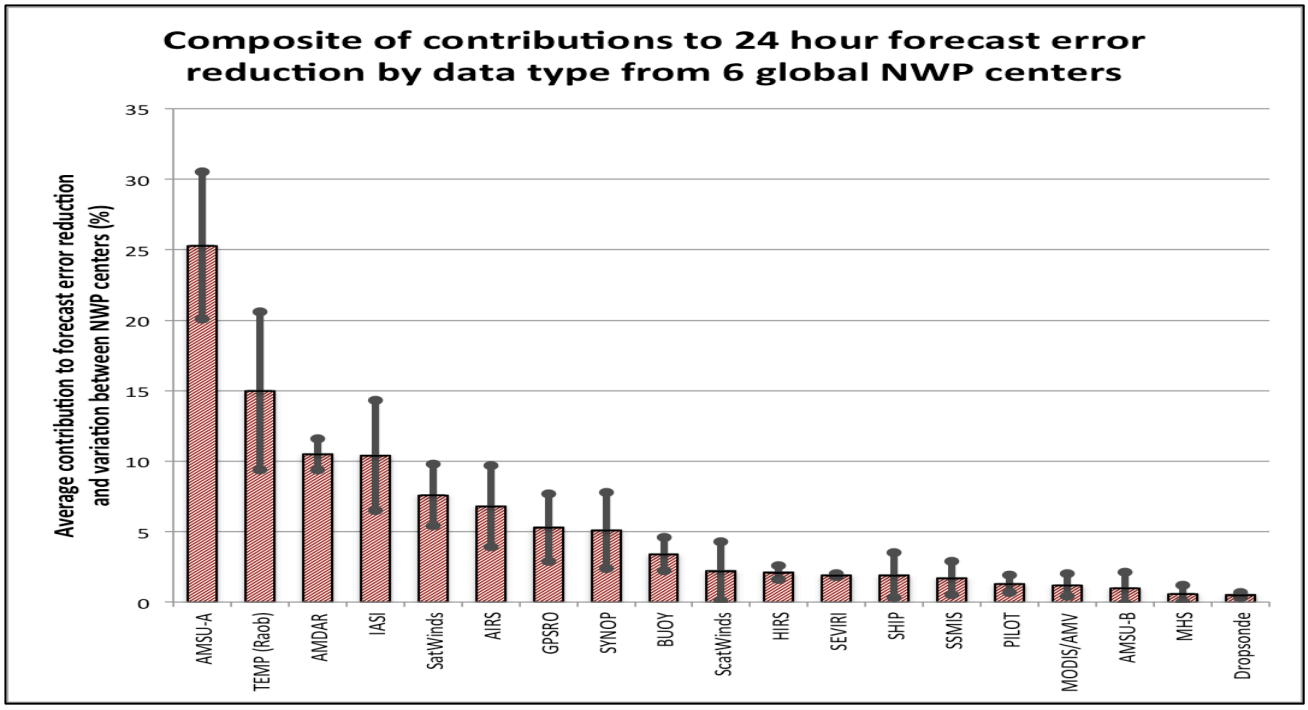

Figure 9: Composite of contributions to 24-h Forecast Error Reduction (%) by data type from five NWP centers using data available in 2012. Gray bars indicate average impact and lines provide an estimate of the variability in impact between centers based on a limited Standard Deviation of % error reduction.

AMDAR reports rank 3rd in importance among all observations for improving 24-h global weather forecasts, behind only microwave satellite observations (primarily AMSU-A observations, which afford more continuous global coverage than AMDAR reports) and RAOB reports (which furnish important information above the highest AMDARreporting levels) when using evaluation criteria similar to those described by Cardinali (2009). Further, AMDAR data exhibit the most consistent impact across the 5 centers, as indicated by its small variability compared to other major data

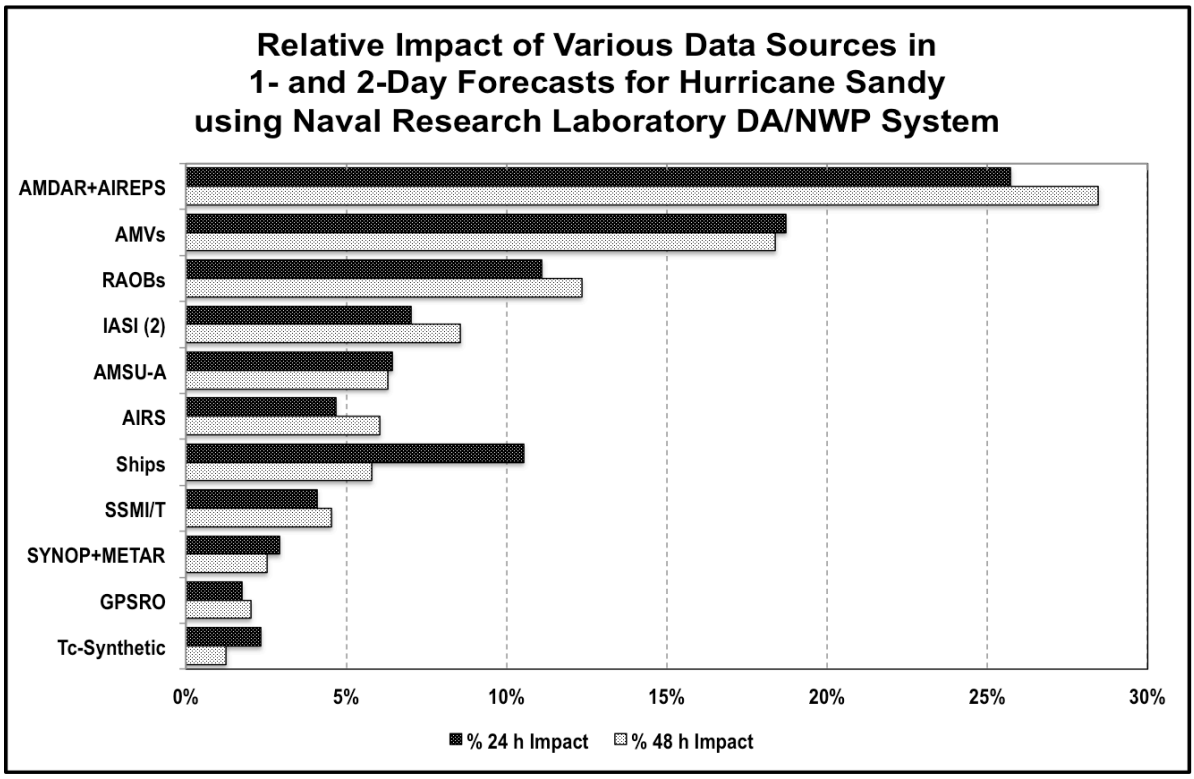

Figure 10: Impact of various data sources on 1- and 2-days forecasts of Hurricane Sandy. (Based on Hoover, et al. 2014)

sets. These results attest not only to the quality of the data, but also to the importance of using reports made both near airports in ascent/descent and near the major source of atmospheric energy near the jetstream, the ease and economy with which the temperature and wind information can be incorporated into DA systems, and the importance of multiple reports along flight routes for use in cross-validating individual observations. Other tests, some using different combination of data sources, show even greater aircraft data impact regionally and globally, in some instances, providing the greatest impact of any data set (e.g., Kang et al. 2014, Alexander et al. 2014, Lupu et al. 2012, Ota et al. 2013).

Several additional studies have addressed other important aspects about the role played by AMDAR data within the total global observing system. For example, Andersson and Radnóti (2012) saw only small degradation in ECMWF forecast skill when the number of RAOBs was reduced selectively but the number and distribution of AMDAR reports was held constant. Cress (2012) also noted that AMDAR data retained impact longer than RAOBs in some regional forecast systems. Other studies indicate that if AMDAR reporting variables are assimilated separately, wind observations had a somewhat greater impact than temperature data, but that the greatest impact occurred when both parameters were assimilated simultaneously (see WMO 2012 for more details).

For individual events, the impact of AMDAR data can be much larger. For example, Hoover et al. (2014) studied the impact of AMDAR data on forecasts of Hurricane Sandy using the Navy Global Environmental Model and Naval Research Laboratory Variational DA System. In these tests (Fig. 10), AMDAR data had a greater impact than any other data source on improving forecasts of the location and timing of landfall of this major storm, both at 24- and 48-h. In this case, the impact was nearly double that of RAOBs. These enhancements can be especially important for airlines to minimize unnecessary disruptions to the flight operations while maximizing the safety of both passengers and their aircraft.

Summary of impacts of AMDAR Temperature and Wind Reports: Tests conducted by numerous NWP centers for over 25 years have demonstrated that high-quality and high-frequency AMDAR temperature and wind observations increase the skill of forecasts at both regional and global scales and for both short- and medium range forecasts. Results show that aircraft data taken at cruise levels and during ascent/descent provide important information for improving forecasts, both in terms of long-term average performance and for individual events. Although global, 'all-weather' satellite microwave observations have the largest average influence on medium-range global forecasting system (especially in the SH), AMDAR observations have become recognized as a critical component of these systems around the world. Aircraft observations rank 3rd in importance globally (especially in the NH) and contribute between 10-15% to 24-h forecast skill improvement, with impacts extending to 48 hours and beyond. In areas with denser data coverage aloft and abundant ascent/descent reports, they have become the single most important data set for use in shorter-range, regional NWP applications.

A unique feature of AMDAR reports is that they provide both temperature and wind data at the same locations and in profiles made during ascent/descent, thereby furnishing explicit two-dimensional information on baroclinic adjustments needed in DA systems. Because the data are available continuously along flight routes, the observations also provide information about gradients of wind and temperature near high-energy jet stream regions. The availability of multiple reports along flight routes is also important for cross-validation and QC (WMO 2014).

Results presented here attest to 1) the quality of the data, 2) the importance of the reports made both as profiles during ascent/descent and at cruise level near the major reservoir of energy in the atmosphere and 3) the ease of use of the wind and bias-corrected temperature information in DA systems. Additional experiments are needed to understand more fully how temperature and wind gradient information that can be derived from cruise-level AMDAR reports may contribute to the enhanced importance of AMDAR data relative to other, more costly data sets.

Brief history of automated moisture data collection from commercial aircraft: Currently, 115 aircraft-based Water Vapor Sensing Systems (WVSS) deliver observations operationally across the globe daily, principally across the US. Although previous studies (summarized by Petersen 2015) have demonstrated the value of aircraft wind and temperature reports obtained through the Aircraft Meteorological DAta Relay (AMDAR) program (WMO 2003a) to both regional and global numerical weather prediction (NWP) scales, the quality and significance of these newly available moisture observations are less well recognized. Because moisture often varies at smaller scales than wind and temperature, temporally and spatially frequent moisture observations can have exceptionally large impacts on forecasts of disruptive weather events and could help offset the dwindling number of upper-air moisture observations available globally. Forecasts of disruptive weather events made at NWS field offices and participating airlines demonstrate the benefits of these newly available observations, particularly profiles made during aircraft ascents and descents.

Various studies over the past decade have shown that, in addition to temperature and wind observations, detailed measurements of the vertical, horizontal and temporal atmospheric moisture and related moisture flux structures are necessary to improve forecasts of location, intensity and timing of precipitation events, including the onset and strength of convective storms (e.g., Hartung et al. 2011 and Otkin et al. 2011). These events can have major impact on public safety and economic efficiency. To meet this need, Fleming (1996) established the Water Vapor Sensing System (WVSS) project with the goal of developing a moisture sensor appropriate for use on commercial aircraft that could offer a cost-effective means of supplementing other in-situ observations, both temporally and spatially.

As an independent component of the WVSS development process, the University of Wisconsin Cooperative Institute for Meteorological Satellite Studies (UW-CIMSS) conducted a series of independent evaluations of the systems over a 10-year period to determine the accuracy of the aircraft humidity observations relative to temporally and spatially co-located RAOBs. WVSS data for these tests were obtained from United Parcel Service (UPS) Boeing 757 aircraft landing at and departing initially from Louisville, Kentucky and later Rockford, Illinois for multiple 2-week long episodes. Because 60-80% of the WVSS equipped planes typically land or take off daily from these major UPS operational hubs, these locations allowed close comparison with RAOBs at the airports, without the logistical complications inherent in launching balloons in congested air traffic areas near more major airports.

The initial design of the WVSS (WVSS-I) used RAOB-like sensors to measure relative humidity (RH). Tests of this system, however, showed that many of the observations were unacceptably affected by a combination of factors, including decreased accuracy over time due to the collection of contaminants on the sensors, the inability to respond quickly to rapid changes in moisture, and excessive relative humidity biases and measurement errors below the reliable minimum threshold of the sensor caused by pressure-induced heating on aircraft traveling at high Mach numbers (Fleming et al. 2002).

A major redesign effort produced the WVSS-II instrument, which measures specific humidity (SH) using a laser-diode approach that senses the number of water vapor molecules moving past the sensor in a specific volume of air. The system is applicable to all aircraft sizes and speeds and does not require frequent recalibration (Fleming and May 2006). The reengineered WVSS-II systems first became available in late 2004.

WVSS-II observations are made independent of temperature and aircraft speed and are available across a wide range of values, from below 50 to over 40,000 ppmv (approximately 0.03 to 24.9 g/kg, respectively), and with an advertised accuracy of ±50 ppmv or ±5%, whichever is greater (Spectral Sensors, 2015). The four time per second internal sample rate (corresponding to one observation every 60-70 m at cruise levels) and 2.3 second data output rate provide vertical moisture profiles comparable in quality and resolution to rawinsonde reports. Observations are made during all phases of flight (ascent, cruise and descent) and are attached to independently measured temperature and wind data to form a single AMDAR report for transmission to the ground. (See Petersen 2015 for details about AMDAR spatial and temporal reporting frequencies.)

Chamber tests were performed by Deutscher Wetterdienst (DWD) to document the accuracy of the WVSS-II system compared with research-grade moisture sensors in a controlled environment (Hoff 2009). These tests showed that the laser diode system exceeded accuracy specification across a wide range of observing environments (Fig. 11), with the only substantial errors of the WVSS-II observations occurring at SH values less than 0.04 g/kg. DWD concluded that WVSS-II data should be valuable in applications where SH remains above this threshold. Climatologically, these include mid-latitudes regions from the ground to at least 400 hPa during winter and to 200 hPa during summer.

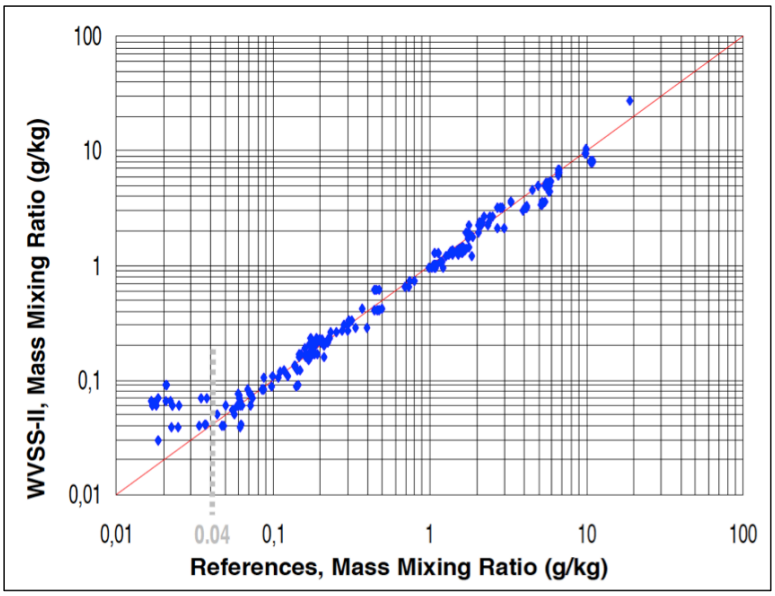

Figure 11: Test results of the 2006 version of WVSS-II against calibrated reference systems performed in a climate chamber at the DWD Meteorological Observatory Lindenberg. (See Hoff 2009 for details)

Installation of the new sensors on UPS aircraft began in 2005. Initial aircraft-to-RAOB evaluations of this system (Petersen et al. 2005, 2006a and 2006b) again revealed a number of performance problems, including: 1) flaws in data-encoding procedures (whereby reports of SH greater than 10 g/kg had a precision of only 1 g/kg), 2) water vapor contamination within the WVSS-II laser-diode sensing chamber that produced moist biases and thereby prevented the systems from observing very small amounts of atmospheric moisture (consistent with the results of DWD chamber tests) and 3) engineering problems caused by temperature-sensitive electronic components which produced large irregular biases and other errors.

After final engineering and communications modifications were completed (Helms et al., 2009), new WVSS-II hardware and software were installed on 25 UPS aircraft beginning in mid-2009. Results described here used data obtained only from these revised sensors. Similar sensors have since been installed operationally on 87 Southwest Airlines Boeing 737 aircraft, as well as on 3 Deutsche Lufthansa Airbus 319 aircraft for evaluation. A map of typical daily WVSS-II ascent/descent coverage currently available over the US is shown in Fig. 12.

A series of assessments are presented here comparing data from WVSS-II sensors installed on Boeing 757 aircraft operated by United Parcel Service (UPS) with co-located rawinsonde observations (hereafter called RAOBs). The results support the hypothesis that the aircraft moisture measurements can help fill data voids over land between conventional upper-air observations, both in time and space. Information derived regarding spatial and temporal moisture variability observed between neighboring aircraft could be important in optimizing the use of these observations in future regional- and storm-scale forecast systems. A series of case studies and a review of initial NWP studies performed elsewhere are also presented to demonstrate the importance of these high temporal- and spatial-resolution data on short-range forecasts over the US.

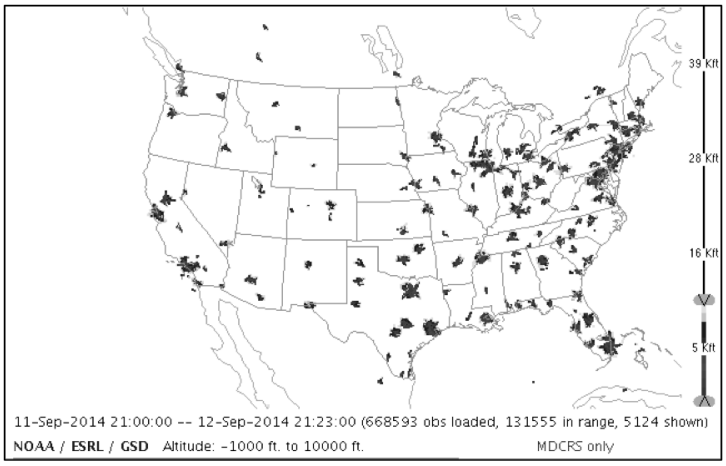

Figure 12: Sample distribution of WVSS-II observations made during takeoff and/or landing between the surface and approximately 3000m (10,000 ft.) during a 24-h period in September 2014. (Courtesy of NOAA/ESRL)

WVSS-II Evaluation Design and Rawinsonde Co-Location Results: Prior to final inter-comparisons of the re-engineered WVSS-II systems with RAOBs, 224 WVSS-II observations from aircraft on the ground were compared with contemporaneous METAR surface observations at 43 airports across the Contiguous US (CONUS) and southern Canada (Petersen et al., 2009). These comparisons were conducted primarily at night when the local effect of thermal mixing and consequent moisture variability should be minimal. Nonetheless, it should be noted that the METAR temperature and moisture are made 2 meters above a grassy surface while the aircraft WVSS-II sensor are made at a higher height above concrete. The results provide a benchmark for assessing instrument accuracy without the influences of aircraft motion. Results in Fig. 13 show good agreement across a range of SH values between 2 and 20 g/kg, with standard deviation (StDev) agreements between independent moisture observations within 0.42 g/kg for SH and a negligible moist bias of approximately 0.01 g/kg. This equates to a RH StDev of 3.53%. (For all RH comparisons shown in this paper, temperatures from the appraisal standard were used in the WVSS-II RH calculations, thus avoiding the effects of known AMDAR temperature biases described by Zhu et al. 2015 and discussed in more detail later.)

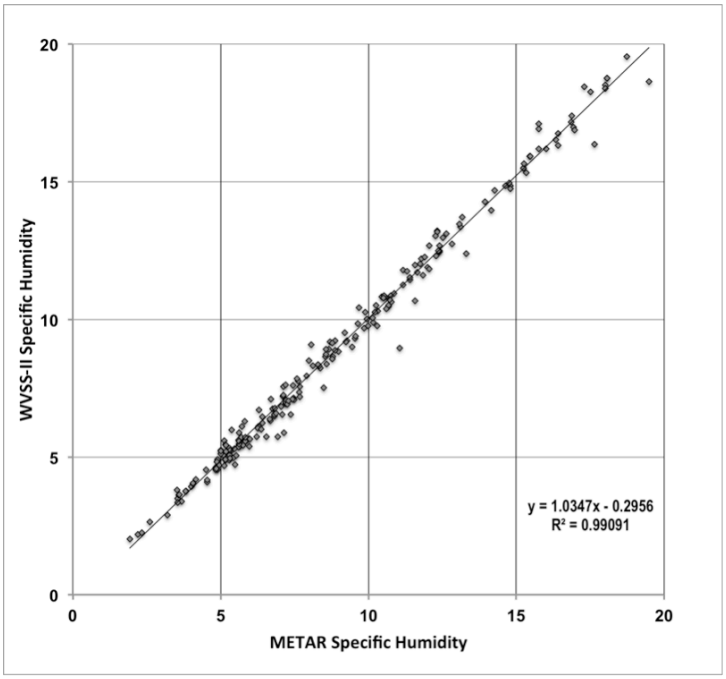

Figure 13: Comparison of 225 AMDAR SH observations (g/kg) with surface METAR reports made at 43 sites across the US and southern Canada for the period from 5-17 September 2009. Linear regression fit statistics shown in lower right.

Comparisons of WVSS-II reports with co-located RAOBs were obtained during 16 evenings over three separate observing periods in fall 2009, spring 2010 and summer 2010 at the Rockford, Illinois airport (RFD). These tests were designed to assess the general performance of the systems and to provide statistical evidence of the accuracy of the re-engineered WVSS-II system. Of the 25 WVSS-II equipped UPS Boeing 757 aircraft, 17 were available for use in the statistical evaluations discussed later.

All RAOBs were made using Vaisala RS92-SGP instruments with Humicap moisture sensors, which employ twin heated thin-film capacitors to provide RH reports. The moisture observations have advertised reproducibility (StDev differences between twin soundings) of 2% and a total uncertainty in a sounding for reports with T > -60°C of 5% (2-sigma confidence level of cumulative effects, including repeatability, long-term stability, measurement conditions and measurement electronics, as well as dynamic effects including response time). All of the RAOBs used in this test were acquired within 60 days of the experiments to minimize the effects of instrument aging on observation accuracy. (See Miller et al. 1999, WMO 2011 and Viasala 2015 and WMO 2011 for more details on instrument details and performance.)

RAOBs were launched adjacent to the RFD runway at approximately 3-hourly intervals. The first launches were made immediately before a period when a group of WVSS-II equipped aircraft landed, the last immediately after the final aircraft departed, with intermediate launches made during the short period between the last landing and first departure.

Direct Inter-comparisons of AMDAR/WVSS-II and RAOB Observations: Before statistical analyses were performed, individual WVSS-II systems were compared with nearby RAOBs. As in all results presented here, the RAOB and aircraft data were vertically interpolated using linear-log pressure methods to common pressure levels based on the nominal reporting frequency of the instantaneous aircraft ascent and descent reports available for this study (10-hPa intervals from the surface to 850 hPa and 25-hPa intervals above that.)

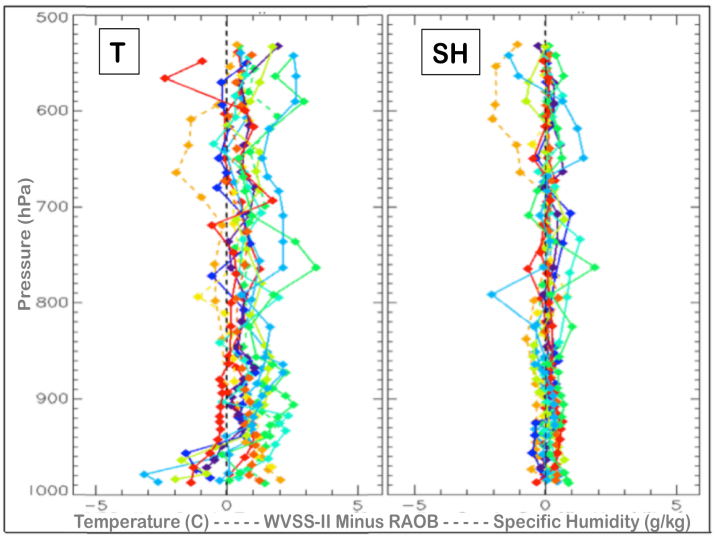

Figure 14: Differences between ascent (solid) and descent (dashed) observations from WVSS-II equipped aircraft (Tail #1370) and co-located RAOBs taken within ±1 h between 27 April and 10 May 2010 at Rockford, IL. T (C) at left, SH (g/kg) at right. Different colors distinguish between individual WVSS-II reports made throughout the period.

Comparisons of each of the individual RAOB profiles with all aircraft observations made within approximately1 hour of the rawinsonde launch time are shown in Appendix B. Fig. 14 shows differences between an individual WVSS-II equipped aircraft and RAOBs throughout the spring 2010 data collection period. The AMDAR temperature (T) reports show a persistent warm bias at all but the lowest levels, although descending data (dashed lines) have slightly smaller biases. The spread of the T difference profiles is indicative of random variations at all levels. These results are consistent with previous studies by Ballish and Kumar (2008) and Zhu et al. (2015).

By contrast, WVSS-II SH reports show little bias and very small random differences in the lowest 200 hPa of the profiles. Larger random differences are seen immediately above 800 hPa in several ascents and above 650 hPa in both some ascent and descent reports, in part a reflection of the greater distance between higher-altitude WVSS-II reports and the validating RAOBs at these levels.

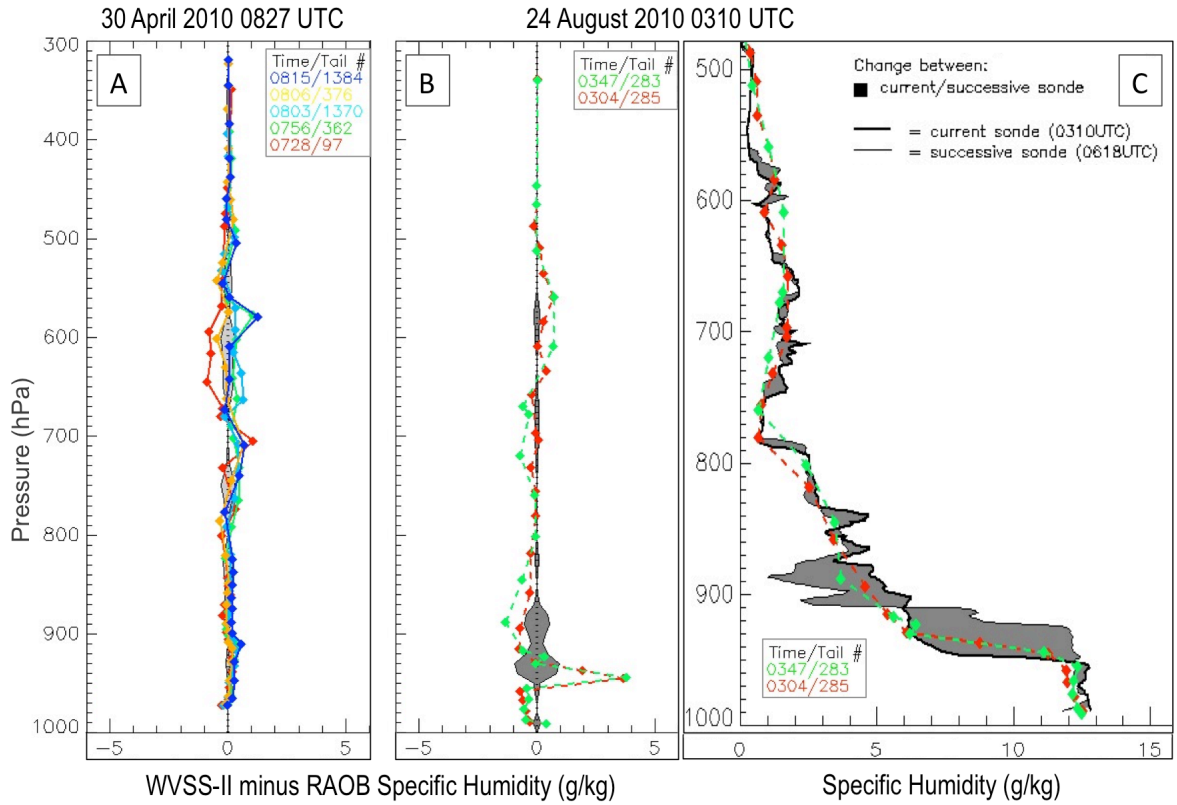

Figure 15: A - Differences between ascending WVSS-II SH (g/kg) observations and RAOBs taken around 0827 UTC on 30 April 2010 at Rockford, IL. Hourly rate of change observed between bounding RAOBs shaded. Colors indicate different aircraft providing reports, with encoded tail numbers and arrival times noted in upper right.
B – Same as 15A, except for descending observations taken around 0310 UTC on 24 August 2010.
C - Plots of co-located WVSS-II SH (g/kg) observations (colored) and RAOBs (black) taken around 0310 UTC on 24 August 2010 at Rockford, IL. Changes observed between bounding RAOBs shaded.

Comparisons between aircraft and individual RAOBs provide another subjective means of evaluating observations from individual WVSS-II equipped aircraft. Differences between WVSS-II and RAOBs for two evenings with different synoptic conditions and seasons are shown in Fig. 15a,b. In both cases, the majority of both ascent (solid) and descent (dashed) profiles showed good agreement with RAOBs taken immediately prior to and following the aircraft reports, including strong gradients across moisture inversions. This was especially true in the lowest 300 hPa of the soundings where all aircraft were flying essentially along the same paths and close to the RAOB launch site. The agreement between the successive, independent WVSS-II profiles provides confidence in the accuracy of and consistency between the individual WVSS-II observations. Aloft, the WVSS-II and RAOB differences show greater variability, part of which may be related to small-scale moisture variations and/or clouds in the area along the aircraft and/or the RAOB path and the increased separation between the paired observations at higher levels.

Ascent WVSS-II moisture observations (Fig. 15a) predominantly agree within ±0.5 g/kg and fall within the hourly variations (shaded) between the temporally bounding RAOBs. It should be noted that ascent reports generally dominated the aircraft data sets and typically show little bias.

Consistency between descent reports (Fig. 15b) was also very good, as illustrated by the fit of the WVSS-II data between the bounding RAOBs across much of the strong low-level moisture inversion in this summer case (see Fig 15c). Although the WVSS-II and RAOB moisture profiles agree very closely, the slight misalignment of observing levels between the WVSS-II observations and the validating RAOBs at the time, location and vertical displacement of the strong inversion led to a large +/- difference couplet between 850 and 950 hPa in Fig 15b. Large individual differences like these, especially in moist environments, can have large impact on the overall statistical evaluation presented later. It should be noted that over-estimates of SH in WVSS-II descent data near the melting level were noted in some of the fall 2009 data, but were not present in later observations. Aircraft temperature profiles, however, continued to have notable warm biases, especially during aircraft ascent (see Appendices for details).

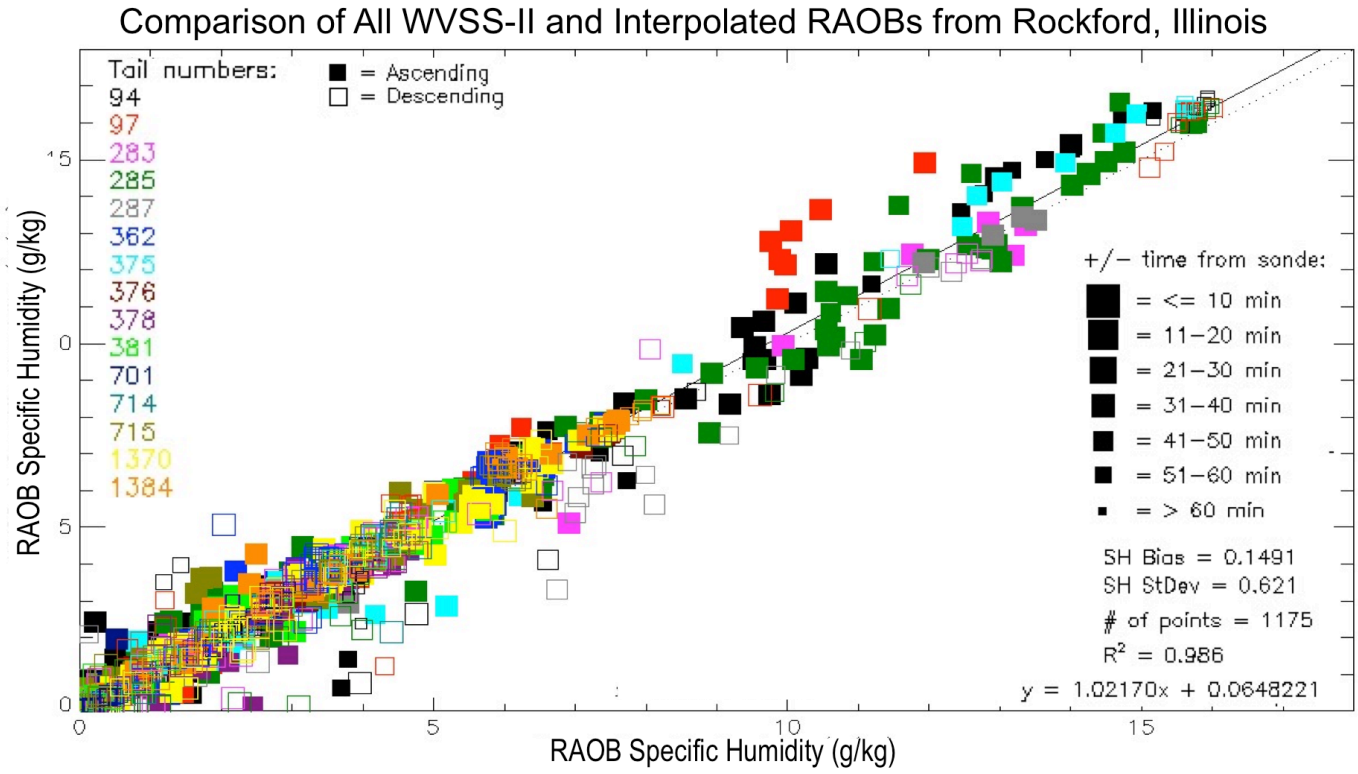

Figure 16: Scatter plot of 1175 co-located WVSS-II and time-interpolated RAOB SH reports for all levels for all inter-comparison periods at Rockford, IL. Markers color-coded for 15 individual aircraft providing WVSS-II reports using encoded tail numbers at left. Marker size indicates time spread between WVSS-II and RAOBs, with larger markers indicate matchups that are closer in time. Ascents presented as solid squares, descents by open squares. Inter-comparison and least-squared fit statistics included in lower right.

Statistical Assessment of co-located AMDAR and RAOB Profiles: The analysis presented here used all available data from 15 UPS aircraft and excluded two early systems that experienced mechanical failures. WVSS-II observations were compared both with the single closest-time RAOBs and with bounding RAOBs interpolated linearly at each level to the aircraft observation time. Because the time interpolation process removed a portion of the random differences noted between the two data sets (11% for SH and lesser amounts for T and Wind), only time-interpolated results are shown here. Co-locations were made using all RAOBs within 60 minutes and 50 km of the WVSS-II reports, with RAOB locations adjusted for balloon drift.

Because the objective of these evaluations was to determine the quality of the WVSS-II data, in-situ observations were sought for comparison in which the effect of small-scale, local atmospheric variability was minimal. Based on the analyses of individual cases described above, additional criteria were applied to restrict evaluations to cases with relatively small changes between successive RAOBs, both in time and between vertical levels. Temporal differences in RH between sequential RAOBs were limited to 7% and vertical differences between adjacent vertical levels in individual profiles to less than 10%. These restrictions diminish both the effects of scattered clouds that could have been along the RAOB trajectory and of vertical motion in shallow banks of moisture and fronts occurring between the 3-hourly ROAB launches. (Examples of different interpolation experiments and Contingency Tables are shown in Appendix C.) In total, 1175 co-locations were used in the assessments, 711 during aircraft ascent and 464 during descent. A minimum of ten observation matchups was required statistics were calculated at individual levels.

Figure 16 compares individual WVSS-II reports with the co-located RAOBs for all levels, all observation periods and both ascents and descents. (Additional plots separated by ascent, descent and time separation are presented in Appendix D.) Several characteristics of the WVSS-II data become readily apparent that are consistent with the individual profiles in Fig. 15. Overall, the more numerous ascent data displayed show fewer outliers than the descent reports. The fits of the ascent data are extremely good for the middle and upper moisture range (> 6 g/kg), although there are a number of outliers from two specific aircraft at larger time differences in the 9-12 g/kg validation range and include the small-scale effects of the strengthening inversion for the August case shown in Fig. 15. It is noteworthy that the highest SH reports (generally obtained near the surface) agreed very closely both with the validation RAOBs and with other WVSS-II observations made at the time, as will be discussed later. Overall, the WVSS-II data set matchups reveal a systematic difference (bias) of 0.15 g/kg and a random difference (StDev) of 0.62 g/kg.

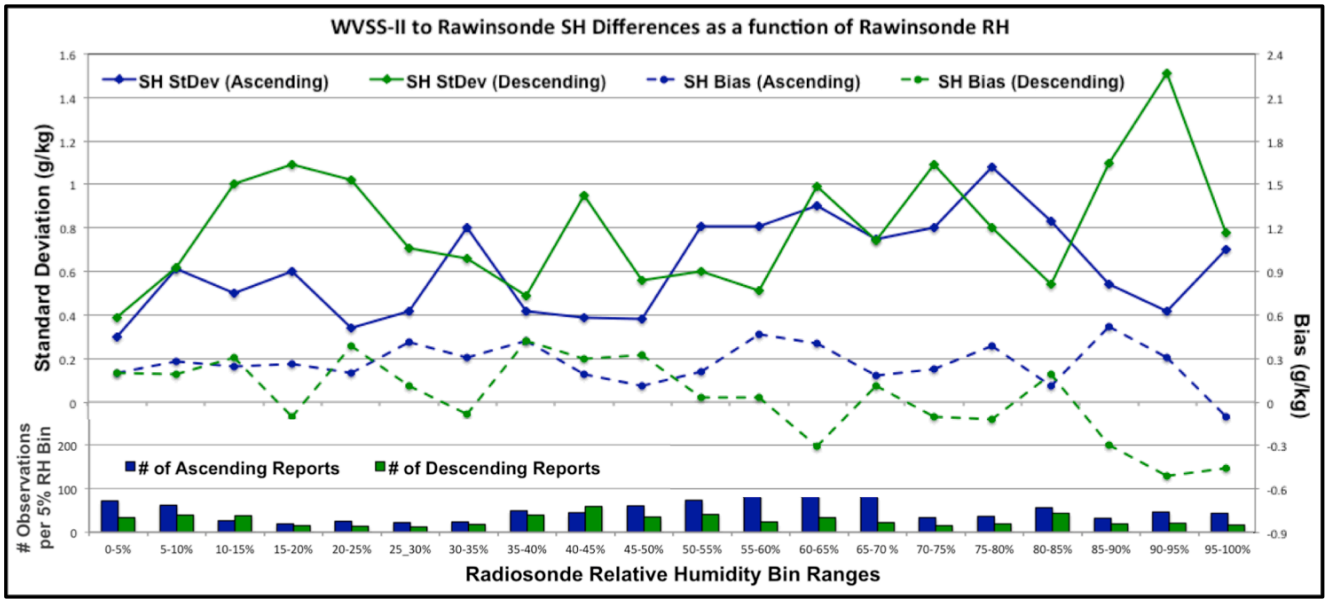

Figure 17: Comparison of systematic (bias) and random (StDev) differences of all WVSS-II SH (g/kg) observations with time-interpolated RAOBs during the full inter-comparison periods at 5% RH intervals during ascent (blue) and descent (green). Number of observations in each RH interval presented in histogram at bottom.

SH data from descending aircraft showed a slightly smaller bias (+0.02 g/kg) and larger random difference (StDev of 0.69 g/kg) when compared with +0.20 g/kg bias and 0.54 g/kg StDev for ascending reports. Flights that descended into moist conditions showed slightly larger systematic moist biases relative to the co-located RAOBs, while the ascending flights showed smaller random differences (StDevs). The fact that multiple aircraft showed these same behaviors points both to good consistency between the aircraft reports and to the possibility that the RAOBs taken at approximately 3-hourly intervals may not have fully captured the small-scale moisture structures observed by the WVSS-II aircraft at intervening times.

To determine whether WVSS-II data showed any degradation as a function of percent saturation, WVSS-II and RAOB SH inter-comparison statistics were collected in 5% bins across the full range of observed RAOB RH values (Fig. 17). The results display only small variations in SH accuracy, especially for RH values less than 85%.

During ascent, WVSS-II biases remain small and positive (moist) except near saturation, where the biases became slightly negative (dry), while during descent, neutral to dry biases are more prevalent across a larger span of higher RAOB RH values, with negative biases noted at RHs greater than 80%. Random differences in the ascent data remain fairly consistent for environments below 50% RH, with StDev near 0.5 g/kg, but approach 1.1 g/kg in environments between 50 and 85% RH, and then return to 0.5 g/kg in the highest RH ranges. The larger StDev observed at higher RHs during descent might have been due in part to possible hysteresis in the instruments when descending through cloudy/moisture layers.

Vertical profiles of the WVSS-II and RAOB SH statistics are shown in Fig. 18. The best agreement between all WVSS-II and RAOB moisture observations appears in the lowest 50 hPa, with random differences (StDev) on the order of 0.5 g/kg and SH biases varying between -0.3 to +0.2 g/kg. At other levels, biases remain between 0.0 and 0.4 g/kg.

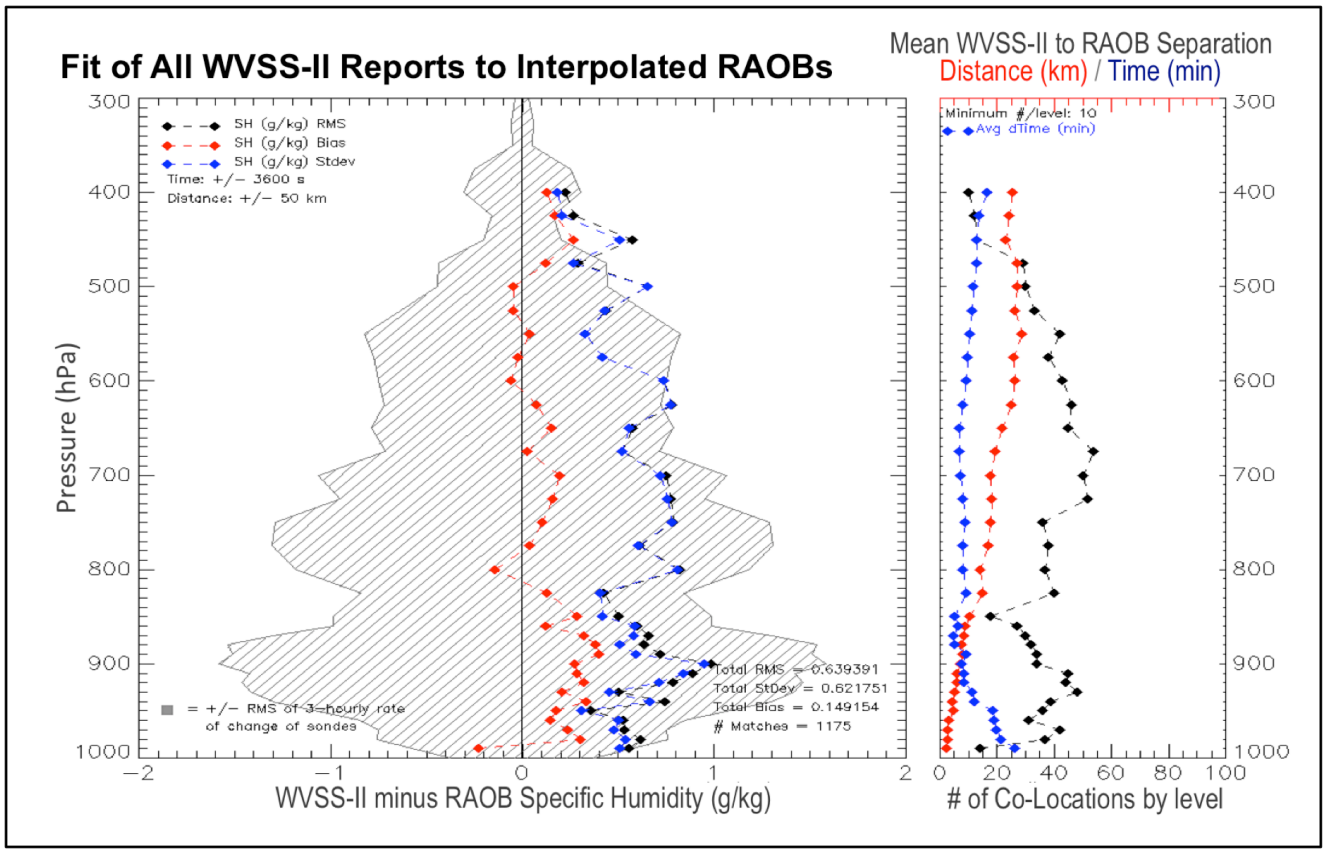

Figure 18: Left - Plots of SH comparison statistics between co-located observations from all WVSS-II and time-interpolated RAOBs taken for all 2009-2010 inter-comparison periods at Rockford, IL (bias, g/kg, red; RMS, g/kg, black; StDev, g/kg, blue). Fit statistics included in lower right indicate a bias of 0.15 g/kg and StDev of 0.62 g/kg over the full assessment period using 1175 data matches. Hatching indicates RMS of change between successive RAOBs throughout test period, normalized to 3-hourly rates. Right - Number of observations inter-comparisons used (black), mean distance between reports (km, red) and mean time difference between reports (minutes, blue).

This systematic behavior of the instrument can readily be removed and modified over time by monitoring instrument performance against a calibrated standard on a regular basis, such as comparing the expanded number of WVSS-II observations to coincident METAR reports and/or nearby operational RAOB profiles.

Above 950 hPa, random differences range between 0.4 and 1.0 g/kg. As shown in the right panel of Fig. 18, the increases above 850 hPa occur as the space and time separation between observations increases. Above 600 hPa, the decrease in random differences is due in part to decreases in magnitude of SH at these levels (not shown). Overall, the majority of the random differences in the WVSS-II-to-RAOB matchups fall within the shaded 3-hourly root mean squared (RMS) changes observed by RAOBs throughout the full test period, indicating that WVSS-II observations are consistent with moisture variations detected between successive RAOBs. Based on these results, WVSS-II performance appears to be well within the current WMO standards for both global and mesoscale weather forecasting applications (WMO, 2003b). (Additional comparisons by ascent/descent and for other AMDAR variables are presented in Appendix E.)

Further partitioning of the profile statistics by ascent and descent (Fig. 19) shows that the time differences between ascents and RAOBs were less than those for descents, and that the distance between the observations made during aircraft descent (which are generally made into the wind and therefore toward the RAOB ascent path) was generally less than during aircraft ascent. The number of upper altitude reports available for comparison was also lower in the descent data set due to the more gradual (and therefore lengthier) descent paths taken by aircraft during landing. Descent data showed slightly smaller random differences when compared with RAOBs in the lowest 70 hPa, with larger differences aloft. Biases during descent were negligible and during ascent averaged < 0.2 g/kg. Overall, random differences during descent of 0.67 g/kg were slightly larger than the 0.58 g/kg StDev noted during ascent.

Investigation of other AMDAR observations show that, as in past tests, T observations (panel Fig. 20a) show positive biases, even for observations that were separated by less than 10 km. It should be noted that the aircraft T observing system is independent of the WVSS-II hardware. Although the bias is small near the surface, it increases rapidly to nearly 0.5°C. between 925 and 850 hPa. Above that level, the bias decreases by half, but then increases again near 600 hPa. Overall, the profiles collected during the three test periods showed a warm bias of approximately 0.36°C and are consistent with, but slightly larger than, results from the same aircraft during earlier WVSS-II tests. (Further discussion of possible sources of this bias, including possible hysteresis

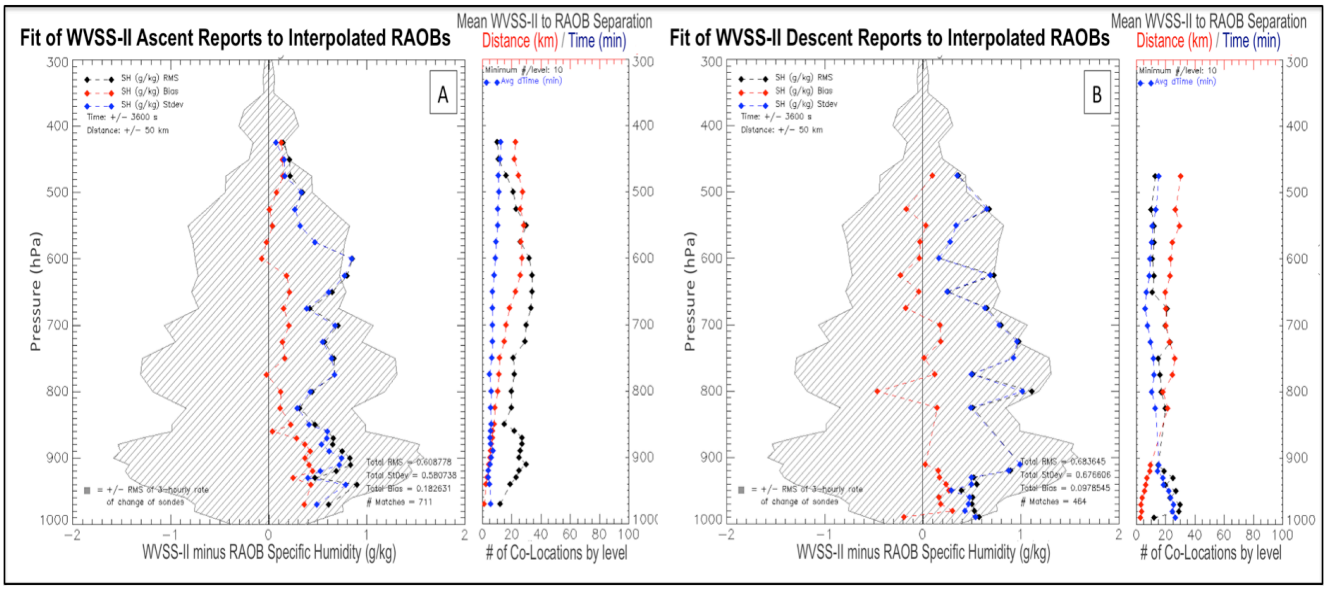

Figure 15: Same as left panel of Fig. 18, except for ascent (a) and descent (b) aircraft data. Fit statistics included in lower right of each panel indicate a bias of 0.18 g/kg and StDev of 0.61 g/kg for 711 reports made during ascent and a bias of 0.1 g/kg and a StDev of 0.68 g/kg for reports made during descent.

effects, is available in Zhu et al. 2015.) By contrast, random variability between the aircraft and RAOB T observations remained fairly uniform, averaging slightly below 0.84°C across all levels.

When the independent aircraft T and SH observations are combined to derive RH, the warm bias in the aircraft T compensates for the small moist bias in the aircraft SH data, producing a RH difference profile with a bias of less than 0.5% throughout the lower troposphere (not shown). These results, however, donot accurately reflect the quality of the WVSS-II data alone. Because aircraft T biases may misrepresent WVSS-II moisture report RH accuracy in a variety of applications, including NWP quality control systems, it is recommended that the WVSS-II SH observations be used in their native form whenever possible.

In order to interpret WVSS-II performance solely in terms of RH, the effects of the aircraft T biases were removed by using RAOB T in both the RAOB and WVSS-II RH calculations, (Fig. 20b), similar to what was done previously using METAR data. Overall, RH biases are approximately 1.8% too moist and StDevs are approximately 10.6%. Although the random differences between WVSS-II and RAOB observations in the lowest 200 hPa were generally between 4 and 6%, RH StDev values in colder environments above 700 hPa (where saturation SH is lower) reached as high as 15%.

Statistical Assessment amongst AMDAR moisture observations from multiple aircraft: Another measure of the robustness of the WVSS-II observations was obtained by inter-comparing reports made between pairs of WVSS-II aircraft within specific time, height and spatial intervals. This approach provides information about the consistency between WVSS-II observations that is independent of possible errors in RAOB moisture reports. Although overall WVSS-II system biases cannot be determined this way, the results provide additional information about atmospheric temporal and spatial variability that could be important in determining how best to use moisture data in future storm-scale forecast models. For this exercise, all pairs of AMDAR observations used in the RAOB inter-comparisons that fell within 50 m of each other in the vertical during 2009-2010 WVSS-II evaluations were used without vertical interpolation. The nearly 4000 data pairs found at and below 5 km altitude were then sorted into a 15-minute time and 15-km distance bins for separation ranges of up to one hour and 60 km.

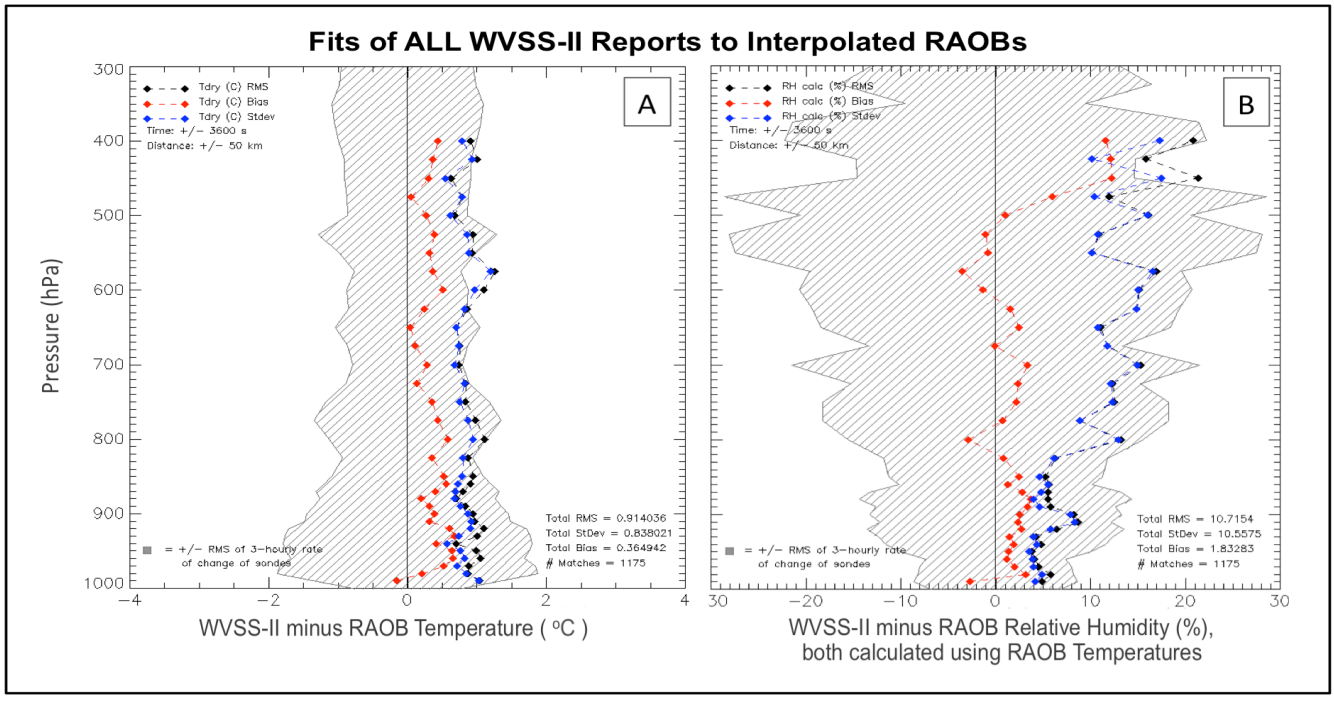

Figure 20: A - Same as left panel of Fig. 18, but for T (°C). T bias of 0.36°C and StDev of 0.84°C using 1175 observation matches. B - Same as Panel A, except for RH calculated from aircraft SH and RAOB T. RH bias of 1.8% and StDev of 10.7%.

Figure 21 shows that the RMS fit of WVSS-II observations made within 60 km of each other improves from about 0.42 g/kg for observations with 45-60 minute separation times to 0.18 g/kg for time differences less than 15 minutes. Likewise, the fits of all observations within 1 hour of each other improves from about 0.47 g/kg to 0.22 g/kg as separation distance between aircraft decreases from 45-60 km to 0-15 km. In both cases, the variability between observations at the shortest ranges is between two and three times less than at the largest intervals, due in part to variations in atmospheric representativeness over the different time and length scales. Projecting these results to simulate perfect co-locations (zero distance and time separations), the observation fits would be within 0.17 g/kg. These differences are several times smaller than those between WVSS-II observations and individual RAOBs using the same time separation intervals, suggesting that errors in the RAOB moisture measurements may be contributing a larger component to the RAOB-to-WVSS-II comparison statistics than the WVSS-II observation errors.

These results, combined with the previously discussed RAOB inter-comparisons, confirm both that WVSS-II observations meet international measurement quality criteria and suggest that they could be considered as a potential new observational comparison standard for a variety of meteorological and climate applications. Further comparisons amongst operational WVSS-II observations could provide a readily available means of understanding moisture variability in different locations, seasons and weather regimes that should be helpful in improving the utility of these high-resolution point observations in the future data assimilation systems of many scales.

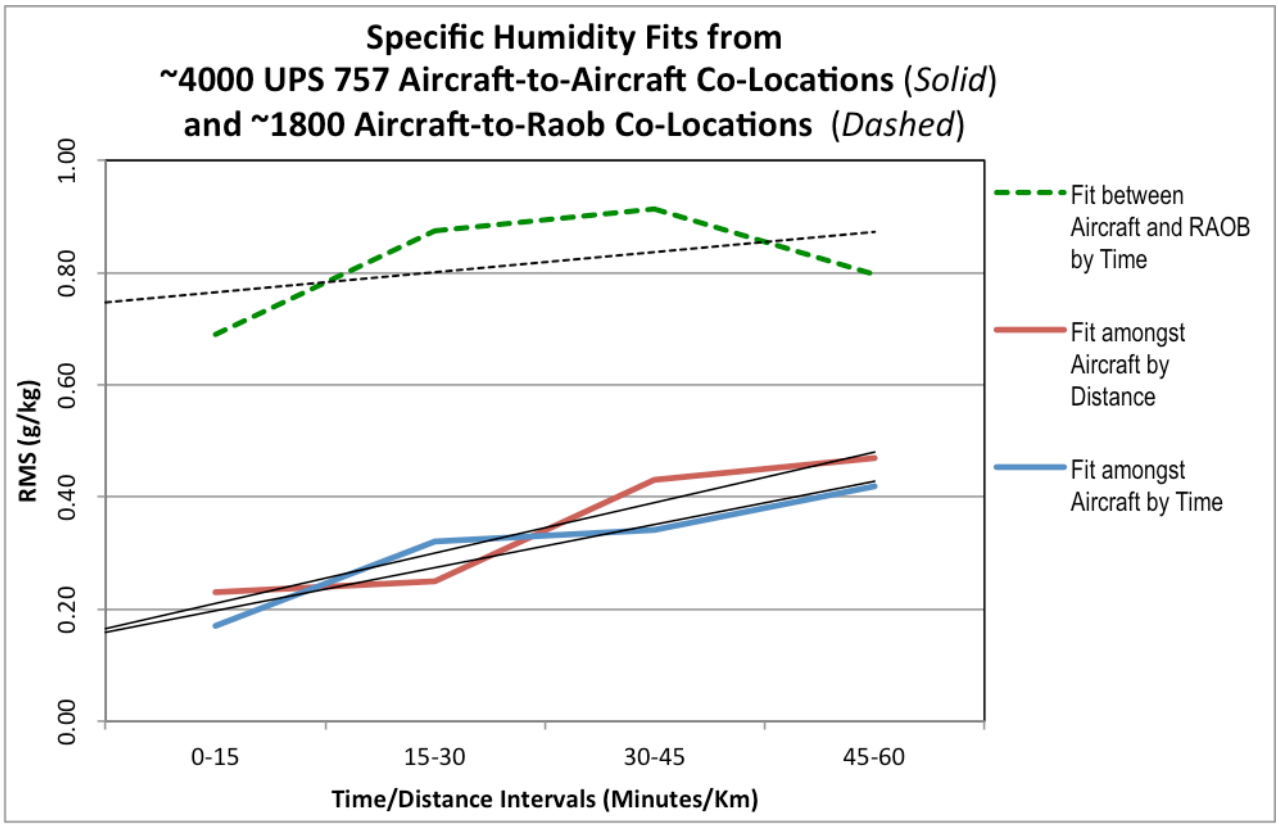

Figure 21: Solid lines show variability (RMS) between SH observations amongst nearby WVSS-II observations made by 15 UPS Boeing 757 aircraft sorted by separation distance (red) and time difference (blue) intervals for all levels from the surface to 5km from six weeks in 3 seasons of 2009-2012. Vertical axis shows RMS differences in g/kg and horizontal axis shows 15-km distance and 15-minute time co-location bins. Thin lines indicate linear fits to observed differences, including projections to fits for perfect co-locations. Dashed green line shows differences between WVSS-II and RAOB SH observations as a function of time differences.

Impacts of aircraft moisture observations on local forecasting: An original justification for the participation of UPS in evaluations of the WVSS-II systems was the need to provide airline forecasters with observations needed for improving predictions of a variety of weather events that have negative impacts on the overnight operations of the airline. Use of the asynoptic aircraft moisture profiles (defined as observations taken at irregular periods throughout the day/night rather than at pre-specified times) has since spread to a growing number of forecast offices (Baker et al. 2011). The following short examples illustrate how local forecasters across the US incorporate AMDAR observations of all three meteorological parameters (temperature, moisture and winds) into their daily operations as a means of monitoring and improving upon standard observations and NWP guidance.

Precipitation Type Forecasts: This case from the afternoon and evening of December 21, 2013 illustrates how WVSS-II observations at 2000 UTC were used to improve the local forecast of sleet for the evening before the busy Christmas travel weekend. Meteorologists at the National Weather Service Chicago office use WVSS-II data to support aviation forecasts for O'Hare (ORD) and Midway (MDW) airports. The data are especially important here, as the nearest twice-daily RAOB soundings are more than 200 km distant.

NWP guidance from 1200 UTC showed a storm system approaching from the Plains was bringing in mild air around 1 km above the ground, while temperatures at the surface remained near freezing, a condition which can be favorable for formation of sleet and impact airport and flight operations if sufficient moisture was also present. As such, the forecast problem was one of determining if the model guidance was providing accurate depictions of the low-level temperature/moisture structures in the Chicago area. The succession of AMDAR soundings throughout the day showed progressively warmer temperatures than expected, with a 2000 UTC AMDAR descent sounding into MDW (Fig. 22) reporting temperatures at 850 hPa (1.5 km) near +5°C. These reports were both warmer than the models forecast and enough to make sleet unlikely. This is significant in that sleet often requires aircraft de-icing, which is costly and causes delays.

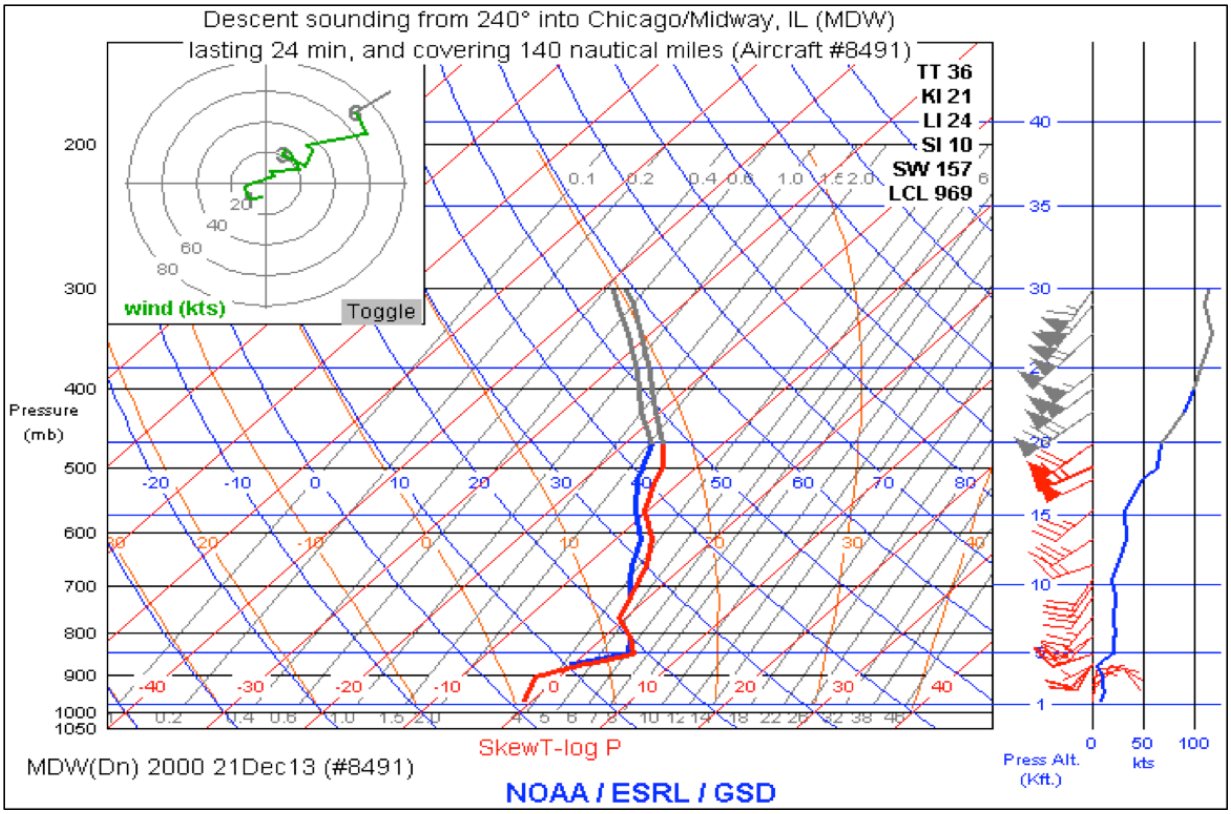

Figure 22: Vertical profiles of temperature, wind and moisture data from AMDAR sounding including WVSS-II reports from aircraft arriving Chicago-Midway Airport (MDW) at 2000 UTC 21 December 2013 showing warm layer between 800 and 875 hPa with a shallow sub-freezing layer below. Plot from NOAA ESRL shows temperature and derived dewpoint profiles on a Skew-T/Log P diagram in large panel, a wind hodograph in the upper left and a variety of stability parameters on the upper right of the diagram and wind plots by level on the right. All winds presented in knots.

Based on these observations, NWS meteorologists correctly modified their 2213 UTC aviation forecast discussion, mentioning the importance of the aircraft soundings in determining the precipitation type of the winter storm. The appended text stated "*Precipitation was moving into the Chicago area this afternoon…mainly in the form of rain/freezing rain*" and included "*Recent aircraft soundings from Chicago-Midway, IL (MDW) and Rockford, IL (RFD) depict warming aloft…with temperatures ranging from around +3°C at RFD to +4/5°C over MDW. This is warmer than most of the model guidance has depicted…which indicates a reduced potential for sleet.*"

Ceiling and Visibility Forecasts: Moisture availability and stratification are important factors for forecasting the formation, maintenance and dissipation of low cloud layers. This case illustrates how frequent WVSS-II soundings from Houston Hobby Airport (HOU) allowed meteorologists to monitor changes in atmospheric water vapor structures over time and update/improve local forecasts. Cloud layer forecasts of 2,000 feet or lower are important to aviation as they require some users to file for alternate airports and carry the additional fuel needed to fly to that airport.

The proximity of Houston to moisture from the Gulf of Mexico results in frequent low cloudiness that can affect air traffic into the busy hub airport by reducing ceiling and visibility below critical operational minima. On the evening of May 21, 2014, a problem facing the night shift forecaster was to determine if low-level moisture would be as pronounced as during the past few evenings (not shown), as was indicated by NWP guidance (not shown).

Several AMDAR soundings were available throughout the afternoon and evening (e.g., Fig. 23). WVSS-II humidity profiles indicated that moisture between 0.5 and 1 km above ground level was both less abundant than the past few evenings and also smaller than indicated by the most recent numerical guidance. The persistent lack of lower-level moisture in the AMDAR soundings provided sufficient information to allow aviation forecasters to modify the 0618 UTC 22 May 2014 aviation forecast discussion to state: "*VFR will slowly turn to MVFR conditions tonight into tomorrow morning. AMDAR soundings show slightly less moisture this evening than at this time yesterday. GFS and NAM forecast soundings both support IFR and MVFR conditions tomorrow morning, but given AMDAR soundings and some possible dry air working its way around the*

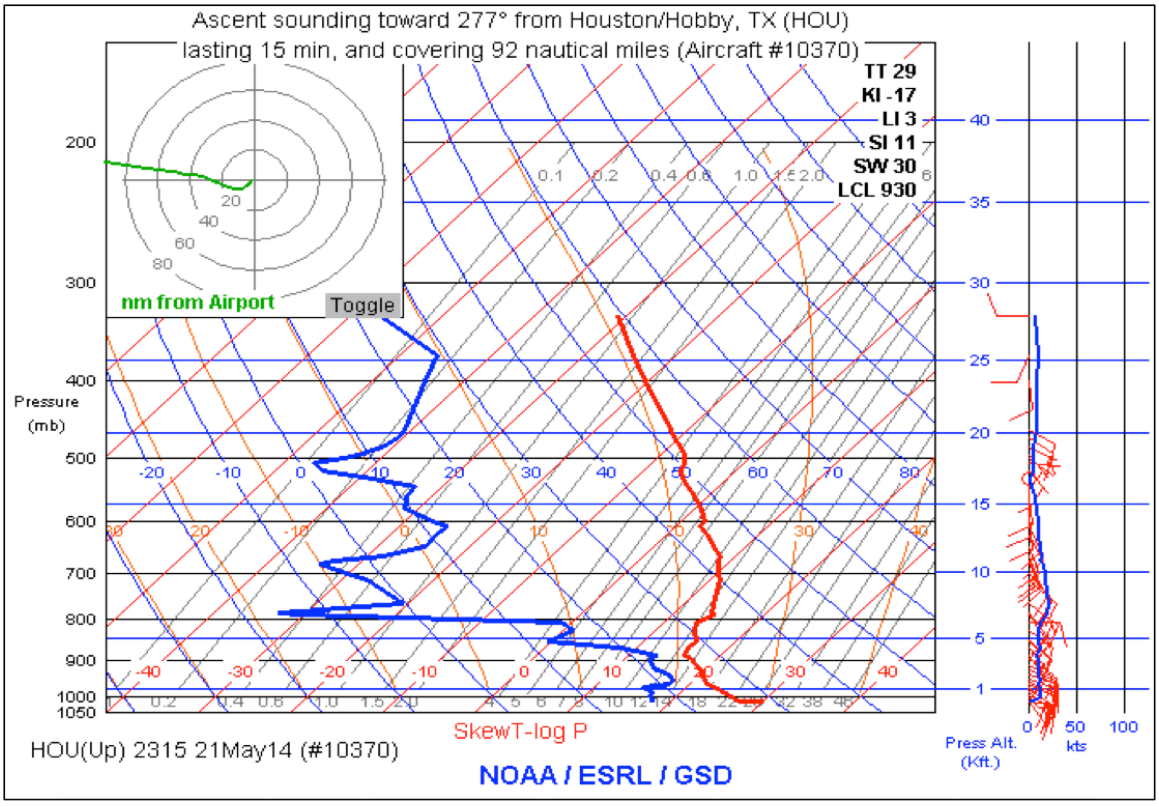

Figure 23: Same as Fig. 22, except from aircraft departing Houston Hobby Airport (HOU) at 2315UTC 21 May 2014.

ridge, (we) think clouds will remain more scattered. TAF sites will likely go between VFR and MVFR though the night until the sun rises, which will help the CIGS rise."

The forecast allowed the airport to operate without concern of delays for either commercial or general aviation. Surface observations (Fig. 24) verify the changes made to the forecast, with clouds remaining few or scattered below 2500 ft for all but a single hour throughout the night and busy morning flight period.

```
KHOU 220553Z 15005KT 10SM FEW019 22/21 A300
KHOU 220653Z 15003KT 10SM FEW019 22/21 A3009
KHOU 220753Z 00000KT 10SM FEW019 22/21 A3008
KHOU 220853Z 00000KT 10SM SCT015 BKN023 22/20 A3009
KHOU 220953Z 00000KT 10SM SCT015 BKN025 22/21 A3008
KHOU 221003Z 00000KT 10SM SCT013 SCT021 22/20 A3008
KHOU 221053Z 00000KT 10SM SCT013 SCT024 22/21 A3009
KHOU 221153Z 00000KT 10SM SCT020 SCT250 22/21 A3010
```

Figure 24: Surface METAR observations from Houston Hobby Airport (HOU) from the morning hours of May 22, 2014. Low cloud observations highlighted.

Fog Forecasting and NWP Validation: For decades, forecasters have used the process described by Petterssen (1956) for forecasting the onset, intensity and dissipation of fog based on a vertical structure in which moisture increases with height below a near-surface inversion, with light winds and clear skies. In many situations, however, the needed vertical profiles of temperature and moisture are not available due to the lack of local and/or real-time RAOBs. AMDAR observations including moisture profiles have helped fill this data gap in many different cases across the country.

For example, on 29 March 2005, UPS meteorologists forecasting for operations at their important Louisville airport hub (SDF) were faced with the problem of determining whether the NWP guidance showing dry advection near the surface until about 0400 UTC, followed by decoupling and possible local fog formation after 0700 UTC, would be applicable at the airport or need to be modified. A series of aircraft descent profiles were investigated (Fig. 25). The first descent report at 0425 UTC (dark blue profile in Fig.25) confirmed the model forecasts of a sharp decrease in moisture with height. Furthermore, a 3°C inversion was capped by winds of nearly 10 m/s, indicating favorable conditions for downward mixing of drier air. Based on these reports, forecasters expected patchy ground fog across the city, but not at SDF airport itself, due to an increased heat island effect there. Subsequent aircraft soundings (later reports in Fig. 25) corroborated the initial profile and confirmed the diagnosis of further localized erosion of the low-level moist layer.

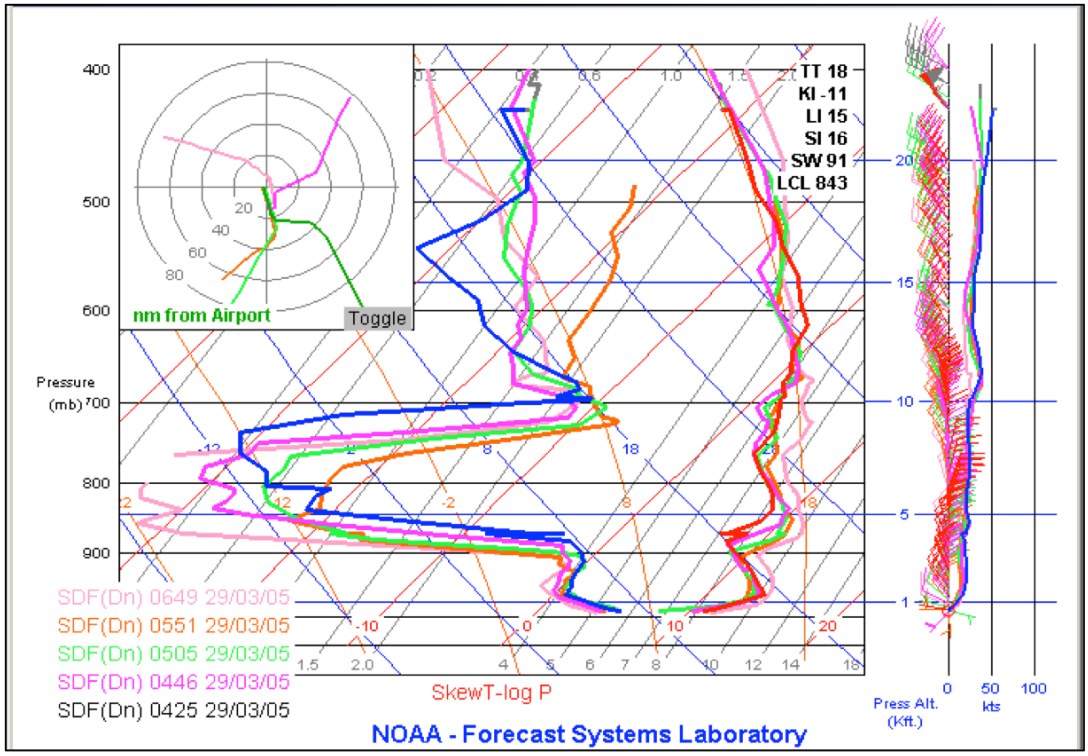

Figure 25: Same as Fig. 22, except from five aircraft arriving at Louisville (KY) International Airport (SDF) between 0425 and 0649 UTC on 29 March 2005. Times of aircraft descents for different noted in lower left.

this case illustrates the important role that AMDAR observations can play in local forecasts. At Louisville Bowman Field (LOU) visibility was reduced to 0.4 km by ground fog later in the evening, extending in patches into low-lying locations across the city and verifying the NWP forecast. However, only 8 km away, the sector visibility at SDF never dropped below 4 km, as indicated by the AMDAR reports that enhanced the NWP guidance there.

Severe Thunderstorm Forecasts: Severe thunderstorm forecasters are often hampered by inadequate knowledge of the temperature, wind field and moisture above the ground. This information is so important that special RAOBs can be launched in the US around 1800 UTC to provide forecasters with added data for the afternoon and evening forecasts. These special launches are costly and are normally reserved for days when organized severe thunderstorms are expected. Forecasters across the US have found AMDAR profiles to be a useful supplemental data source, both for determining the likelihood and strength of severe thunderstorms as well as differentiating between severe and non-severe events.

Such a situation occurred during the midday hours of 29 May 2014. Forecasters in Tulsa, Oklahoma were faced with determining the severity of thunderstorms expected that afternoon. A series of AMDAR soundings were available throughout the day. The combination of temperature, WVSS-II moisture and wind information contained in the AMDAR sounding (e.g., Fig. 26) showed a persistent lack of not only suitable instability and a capping inversion but also insufficient wind shear to support severe thunderstorm development. Using this information, the area forecast discussion was modified to indicate that, although scattered thunderstorms were likely to occur, the chance of severe thunderstorms was very low**,** stating: "*The 1450 UTC AMDAR sounding is not overly favorable for convection…despite being virtually uncapped. Lapse rates from 700 hPa on up are either moist adiabatic or less…with a unidirectional northeast flow thru the column at less than 20 kts. Nevertheless…with insolation ongoing, there will be scattered showers and a few storms, but instability will be limited by the poor lapse rates aloft and there will be virtually no storm relative flow. Thus…severe weather is not expected this afternoon.*"

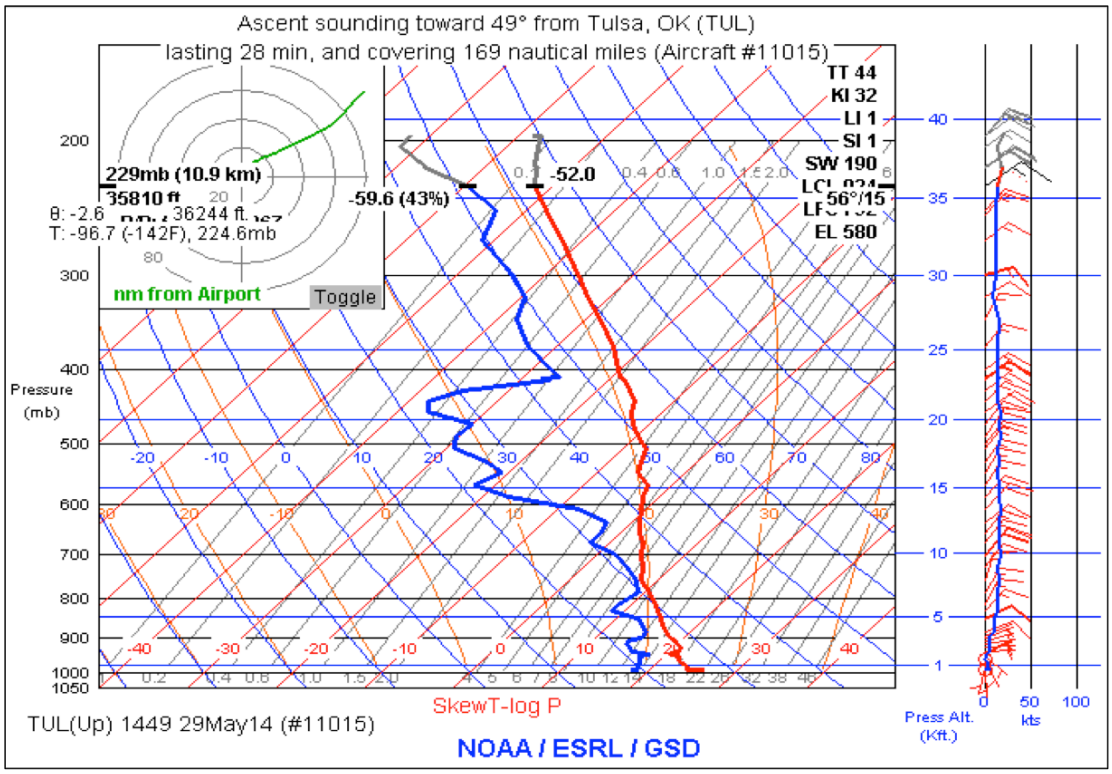

Figure 26: Same as Fig. 22, except from aircraft departing Tulsa International Airport at 1449 UTC 29 May 2014.

Impacts of WVSS-II on NWP models: The recent expansion in the number of AMDAR aircraft providing WVSS-II observations has allowed several NWP centers adequate data to begin conducting impact tests using these spatially and temporally denser moisture observations. Although these tests have been much less extensive than those for AMDAR temperature and wind observations (see Petersen 2015 for discussion and further references), all tests show positive impacts on short-range forecasts over the US. Several efforts by other authors are noteworthy.

Benjamin et al. (2010, 2012 and 2014) have conducted a succession of studies of the combined impact of the full sets of aircraft observations (temperature, wind and, when available, humidity) relative to RAOBs, surface observations, satellite-derived atmospheric motion vector winds and GPS-Met Total Column Precipitable Water data. Figure 27 synthesizes the results of a chain of data denial experiments designed to determine the effect of individually removing different data sources on 3-, 6- and 9-hour forecasts from the Rapid Update Cycle (RUC) and Rapid Refresh (RAP) models over the US. Between these tests, the number of available aircraft humidity reports increased progressively, starting with a limited number of TAMDAR moisture observations concentrated primarily near the Great Lakes in 2006 (see Moninger et al 2010 for details), increasing to include WVSS-II reports from up to 60 aircraft available to provide WVSS-II observations across CONUS in 2011 and reaching approximately 90 WVSS-II-equipped aircraft in 2013.

Although it is difficult to separate effects of improvements in the forecast models and associated data assimilation systems from influences due to changes in the input data used in these tests, a subjective review of trends in the results is useful. While RAOBs were the most important contributor to improving humidity forecasts using data from 2006, by 2011, AMDAR observations had become the most important data set by a slight margin. By 2013, the impact of the full set of AMDAR reports was more than four times that of any other regional data source, including balloon-based RAOBs. The increase in influence of AMDAR reports between the last two test periods was greater for RH than T or Wind (not shown) and coincided with an expansion in the available WVSS-II reports. The importance of the AMDAR data was greater for shorter forecast periods (not shown), when AMDAR observations provide the only source of upper-atmospheric data, including moisture observations.

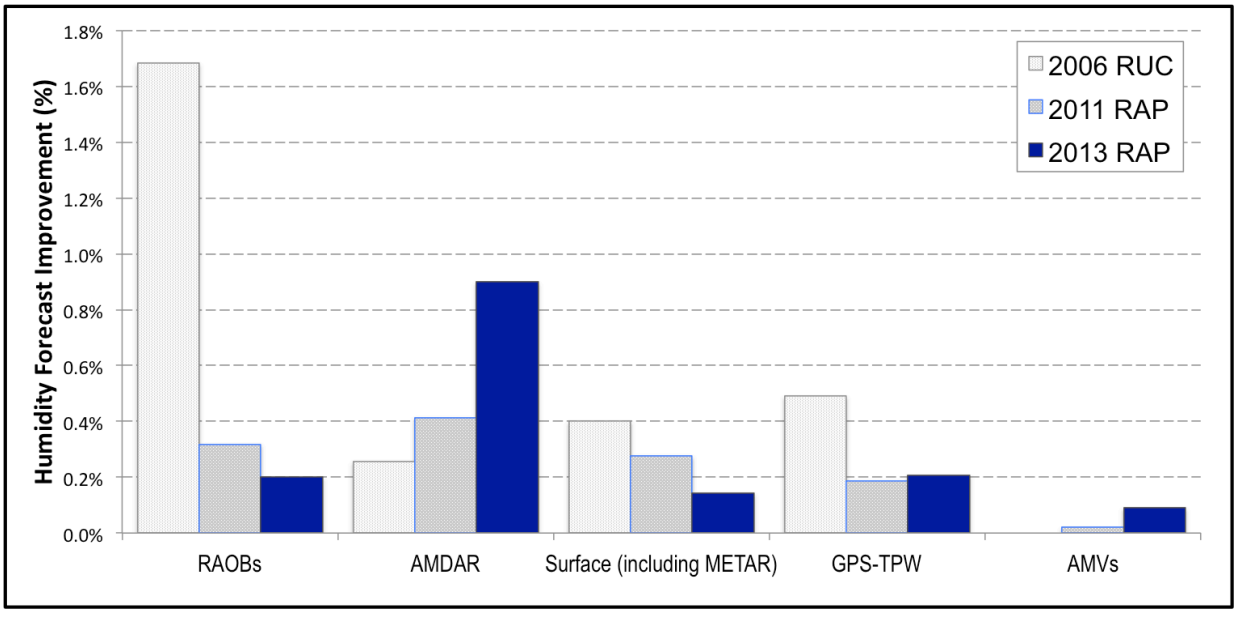

Figure 27: Impact of five major data sources averaged over 3-, 6- and 9-h RH (%) forecasts from the Rapid Update Cycle (RUC) and two versions of the Rapid Refresh (RAP) model over the US. Impact measured by the difference between forecasts using all data sets and those in which all types of observations provided by each data source were removed. Data sources included RAOBs, all forms of automated aircraft (labeled AMDAR), surface reports (including hourly METAR observations), surface-based GPS Total Precipitable Water measurements (GPS-TPW) and satellite-based Atmospheric Motion Vector winds (AMVs). (Data derived from Benjamin et al. 2010, Benjamin et al. 2012 and Benjamin et al. 2014 using data from multiple-week periods in warm seasons during 2006, 2012 and 2013.)

Recent tests by Pauley et al. 2014 and Pauley and Baker 2014 using the Navy Global Environmental Model (NAVGEM) provide more specific insight into the value of AMDAR moisture observations. Tests of forecast sensitivity to observations (FSO, Langland and Baker 2004) were conducted on the 1- to 2-day forecast from mid-April to mid-May 2013 and evaluated both globally and regionally. In areas of plentiful aircraft moisture observations, the collection of AMDAR WVSS-II profiles available throughout the day over the US had double the impact of the twice-daily, and more costly RAOBs (Fig. 28). Data taken during ascent were more numerous and had slight larger impact per observations than descent reports. Improvements were noted in both the timing and location of precipitation forecasts, factors that impact multiple forecast problems. These preliminary results signal that aircraft-based WVSS-II observations could become a primary source of upper-air moisture observations over the US for very-short-range NWP. Increased impacts are anticipated as the network of WVSS-II equipped aircraft expands further. On the global scale, however, results (not shown) indicated that balloon-borne observations will continue to be the primary source of moisture globally until a broader international WVSS-II network becomes available elsewhere, followed by surface weather observations, including hourly METAR and ship reports.

Comparisons of moisture transport observations obtained from RAOBs and AMDAR are shown in Appendix F. Though not discussed here, these dynamical-important derived have been shown to be critical for improving NWP precipitation forecasts.

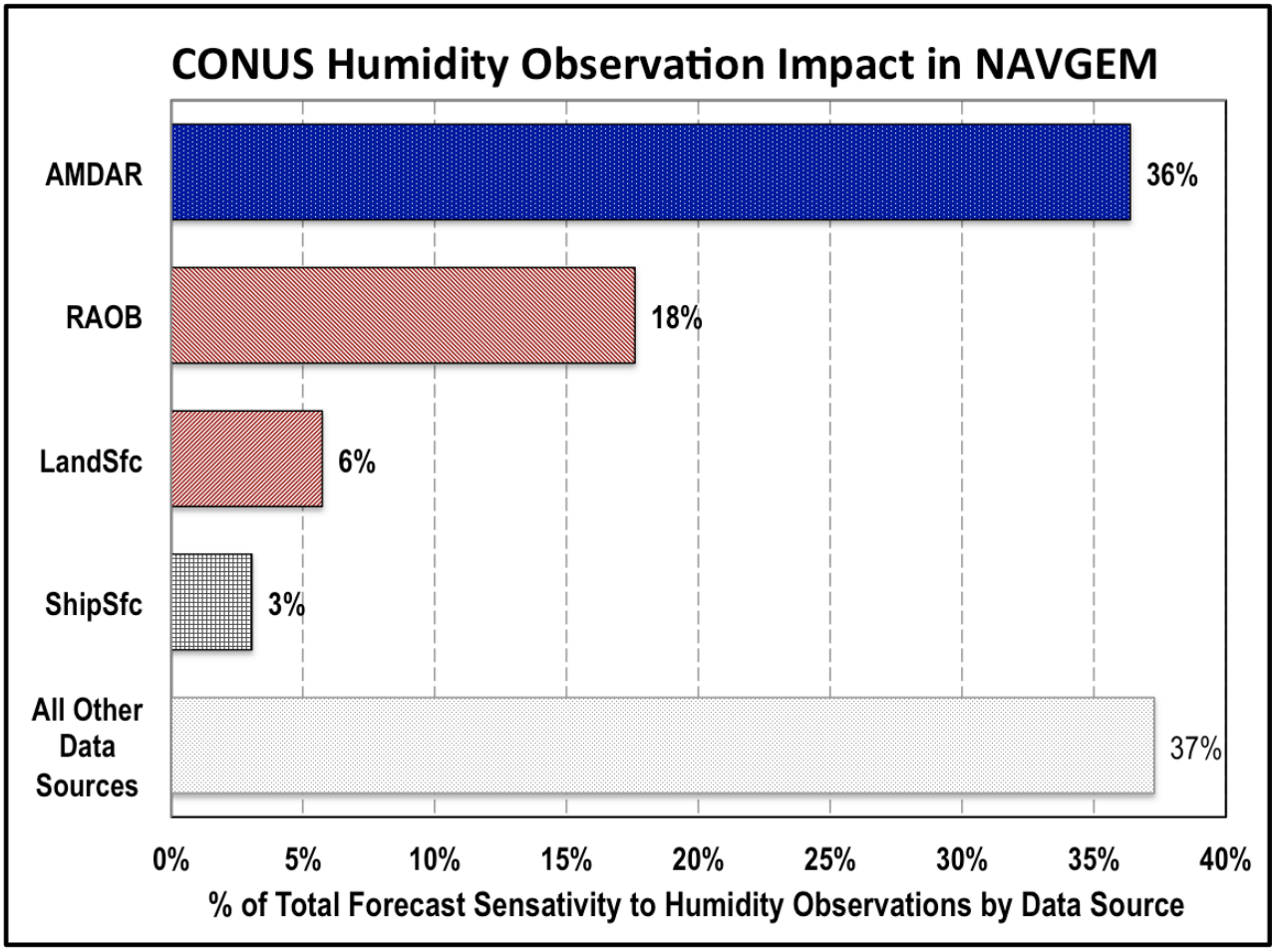

Figure 28: Relative Forecast Sensitivity to Observations over the CONUS in the Navy Global Environmental Model (NAVGEM) of humidity data from different data sources for a 4-week period from mid-April to mid-May 2013. (Based on date provided from Pauley et al. 2014 and Pauley and Baker 2014.)

Summary of AMDAR Water Vapor Observation Assessments: Tests conducted by numerous NWP centers over the past decade have concentrated on assessing the impact of AMDAR temperature and wind observations on the skill of regional and global NWP systems. Results show that aircraft data taken en-route and during ascent/descent provide important information for improving forecasts, both for individual events and for long-term performance. These tests, however, did not take into account the additional improvements that can occur from the new moisture observing systems being deployed as part of the global AMDAR enhancement effort.

Evaluations of new WVSS-II moisture observing systems being deployed on aircraft in the US show that WVSS-II observations:

1) Provide excellent quality horizontally and vertically, even across sharp inversions,
2) Agree with co-located RAOBs to within 0.6 g/kg, with minimal biases (approximately 0.15 g/kg), and
3) Display consistency between observations from different aircraft of at least 0.2 g/kg, indicating that WVSS-II observations perform as well as high-quality RAOBs.

Forecasters have been able to readily incorporate WVSS-II reports (along with AMDAR temperature and wind profiles) into their forecasting process. The availability of the data throughout the day has proven valuable in improving local, short-range forecasts of a number of high-impact weather phenomena, ranging from forecasts of fog and ceiling height to determining precipitation type and improving severe weather outlooks. Finally, a review of initial NWP impact studies shows that WVSS-II reports obtained throughout the day have greater influence than twice-daily RAOBs on 1-2 day forecasts over the US.

The volume of WVSS-II data available over the US has recently grown to a level that can support initial data impact tests in NWP models. Initial results using SH observations from the expanded fleet of WVSS-II equipped aircraft over the US have shown short-range forecast impacts larger than from any other moisture observations, including twice-daily RAOBs. Humidity forecast improvements like these are essential to enhance prediction of both the timing and location of precipitation events.

Economic Aspects of AMDAR Temperature and Wind Observations: Although the lack of sufficient AMDAR moisture observations has limited assessments of the economic value of these newly arriving data sets, Eyre and Reid (2014) have introduced an approach to obtain needed information about the cost effectiveness of the temperature and wind AMDAR observations relative to all other data sources used in global NWP systems. They first showed the impact of each of the individual data systems available for real-time application in 2013 using the UK Met Office Global analysis and forecastmodel assimilation and forecast system. Results indicate that the largest global forecast improvements are due to Microwave (μ-wave) and Hyperspectral Infra-Red (H-IR) observations from multiple (4 or more) polar-orbiting satellites, as shown by the gray bars in the left side of Fig. 29.

Other analyses have also shown that increasing the amount of satellite data increases their impacts at least linearly. The remaining members of the five highest impact data sets have similar magnitudes and include rawinsonde reports and two other aviation-related observing systems, SYNOP+METAR surface observations and AMDAR+AIREP aircraft reports.

When estimates of the costs of each observing system are included to approximate which observations have the largest impact per unit cost, the rankings change. (*It must be noted that, because of large uncertainties in the costs for many of the observing systems, readers should be careful not to draw quantitative conclusions about all systems.*) As shown in the right side of Fig. 29, by far the two most cost effective observing systems are AMDAR/AIREP and Drifting Buoys, with the aircraft reports having approximately five times more impact than the bouy data.

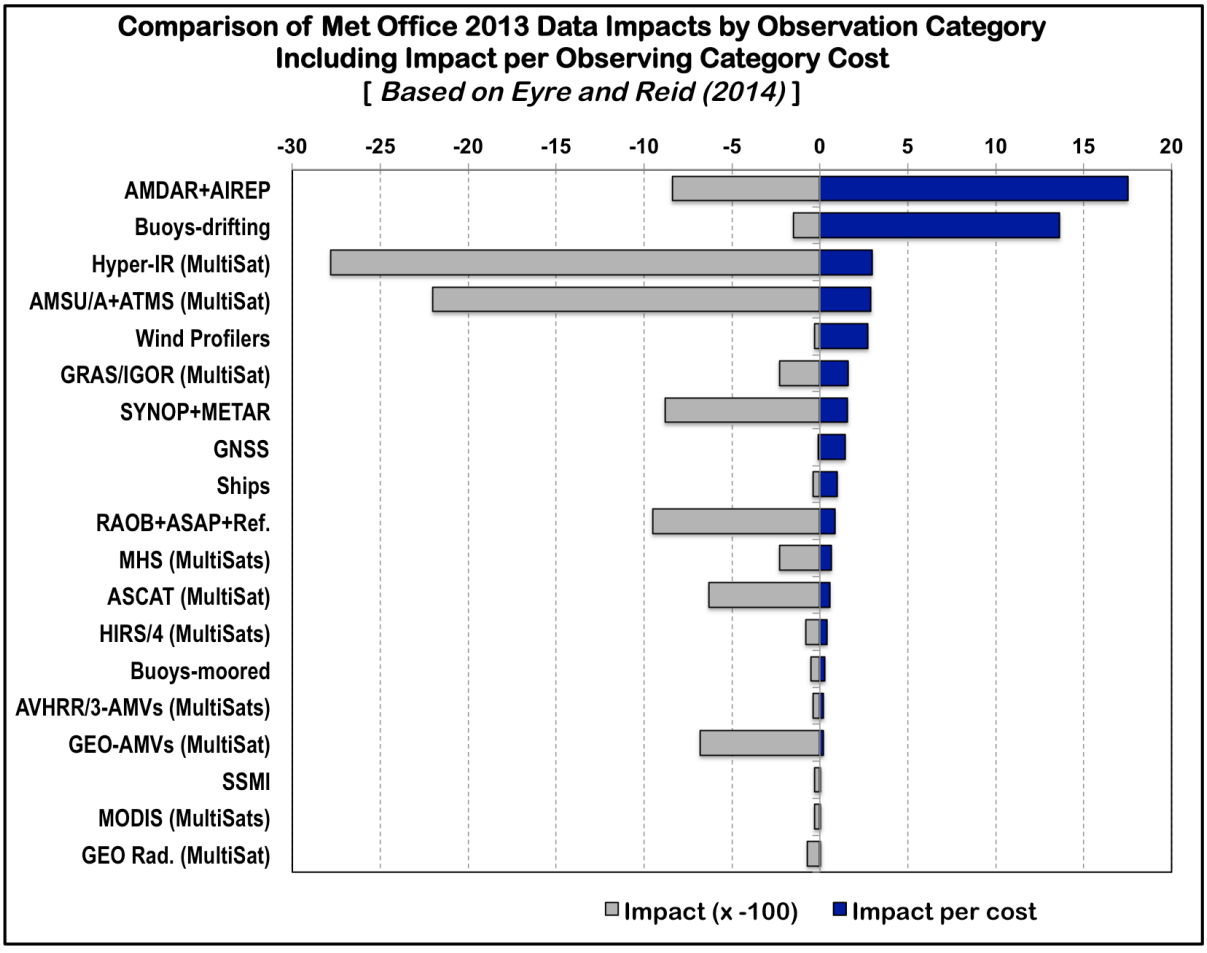

Figure 29: Left: Impacts of various observing systems using in UK Met Office Global model on 24 hour forecast skill (indicated by gray bars on left of figure with longest bars indicating greatest importance). Right: Approximate measure of Cost Effectiveness of each observing system calculated as Impact per unit Cost. Data sorted by observing systems with largest Impacts per unit Cost (i.e., most cost effective) at top. [Derived from Eyre and Reid (2014). Note that, because of large uncertainties in the costs for many of the observing systems, readers should be careful not to draw quantitative conclusions about all systems shown.]

Confidence in the relative rankings of these two systems was quite high, despite the uncertainties in the precise costs estimates used in the study. For reference, AMDAR/AIREP observations have an annual cost globally on the order of $6-8M (about 1/400th of the annual cost of the total GOS).

Of the five highest-impact systems, all others appear to be less cost effective than AMDAR observations and contribute substantially larger portions of the total GOS costs that can be attributable to NWP use, with RAOBs appearing to be the least economically effective.

Based on results shown earlier in this paper and findings from multiple previous studies that varied the amounts of satellite data available to NWP systems, it is anticipated that increasing the spatial coverage of AMDAR reports will further enhance their impact and continue to improve the quality of operational NWP products used by the general public and aviation community, including terminal and en-route forecasts. Even in the unlikely scenario that there would be no change in impact, a doubling of the current number of AMDAR reports would still leave the observations nearly three times more cost effective than any other observing system. Although an amalgam of many different data sets is essential for sustaining improvements in NWP into the future, AMDAR data are the most cost-effective of any global data set and one that can be expanded quickly and easily, making them particularly attractive for use in areas where RAOB availability may be in jeopardy. In particular, expansion of automated aircraft reporting systems may offer a highly cost effective means of improving local aviation services, as well as short- and medium-range weather prediction, for regions such as Africa and South America, as well as outlying areas, such as Pacific Islands and data sparse, high-latitude areas such as Alaska and Russia.

Summary and Recommendations: The long-term, consistently positive impacts of automated aircraft reports on regional and global operational NWP presented here provide ample evidence that the collaborative effort between airlines and National Meteorological Services to improve access to and use of automated wind and temperature reports has benefited both the data providers and other users of the other products issued by NWP centers and forecasters using these data. AMDAR growth has occurred chiefly over developed countries whereas, for developing and least-developed countries, the progress in implementation has lagged and is now well behind. Because improvements attributable to AMDAR observations have been concentrated in areas of highest data availability, greater improvements can be expected in other more data sparse regions as the spatial and temporal coverage of AMDAR reports increases globally. As a means of fostering further AMDAR expansion, cooperative means (including possible cost sharing opportunities) should be developed both to continue expanding the AMDAR observing network into areas not currently covered adequately and to increase the number of aircraft providing data, especially over data sparse regions of the globe. This should include establishing dedicated efforts at regional and global NWP centers to continue evaluation of the impact and cost effectiveness of all observing systems components, with the goal of promoting rapid expansion of those systems that have both high value and low cost.

Although the improvements attributable to AMDAR observations have been concentrated in areas of highest data availability, similar improvements are expected in other areas as the spatial and temporal coverage of the reports increases globally, especially if water vapor measurements are included. This will be particularly important both in areas where the continuation of upper-air observing programs are under budgetary threat and in forecast situations where additional observations are needed to fill the time and space gaps between once- or twice-daily RAOB launches.

Based on these findings, it is recommended that cooperative means, including possible cost-sharing opportunities, be developed simultaneously 1) to expand the AMDAR observing network into areas not currently covered adequately and 2) to increase the number of aircraft providing humidity information.

Both of these recommendations are financially and logistically viable. AMDAR observations are extremely cost effective, currently contributing only about 0.25% of the expense of the global observing system (Eyre and Reid 2014), with temperature/moisture/wind profiles typically costing less than 5% of a full ROAB launch. Because the AMDAR observing system can be attached to commercial aircraft from many airlines that already have well-established air-to-ground communications systems, the systems can be implemented with only minor impact on other operational and engineering resources available at local meteorological services.

It should be recognized that AMDAR reports will not meet all balloon-borne observing requirements (in particular, data in and above the stratosphere needed for both weather and climate purposes). However, the availability of high-quality tropospheric information over land at space and time resolutions not affordable using conventional observing systems offers a unique opportunity for improving weather forecasts across the globe, including terminal and weather hazard forecasts benefiting airlines. Improvements in safety-related forecasts used for aircraft and airspace operations could be enhanced further through incorporation of additional turbulence and icing observations in future AMDAR reports.

Appendix A: Description of AMDAR Data Reporting Processes

Early automated aircraft meteorological observations used a number of formats, as well as different reporting frequencies, spatial density, reporting precisions or phase of flight needed to assess potential wind and temperature errors. As part of the WMO AMDAR effort, standard reporting practices were adopted by the participating airlines and air-to-ground communication centers, as shown schematically in Fig. A-1.

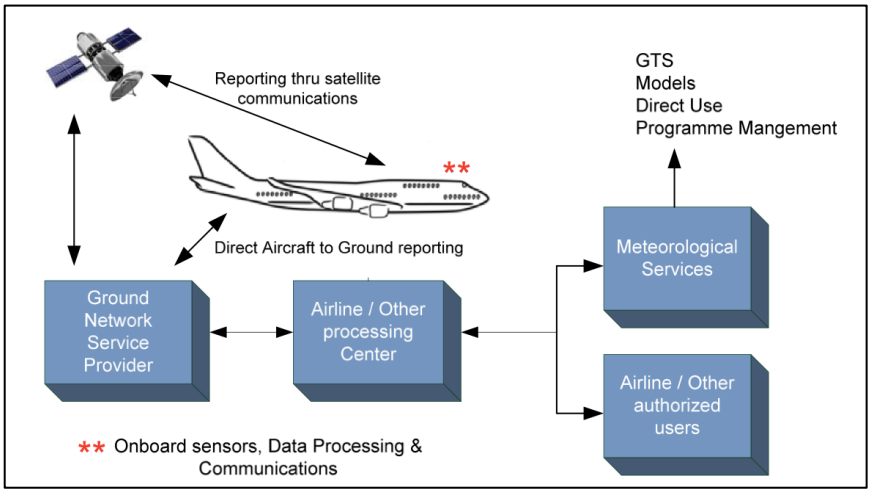

Figure A-1: Schematic of AMDAR data flow from aircraft to end-users. (From WMO 2014b)

Observations of aircraft location, time, phase of flight and altitude, along with the primary temperature and wind observations (as well as moisture, turbulence and other optional variables if available) are made at specific intervals throughout an aircraft's flight. These data are collected onboard the aircraft using specially developed software, stored for a short interval and then transmitted to the ground via radio or satellite as a small addition to normal messages containing information about engine performance, fuel use, etc. using existing digital air-to-ground communications systems. The meteorological portions are then encoded into WMO standard formats and forwarded to operational meteorological services via the WMO Global Telecommunications System (GTS).

A consolidated set of standards for providing AMDAR observations has been recently updated by the WMO (2003a, 2014a). Meteorological variables are reported at different intervals depending on aircraft phase of flight, as shown in Fig. A-2. Increased reporting during takeoff and landing captures thermal structures and shear zones across narrow inversions and fronts. Nominally, reports are obtained or calculated from the highest frequency (typically 1 per second) instantaneous measurements available made closest to the observation time, using minimal smoothing, and subject to established data validation requirements procedures. On occasion, reporting data precisions can exceed the accuracy of the aircraft onboard measurements, resulting in data rounding or truncation.

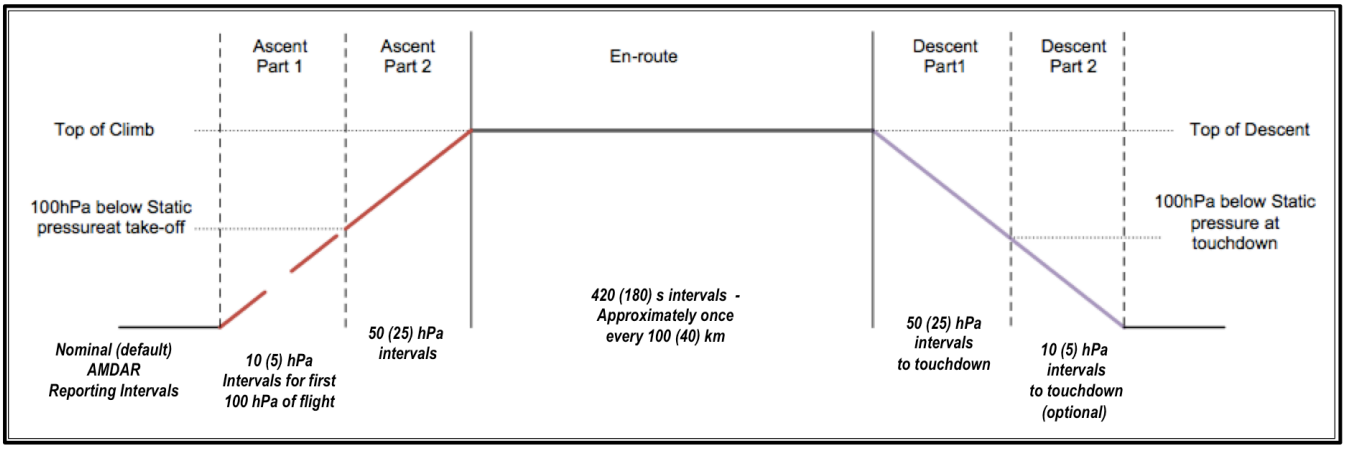

Figure A-2: Phases of flight and associated suggested nominal reporting frequencies of AMDAR observations (Italics, with options in parentheses). Primary variables included in AMDAR reports [with precisions in brackets] include Latitude/Longitude location [0.1 degree], Date/Time [second], Pressure Altitude [10 ft], Temperature [0.1 C], Wind Direction [1 degree], Wind Speed [1 knot], Mixing Ratio [10^6 kg/kg] and Roll Angle [discrete, used for Wind QC]. (Adapted from WMO 2003)

Appendix B: Comparisons of individual RAOB observations with co-located AMDAR reports for entire 2010-2011 test perid.

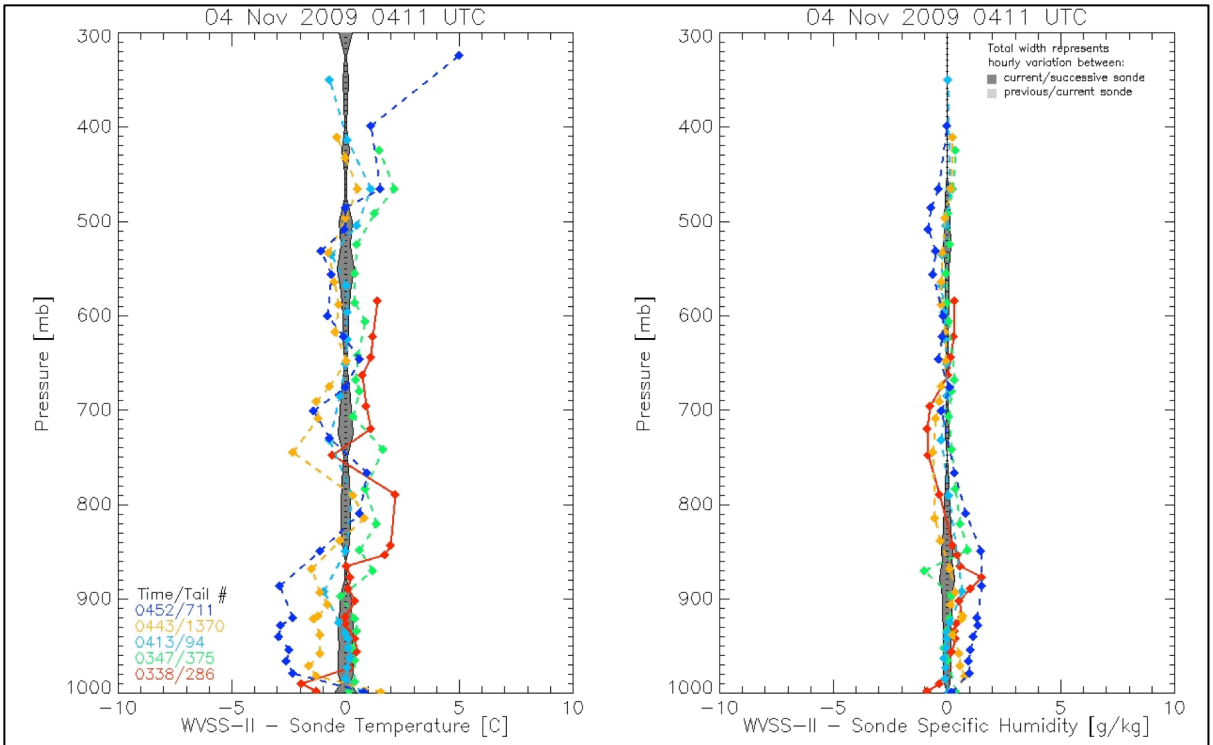

Figure B-1: Differences between RAOB and aircraft temperature and moisture profiles from within one hour of RAOB launch time of 0411 UTC on 04 Nov. 2010 at Rockford Illinois. Gray shaded indicate change between successive RAOB launches

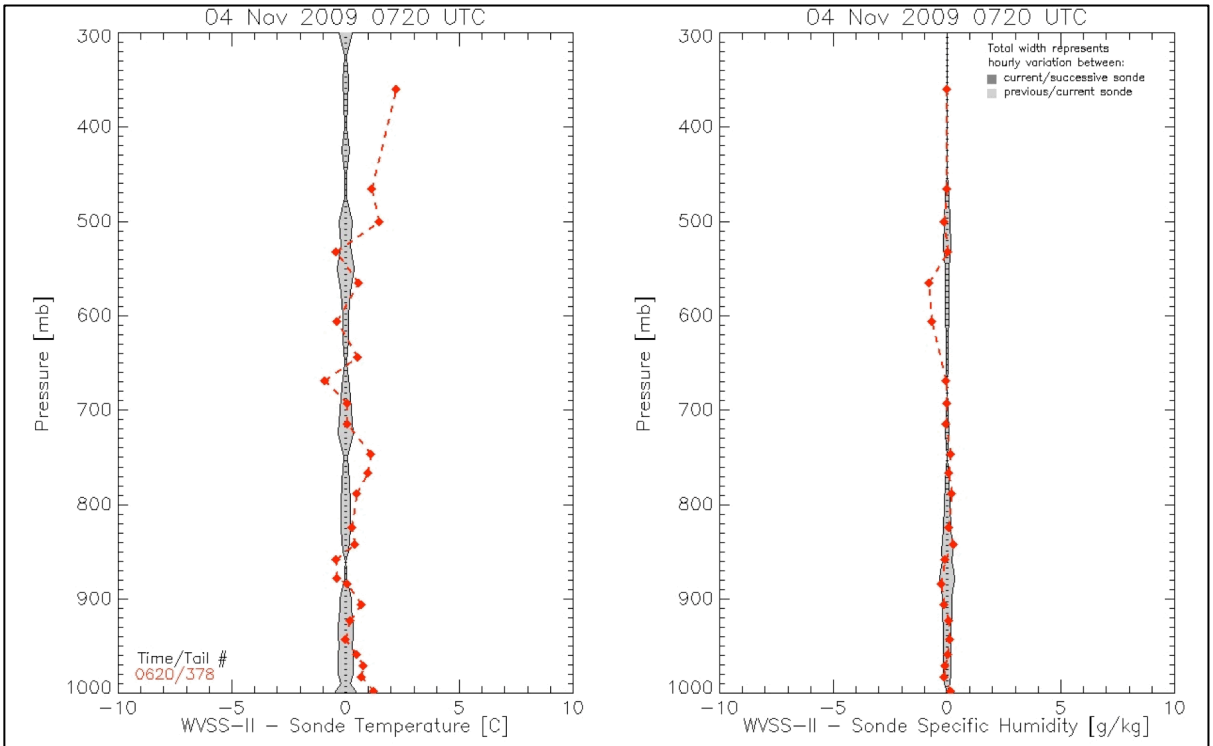

Figure B-2: Differences between RAOB and aircraft temperature and moisture profiles from within one hour of RAOB launch time of 0720 UTC on 04 Nov. 2010 at Rockford Illinois. Gray shaded indicate change between successive RAOB launches

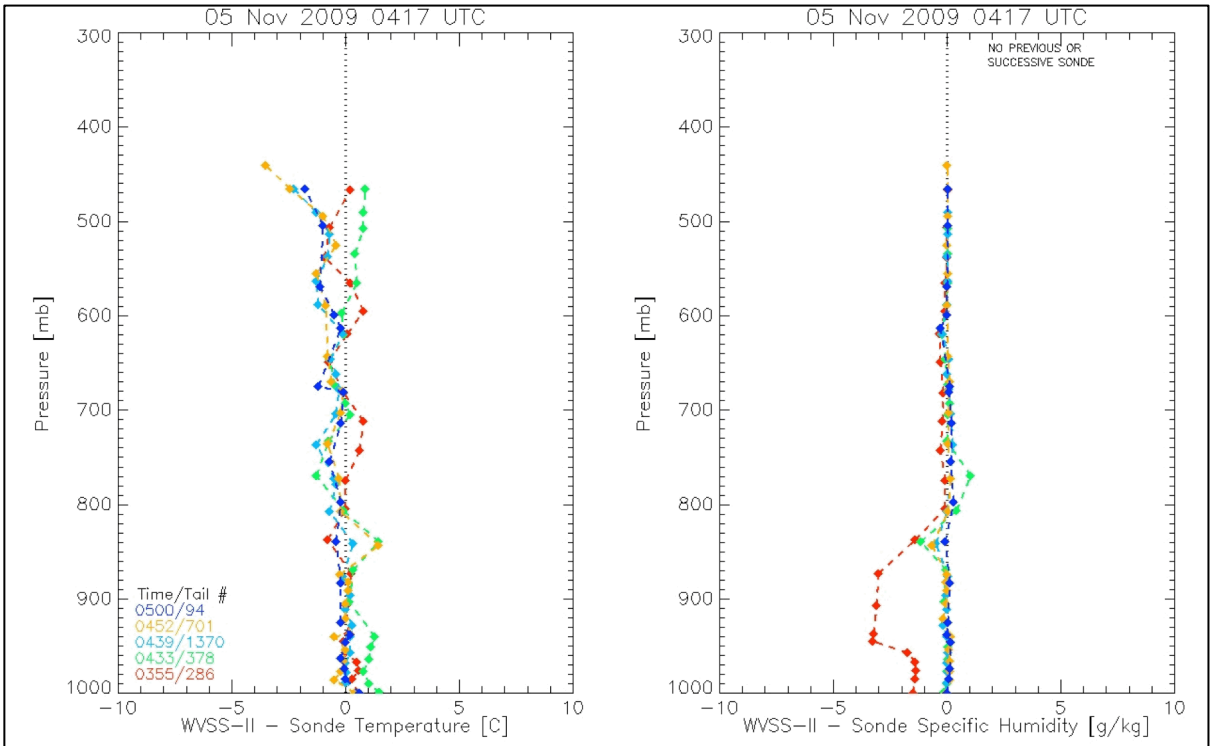

Figure B-3: Differences between RAOB and aircraft temperature and moisture profiles from within one hour of RAOB launch time of 0417 UTC on 05 Nov. 2010 at Rockford Illinois. Gray shaded indicate change between successive RAOB launches

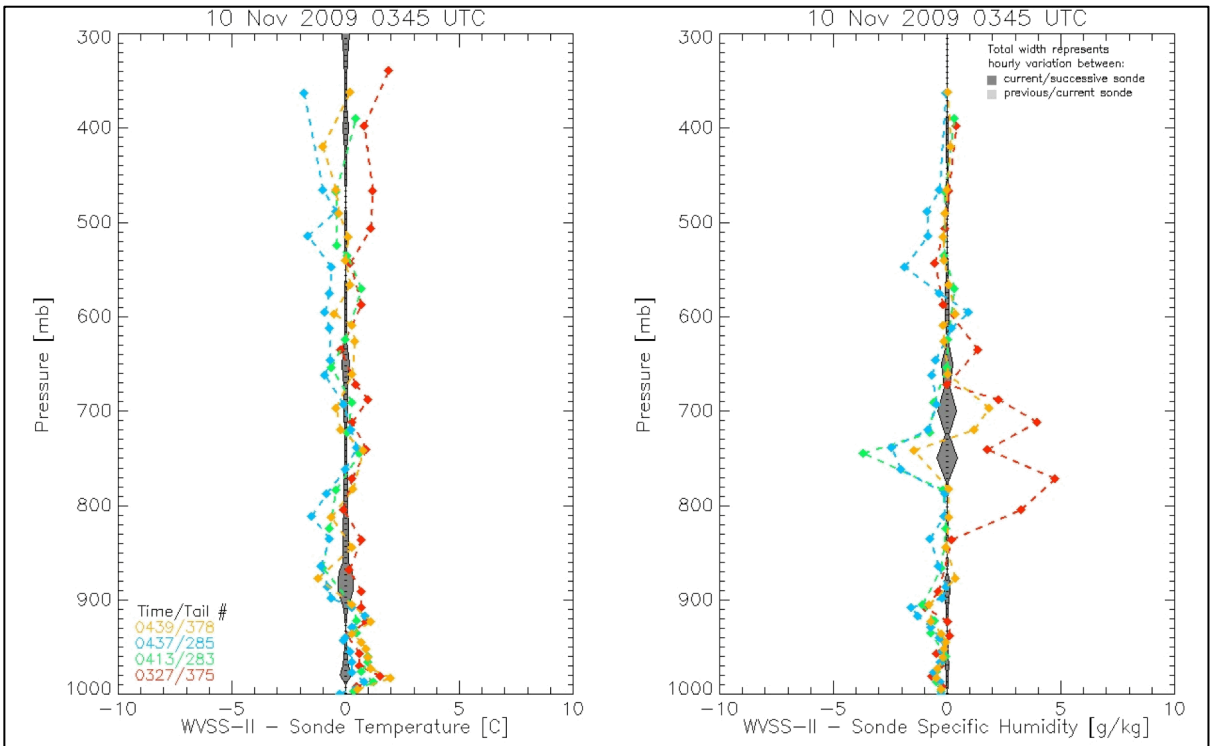

Figure B-4: Differences between RAOB and aircraft temperature and moisture profiles from within one hour of RAOB launch time of 0345 UTC on 05 Nov. 2010 at Rockford Illinois. Gray shaded indicate change between successive RAOB launches

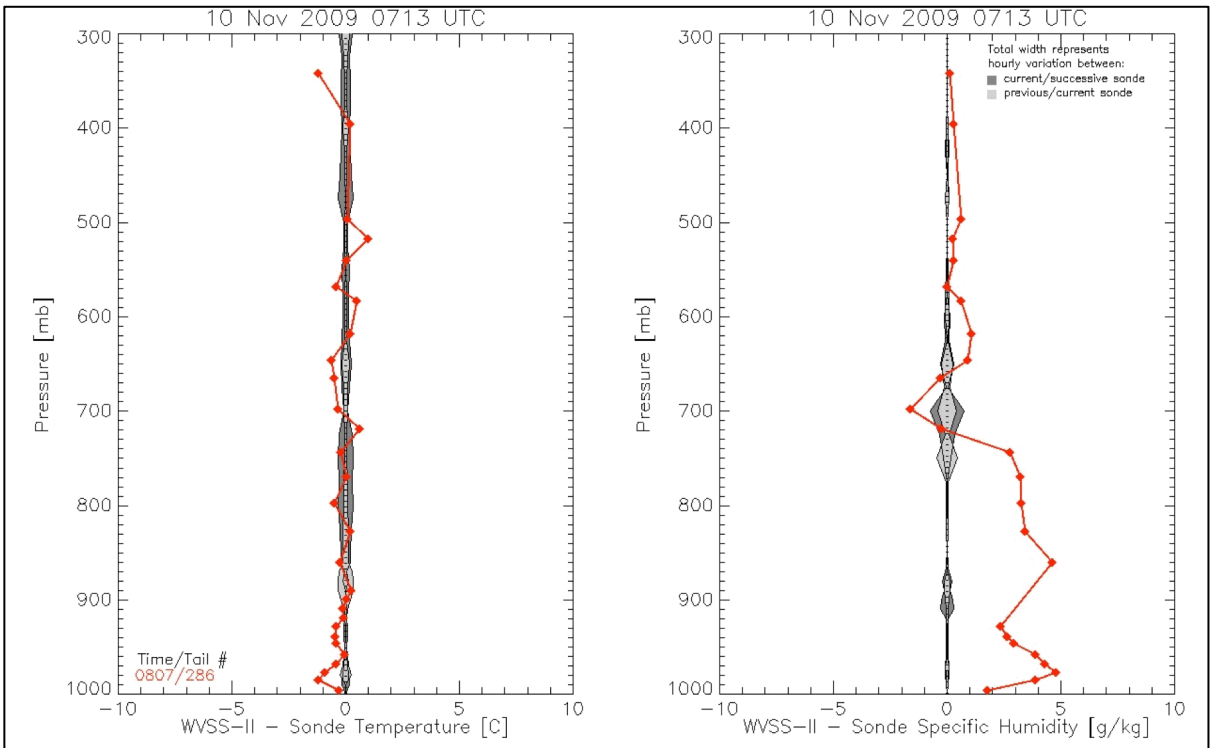

Figure B-5: Differences between RAOB and aircraft temperature and moisture profiles from within one hour of RAOB launch time of 0713 UTC on 10 Nov. 2010 at Rockford Illinois. Gray shaded indicate change between successive RAOB launches

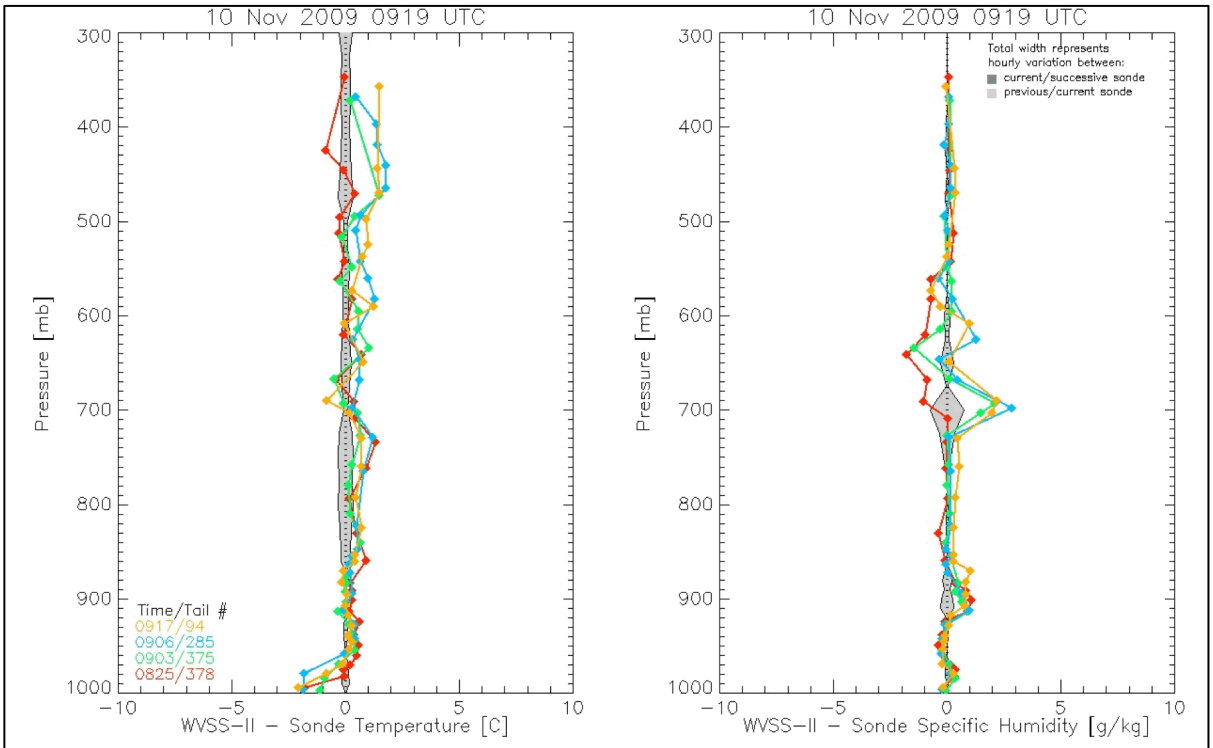

Figure B-6: Differences between RAOB and aircraft temperature and moisture profiles from within one hour of RAOB launch time of 0919 UTC on 10 Nov. 2010 at Rockford Illinois. Gray shaded indicate change between successive RAOB launches

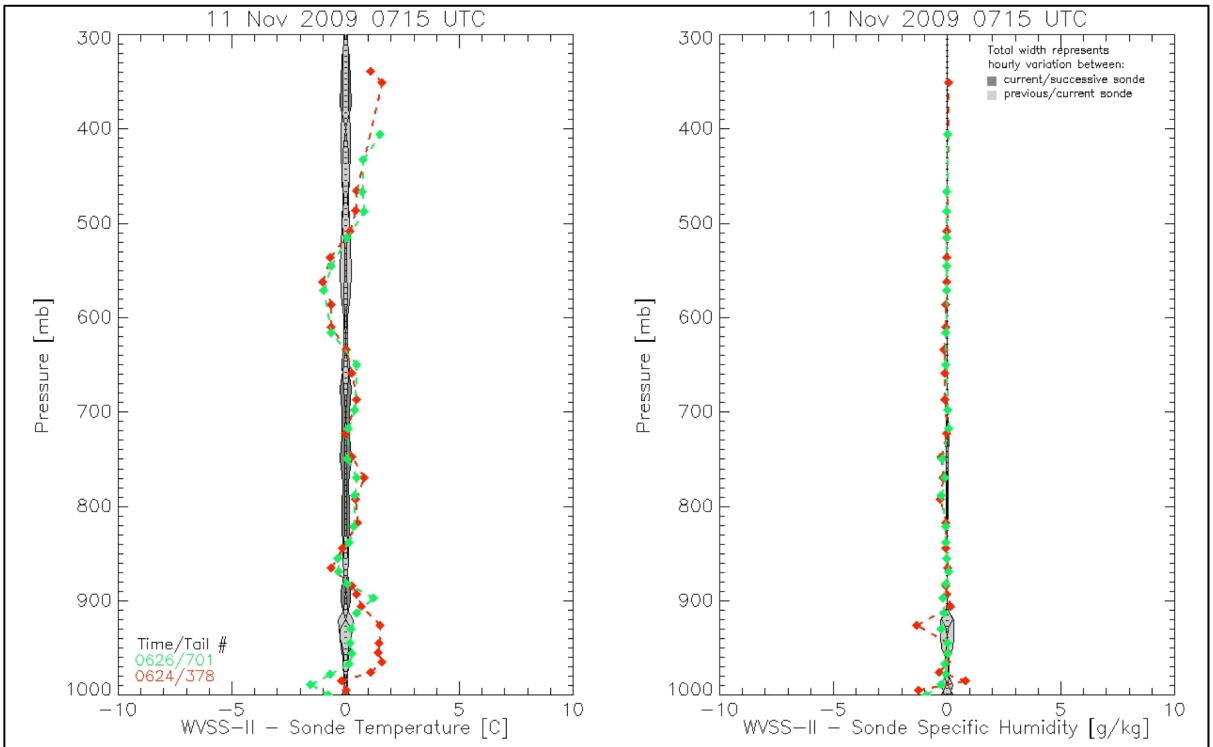

Figure B-7: Differences between RAOB and aircraft temperature and moisture profiles from within one hour of RAOB launch time of 0715 UTC on 11 Nov. 2010 at Rockford Illinois. Gray shaded indicate change between successive RAOB launches

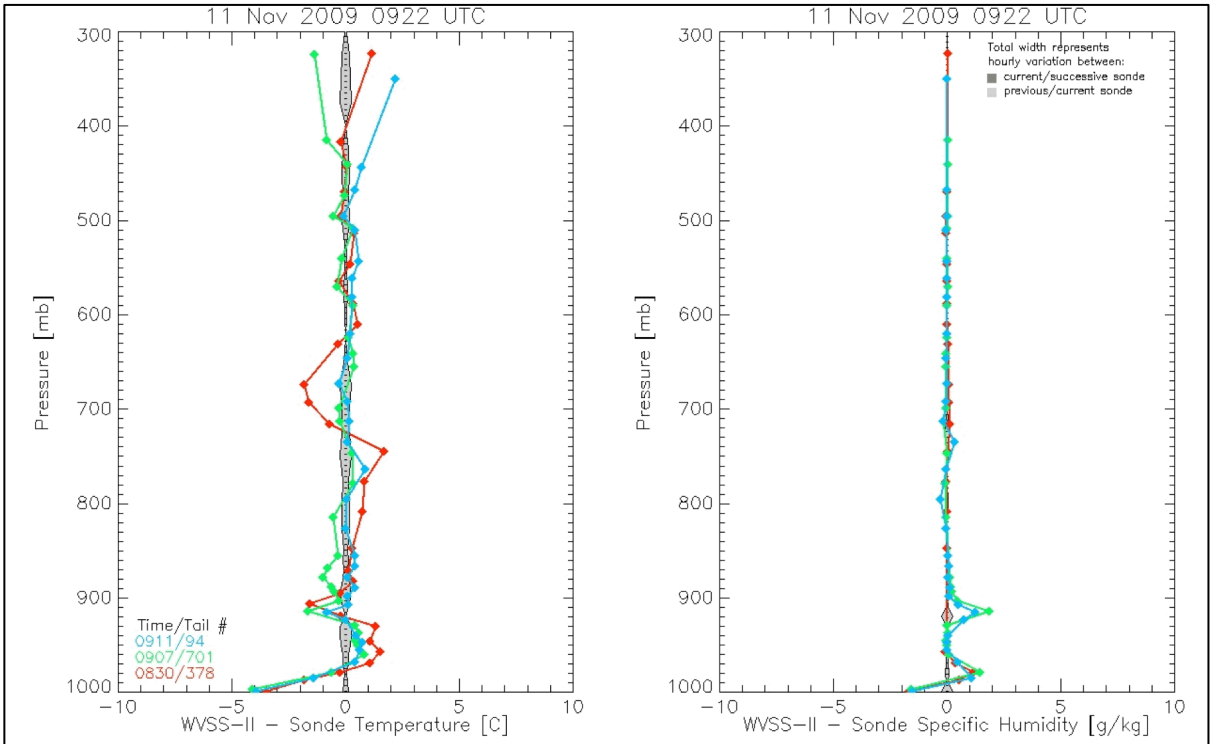

Figure B-8: Differences between RAOB and aircraft temperature and moisture profiles from within one hour of RAOB launch time of 0922 UTC on 11 Nov. 2010 at Rockford Illinois. Gray shaded indicate change between successive RAOB launches

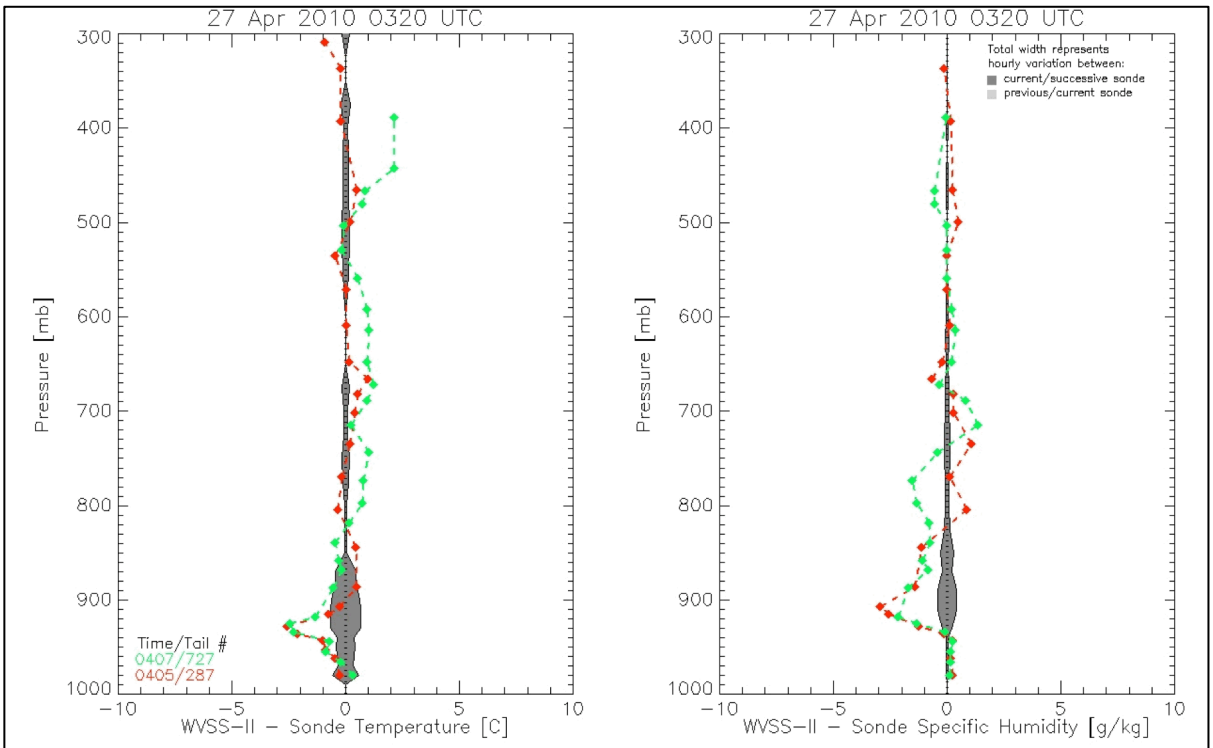

Figure B-9: Differences between RAOB and aircraft temperature and moisture profiles from within one hour of RAOB launch time of 0330 UTC on 27 Apr. 2010 at Rockford Illinois. Gray shaded indicate change between successive RAOB launches

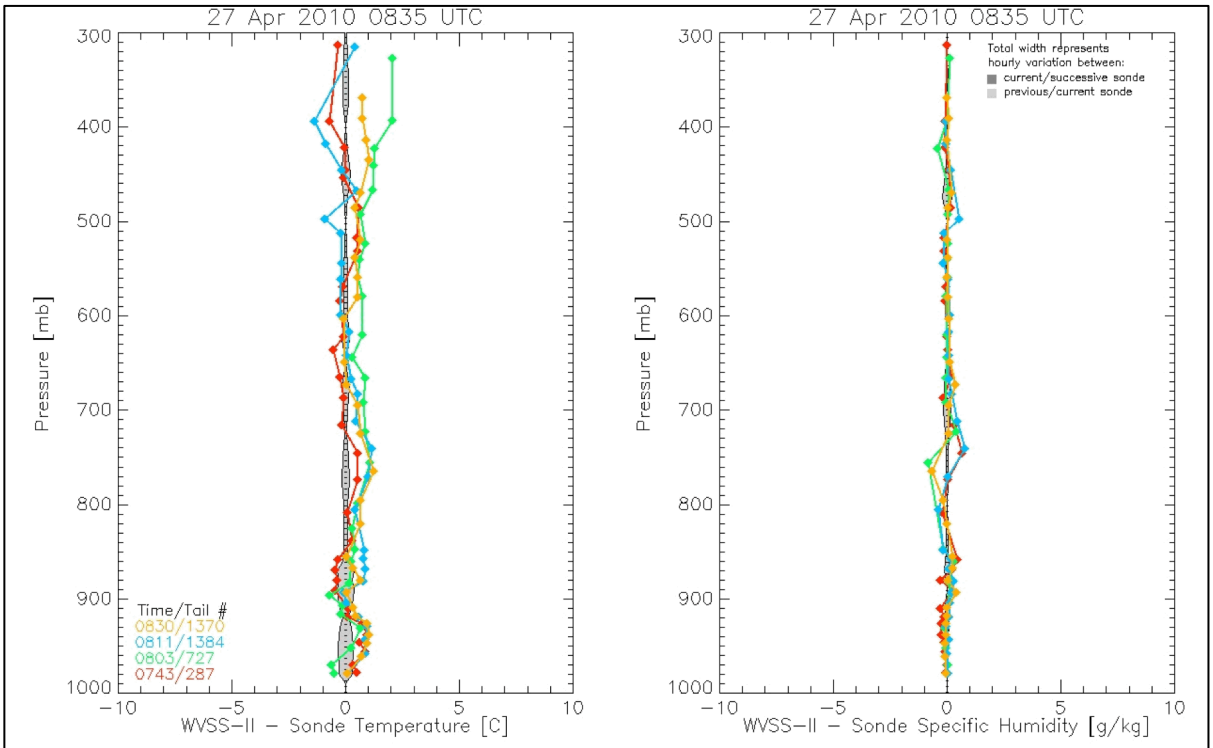

Figure B-10: Differences between RAOB and aircraft temperature and moisture profiles from within one hour of RAOB launch time of 0835 UTC on 27 Apr. 2010 at Rockford Illinois. Gray shaded indicate change between successive RAOB launches

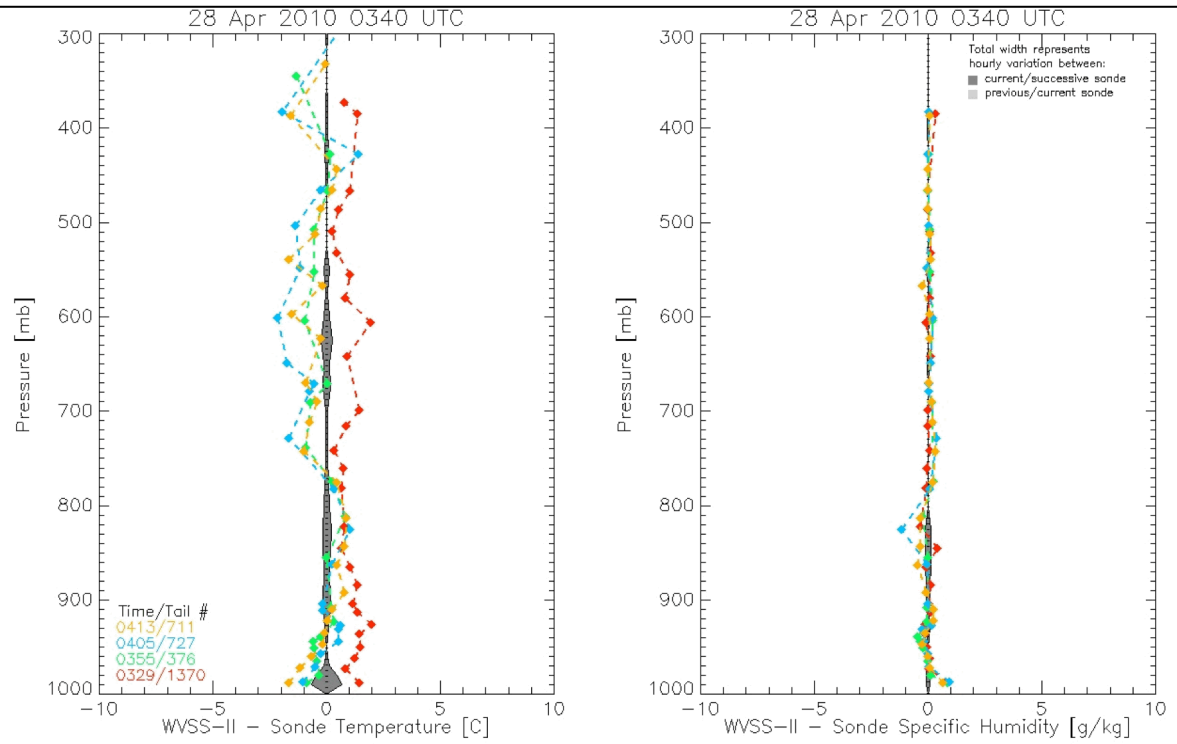

Figure B-11: Differences between RAOB and aircraft temperature and moisture profiles from within one hour of RAOB launch time of 0340 UTC on 28 Apr. 2010 at Rockford Illinois. Gray shaded indicate change between successive RAOB launches

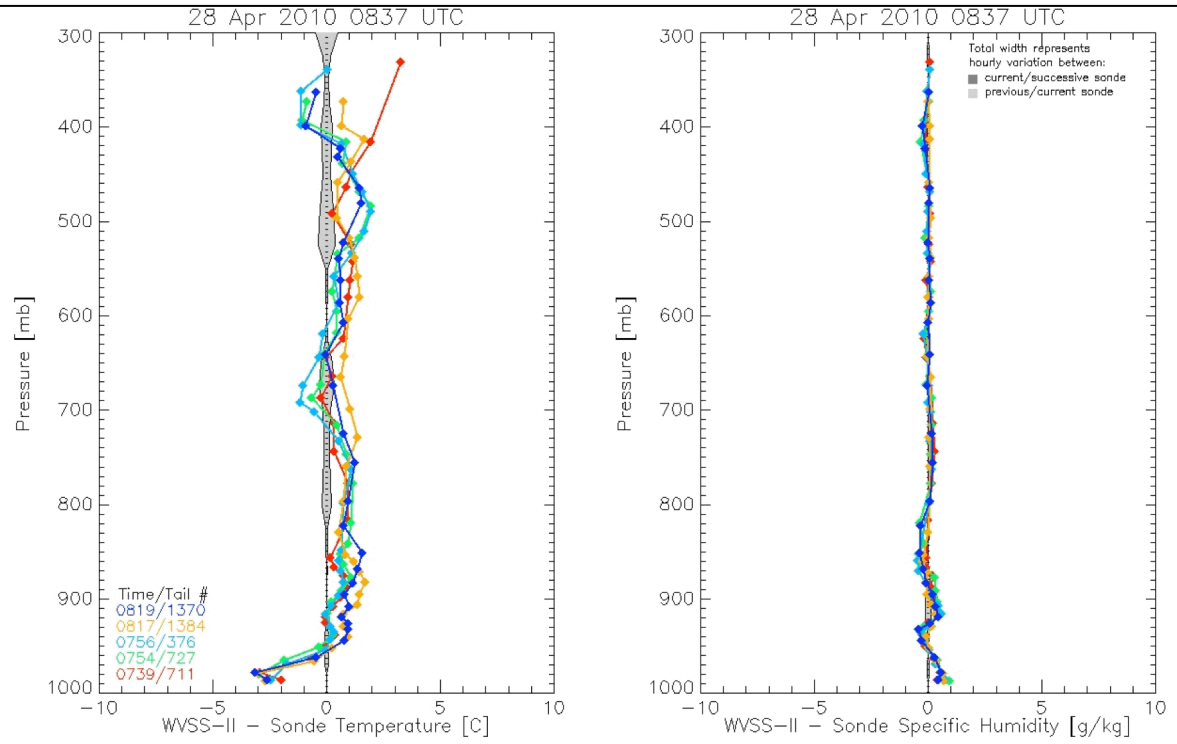

Figure B-12: Differences between RAOB and aircraft temperature and moisture profiles from within one hour of RAOB launch time of 0837 UTC on 28 Apr. 2010 at Rockford Illinois. Gray shaded indicate change between successive RAOB launches

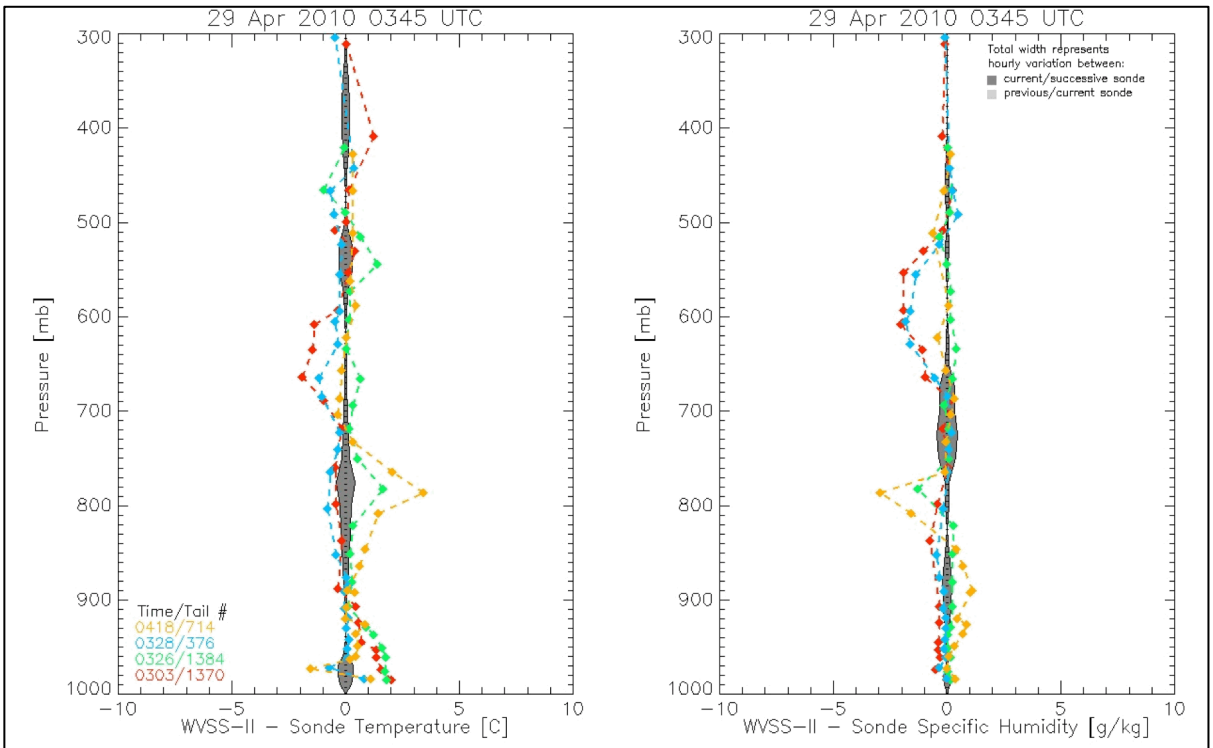

Figure B-13: Differences between RAOB and aircraft temperature and moisture profiles from within one hour of RAOB launch time of 0345 UTC on 29 Apr. 2010 at Rockford Illinois. Gray shaded indicate change between successive RAOB launches

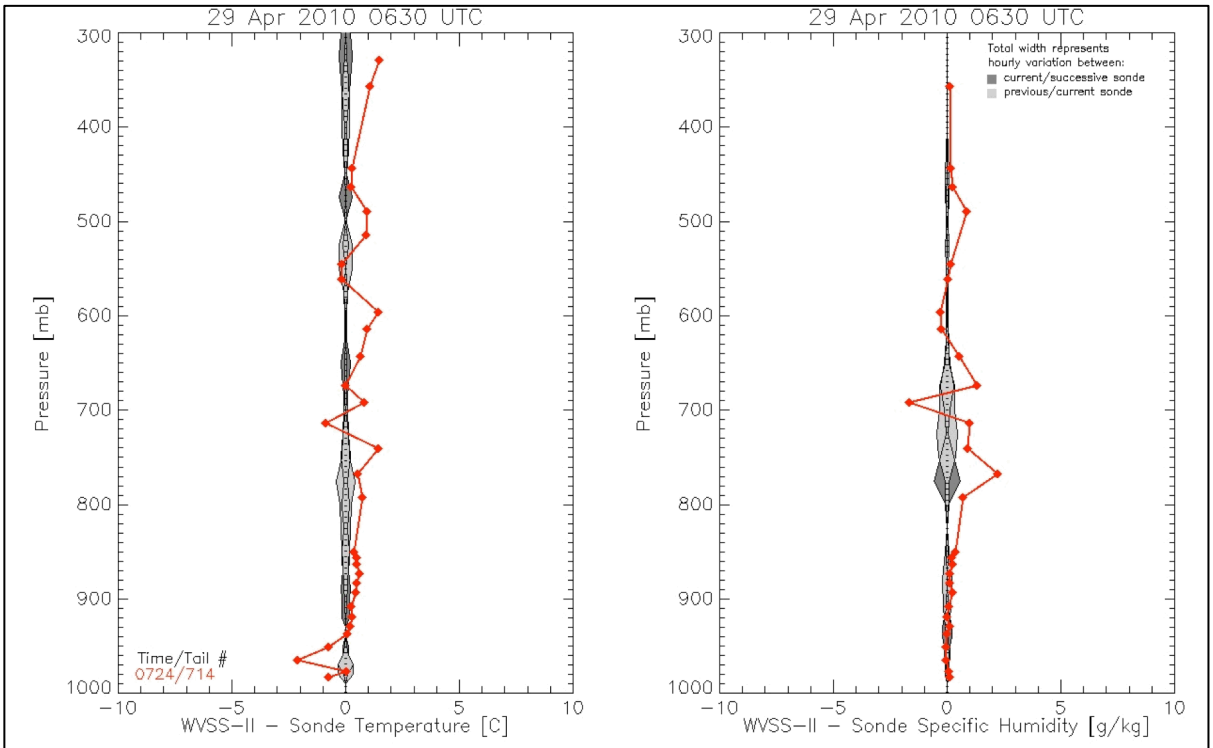

Figure B-14: Differences between RAOB and aircraft temperature and moisture profiles from within one hour of RAOB launch time of 0630 UTC on 29 Apr. 2010 at Rockford Illinois. Gray shaded indicate change between successive RAOB launches

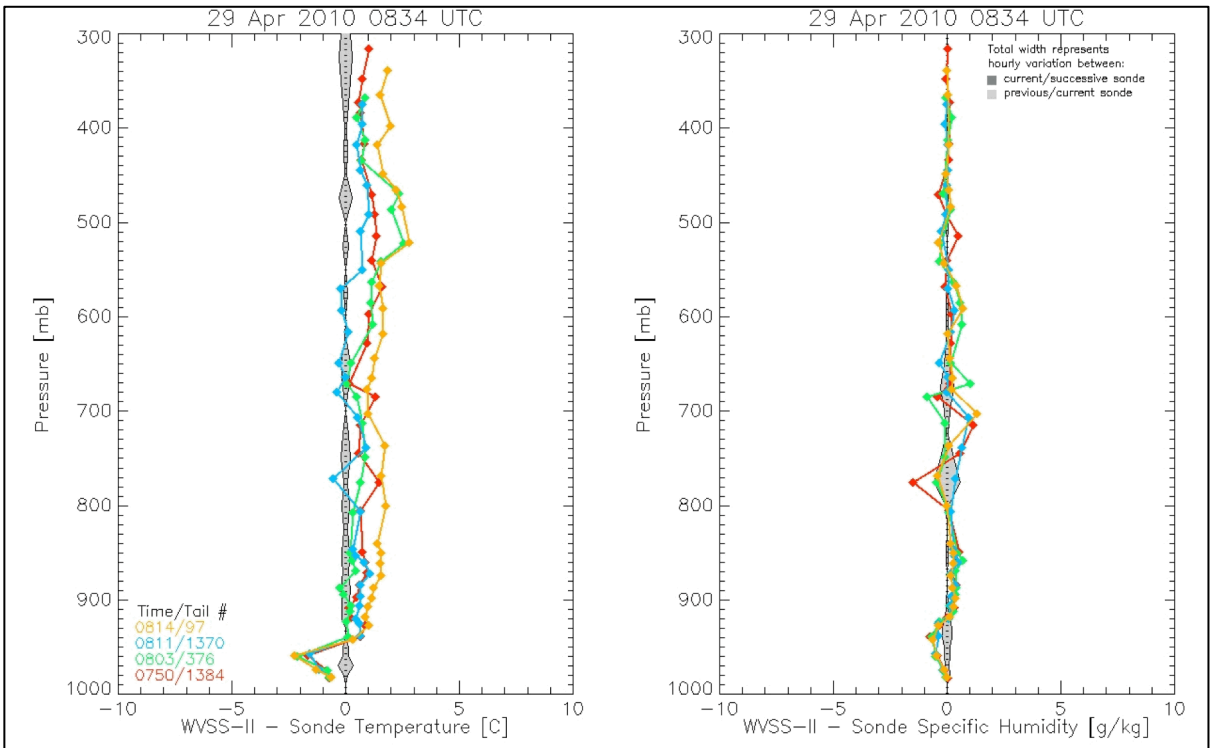

Figure B-15: Differences between RAOB and aircraft temperature and moisture profiles from within one hour of RAOB launch time of 0834 UTC on 29 Apr. 2010 at Rockford Illinois. Gray shaded indicate change between successive RAOB launches

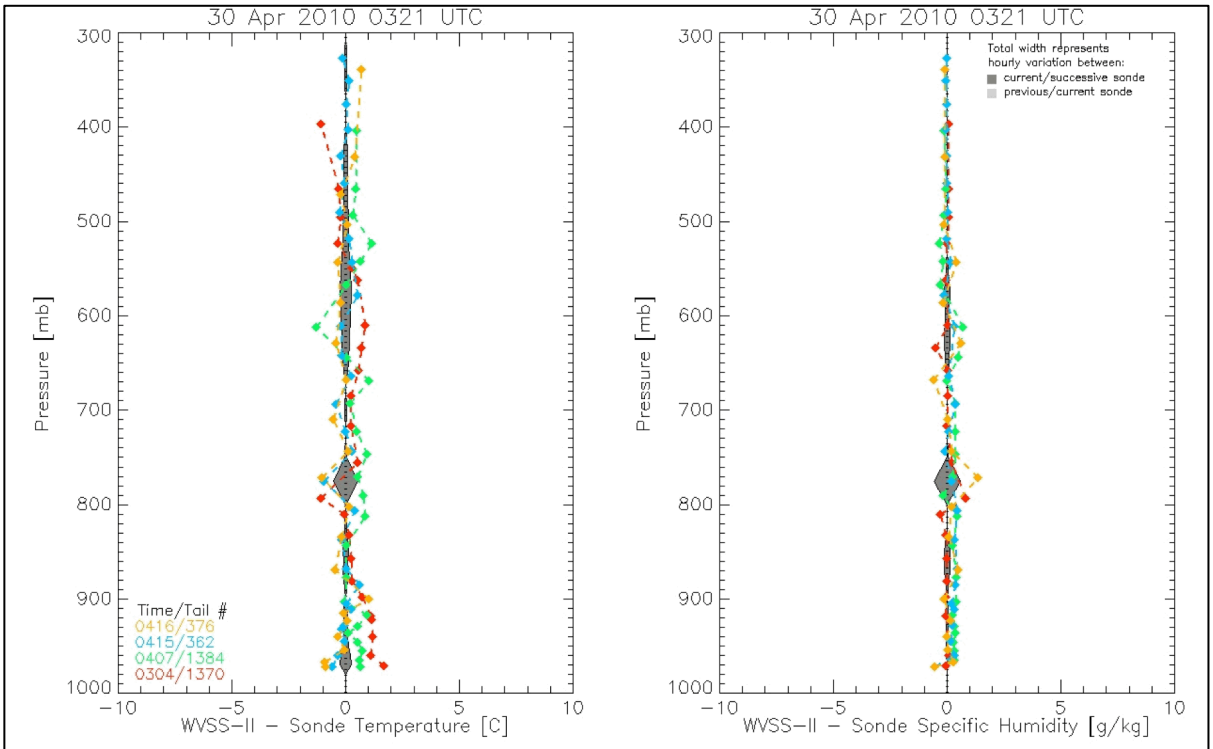

Figure B-16: Differences between RAOB and aircraft temperature and moisture profiles from within one hour of RAOB launch time of 0321 UTC on 30 Apr. 2010 at Rockford Illinois. Gray shaded indicate change between successive RAOB launches

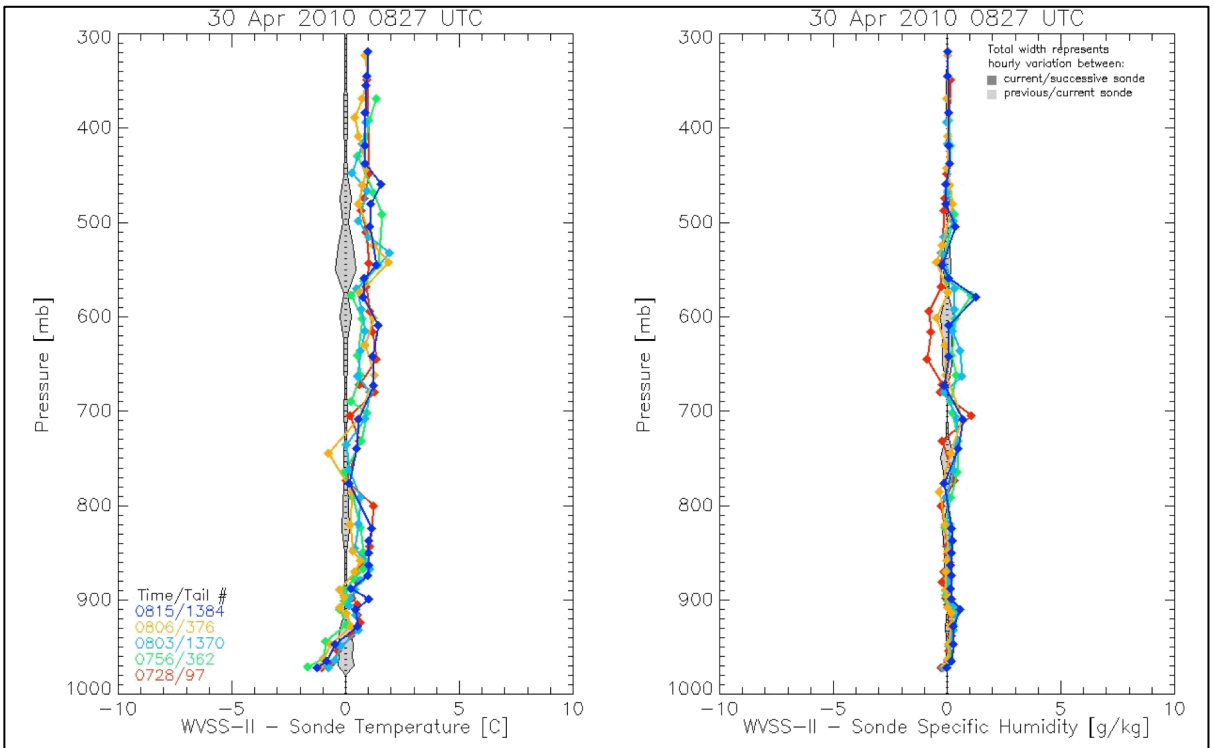

Figure B-17: Differences between RAOB and aircraft temperature and moisture profiles from within one hour of RAOB launch time of 0827 UTC on 30 Apr. 2010 at Rockford Illinois. Gray shaded indicate change between successive RAOB launches

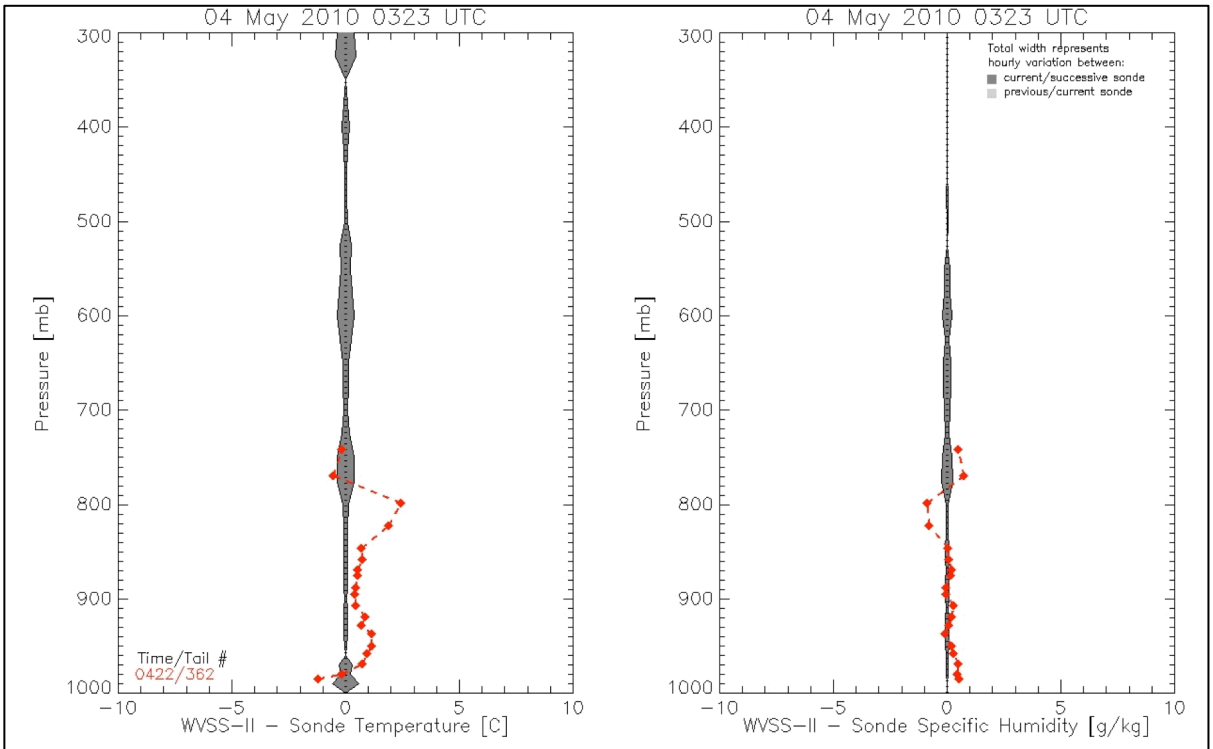

Figure B-18: Differences between RAOB and aircraft temperature and moisture profiles from within one hour of RAOB launch time of 0323 UTC on 04 May2010 at Rockford Illinois. Gray shaded indicate change between successive RAOB launches

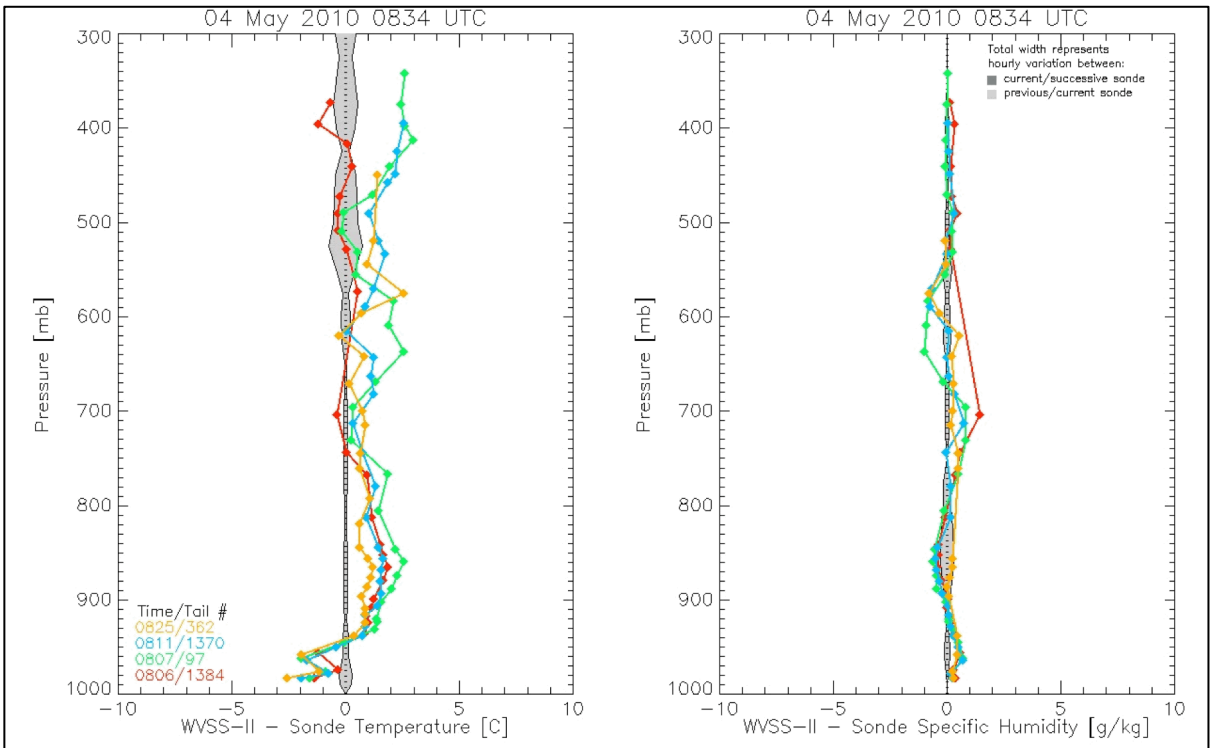

Figure B-19: Differences between RAOB and aircraft temperature and moisture profiles from within one hour of RAOB launch time of 0834 UTC on 04 May2010 at Rockford Illinois. Gray shaded indicate change between successive RAOB launches

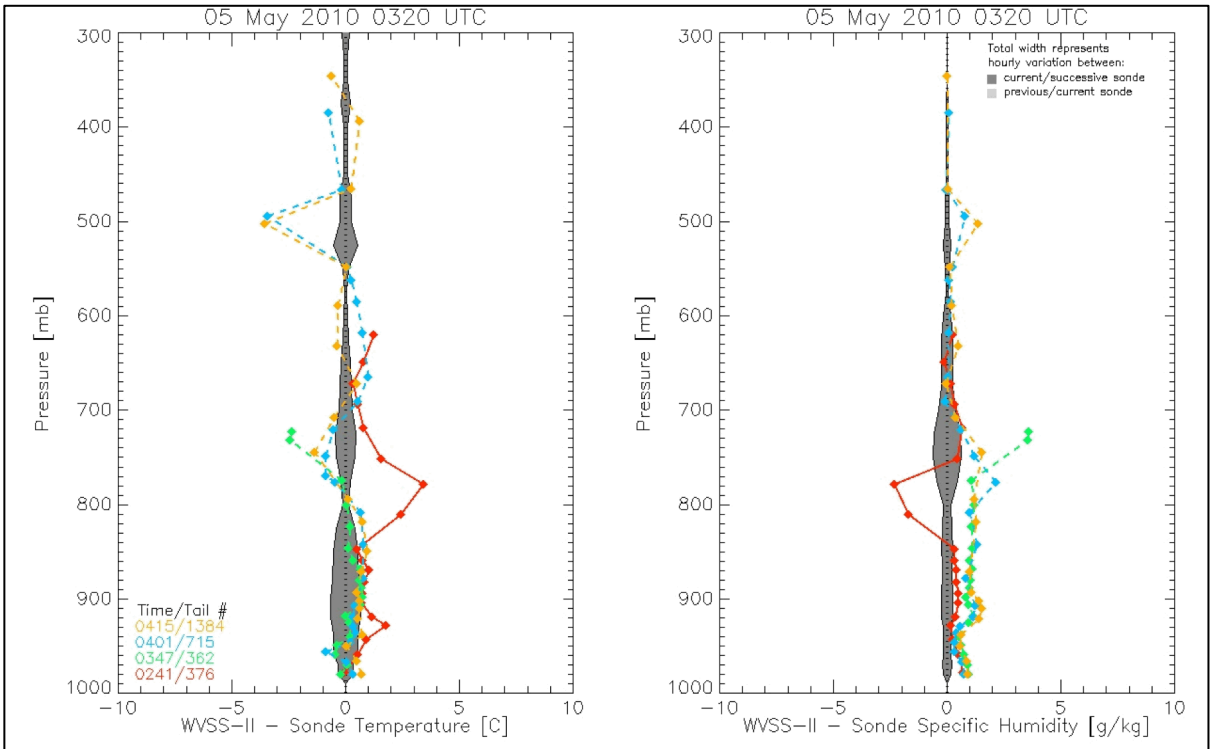

Figure B-20: Differences between RAOB and aircraft temperature and moisture profiles from within one hour of RAOB launch time of 0320 UTC on 05 May2010 at Rockford Illinois. Gray shaded indicate change between successive RAOB launches

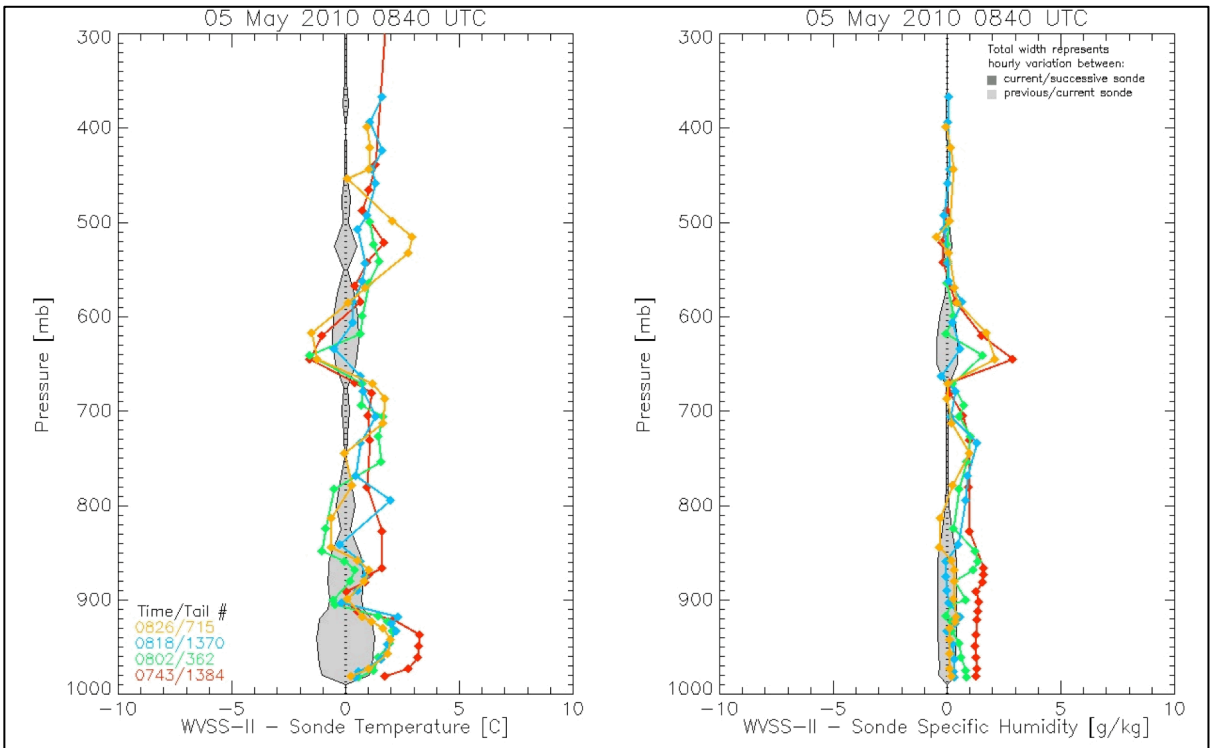

Figure B-21: Differences between RAOB and aircraft temperature and moisture profiles from within one hour of RAOB launch time of 0840 UTC on 05 May2010 at Rockford Illinois. Gray shaded indicate change between successive RAOB launches

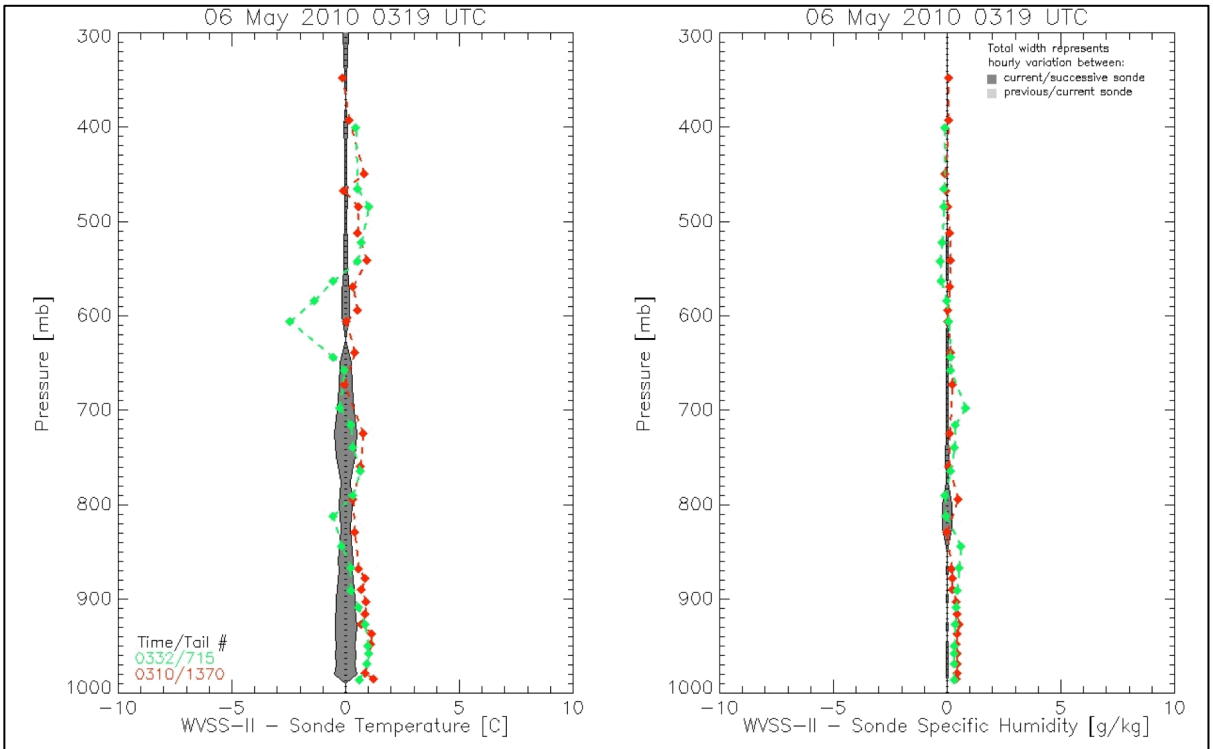

Figure B-22: Differences between RAOB and aircraft temperature and moisture profiles from within one hour of RAOB launch time of 0319 UTC on 06 May2010 at Rockford Illinois. Gray shaded indicate change between successive RAOB launches

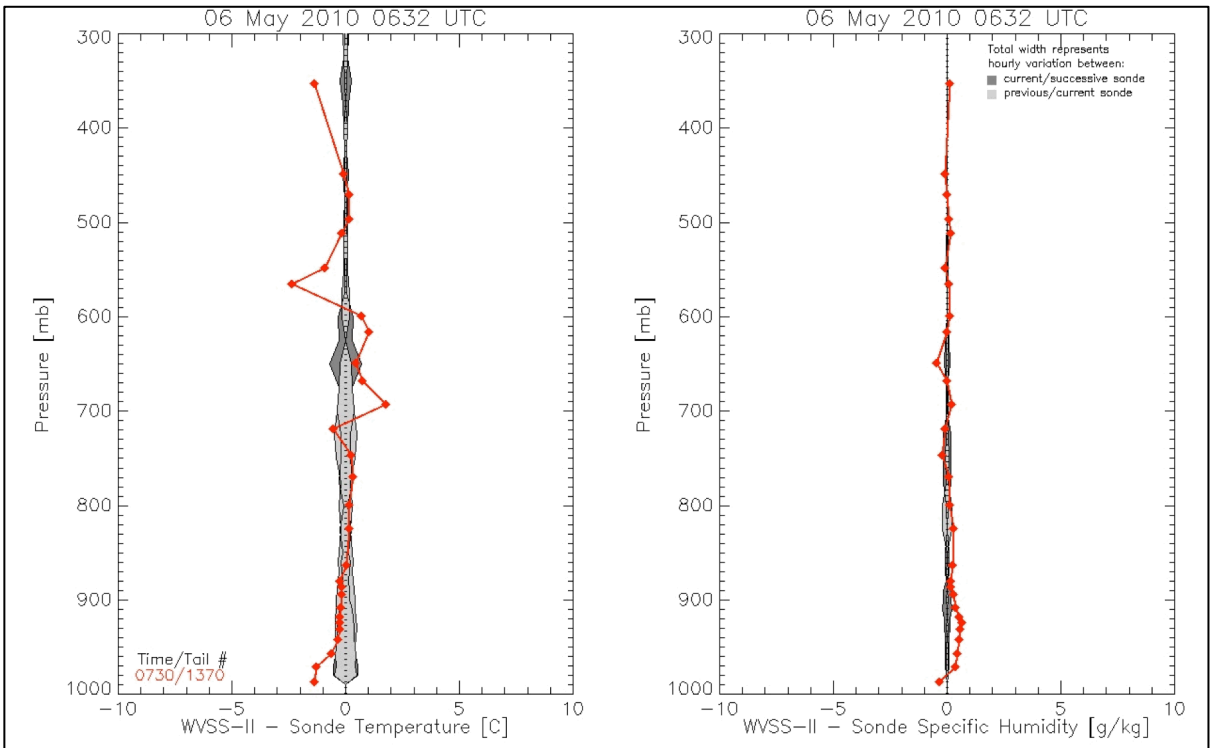

Figure B-23: Differences between RAOB and aircraft temperature and moisture profiles from within one hour of RAOB launch time of 0632 UTC on 06 May2010 at Rockford Illinois. Gray shaded indicate change between successive RAOB launches

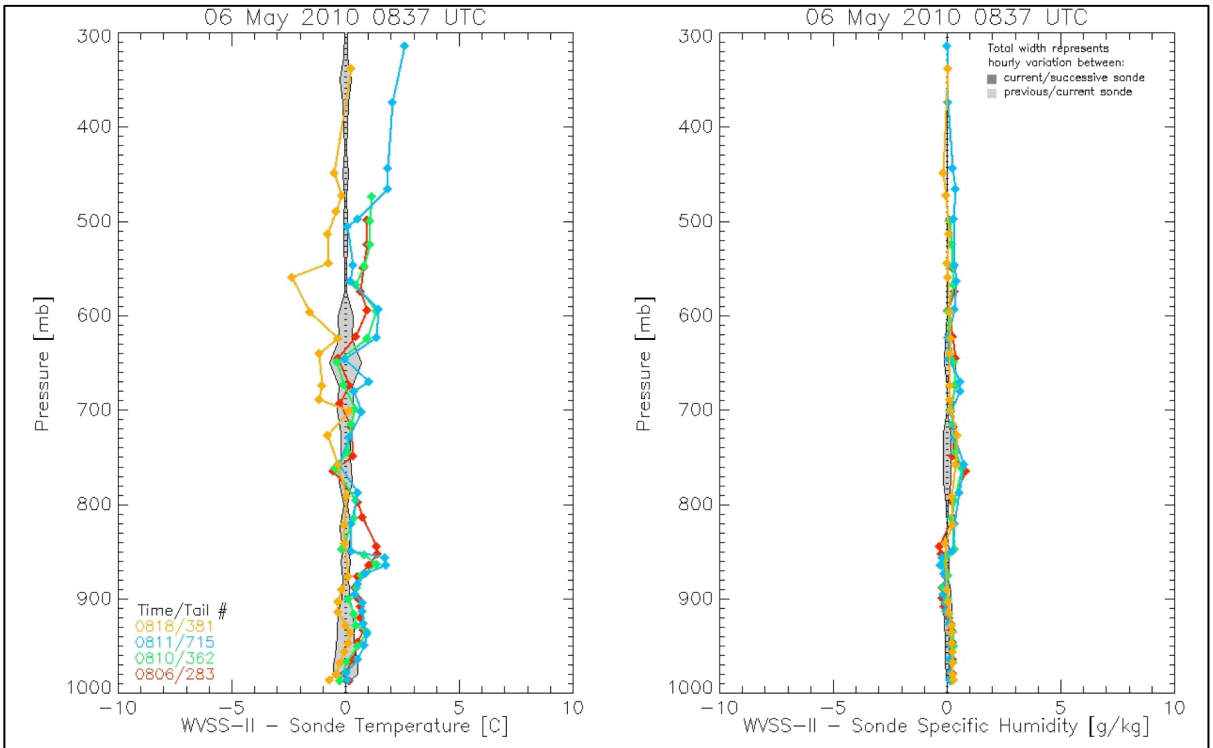

Figure B-24: Differences between RAOB and aircraft temperature and moisture profiles from within one hour of RAOB launch time of 8374 UTC on 06 May2010 at Rockford Illinois. Gray shaded indicate change between successive RAOB launches

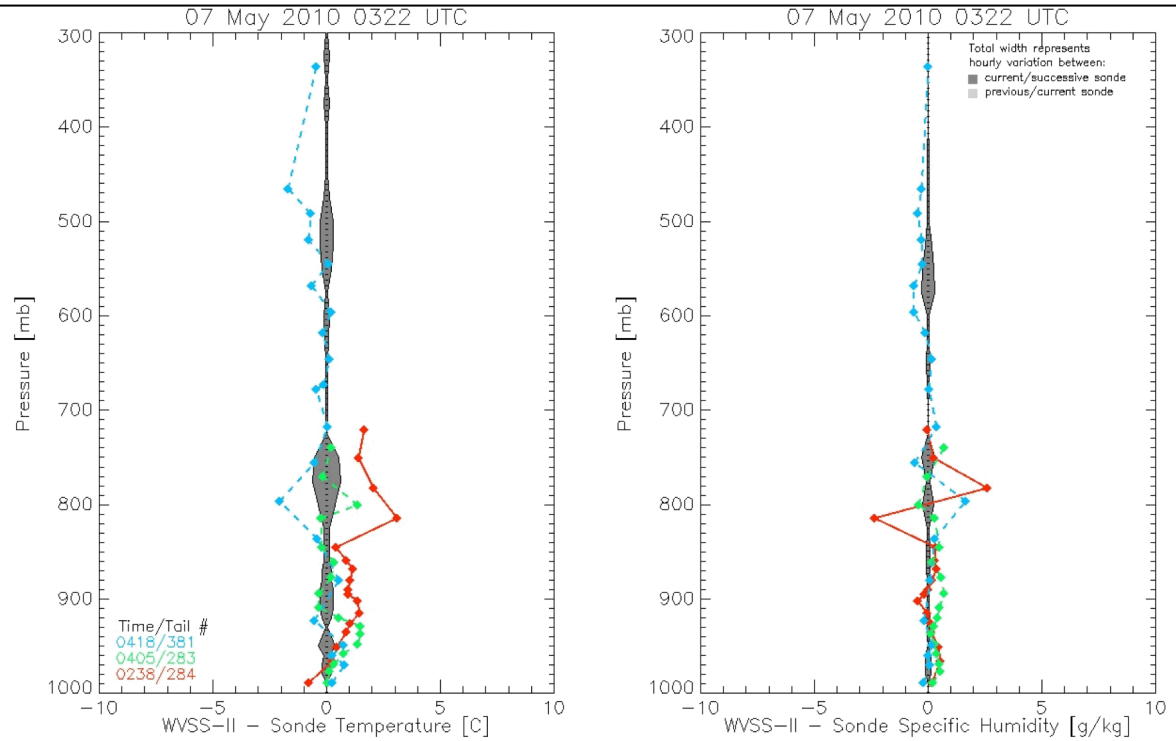

Figure B-25: Differences between RAOB and aircraft temperature and moisture profiles from within one hour of RAOB launch time of 0322 UTC on 07 May2010 at Rockford Illinois. Gray shaded indicate change between successive RAOB launches

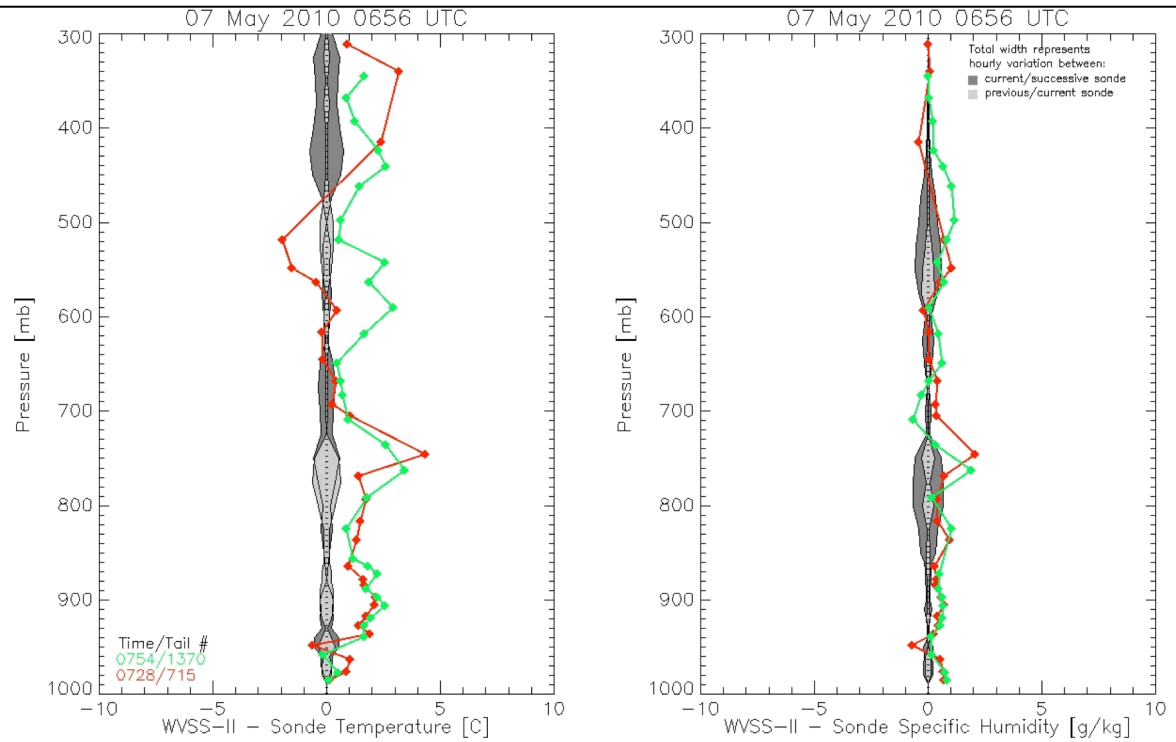

Figure B-26: Differences between RAOB and aircraft temperature and moisture profiles from within one hour of RAOB launch time of 0656 UTC on 07 May2010 at Rockford Illinois. Gray shaded indicate change between successive RAOB launches

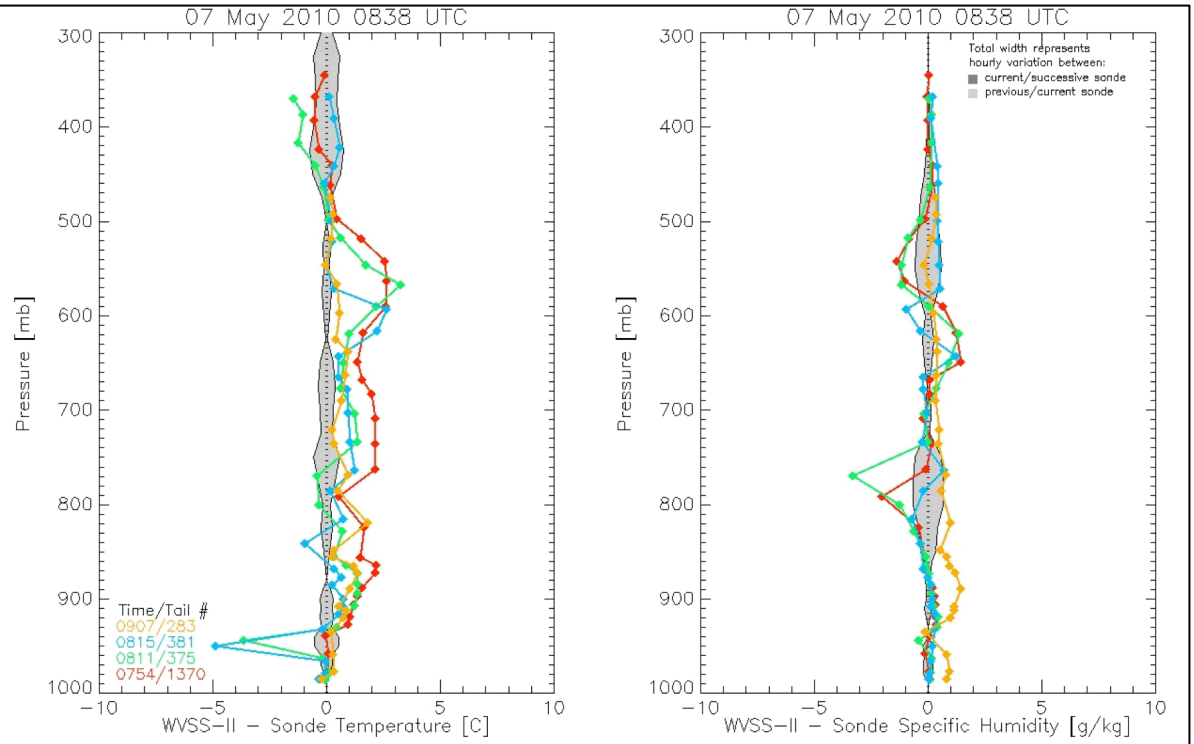

Figure B-27: Differences between RAOB and aircraft temperature and moisture profiles from within one hour of RAOB launch time of 0838 UTC on 07 May2010 at Rockford Illinois. Gray shaded indicate change between successive RAOB launches

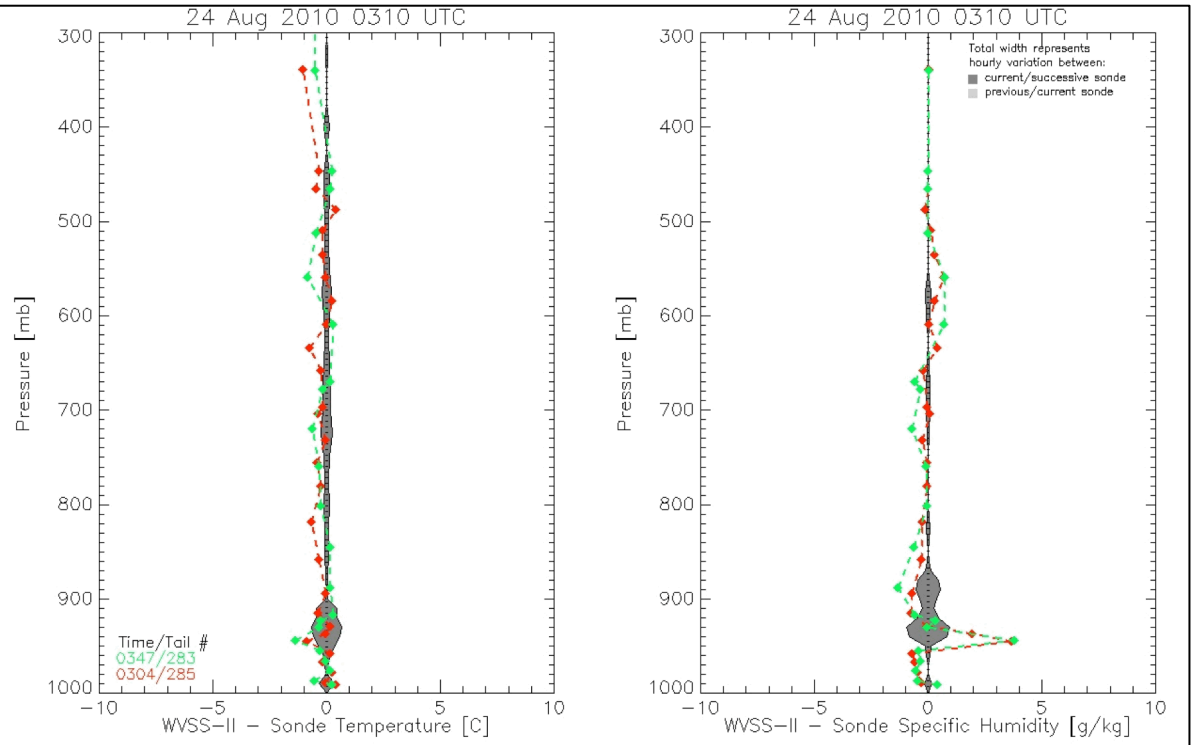

Figure B-28: Differences between RAOB and aircraft temperature and moisture profiles from within one hour of RAOB launch time of 0310 UTC on 24 Aug. 2010 at Rockford Illinois. Gray shaded indicate change between successive RAOB launches

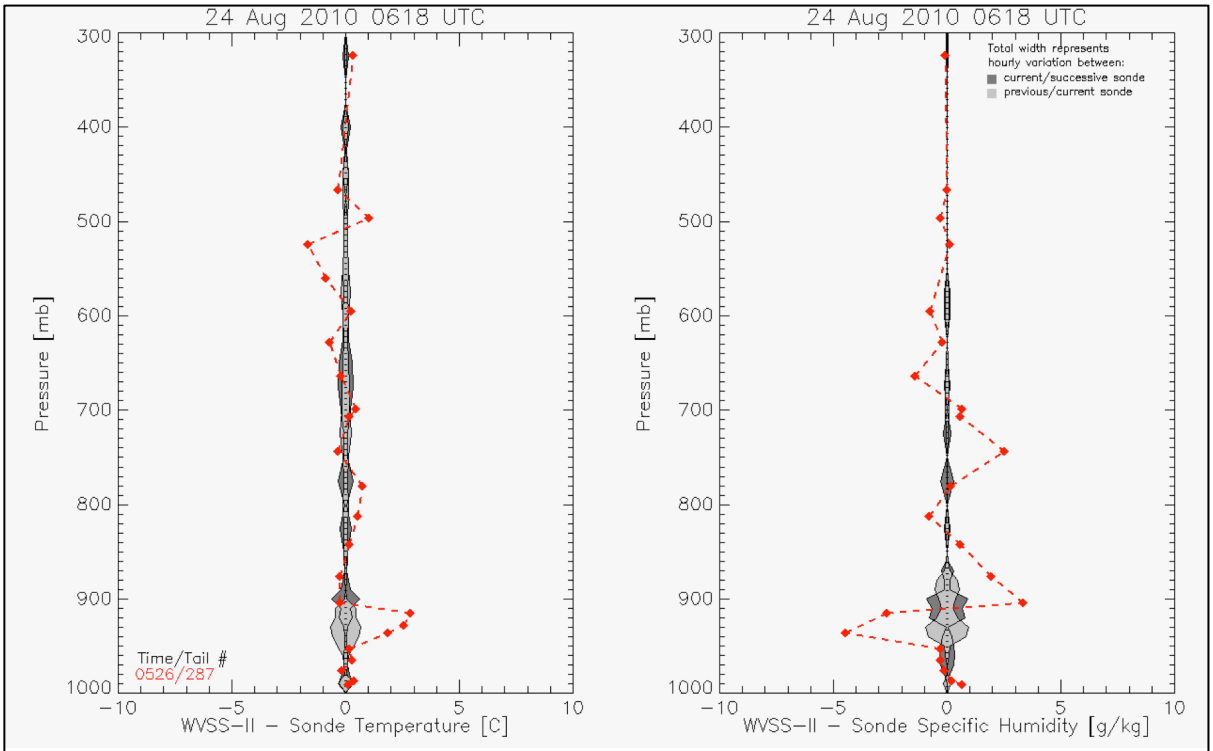

Figure B-29: Differences between RAOB and aircraft temperature and moisture profiles from within one hour of RAOB launch time of 0618 UTC on 24 Aug. 2010 at Rockford Illinois. Gray shaded indicate change between successive RAOB launches

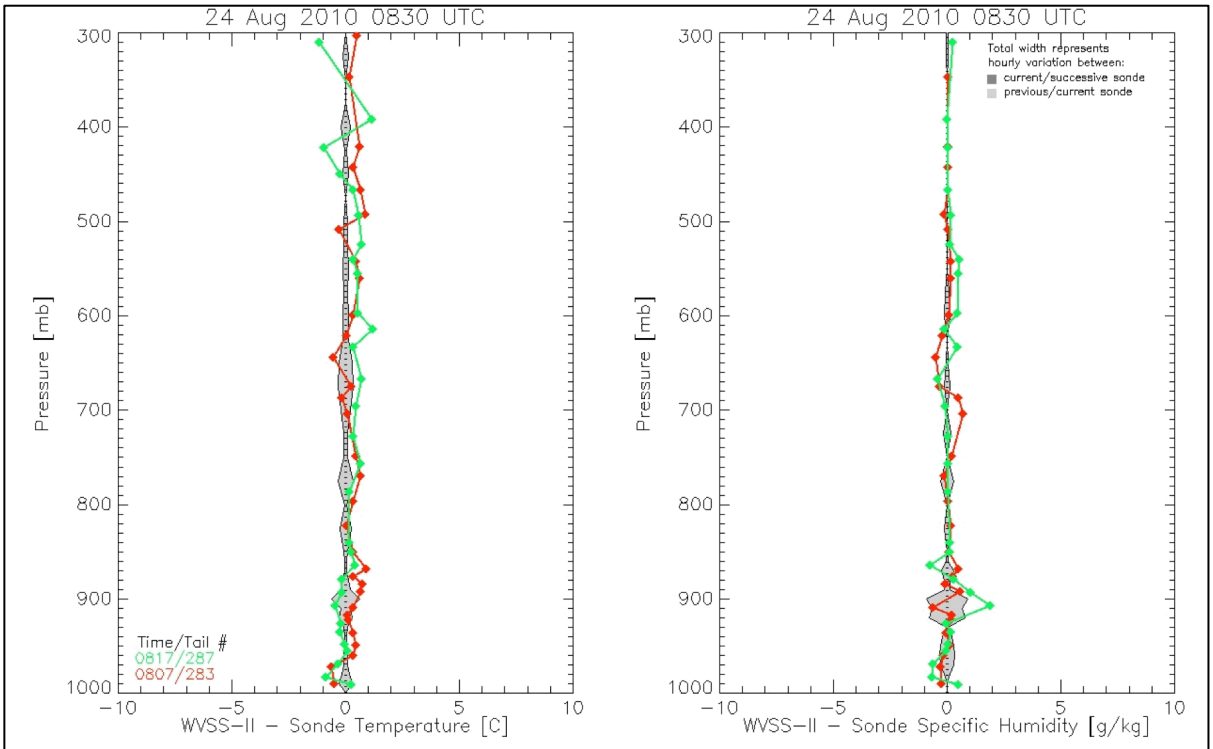

Figure B-30: Differences between RAOB and aircraft temperature and moisture profiles from within one hour of RAOB launch time of 0830 UTC on 24 Aug. 2010 at Rockford Illinois. Gray shaded indicate change between successive RAOB launches

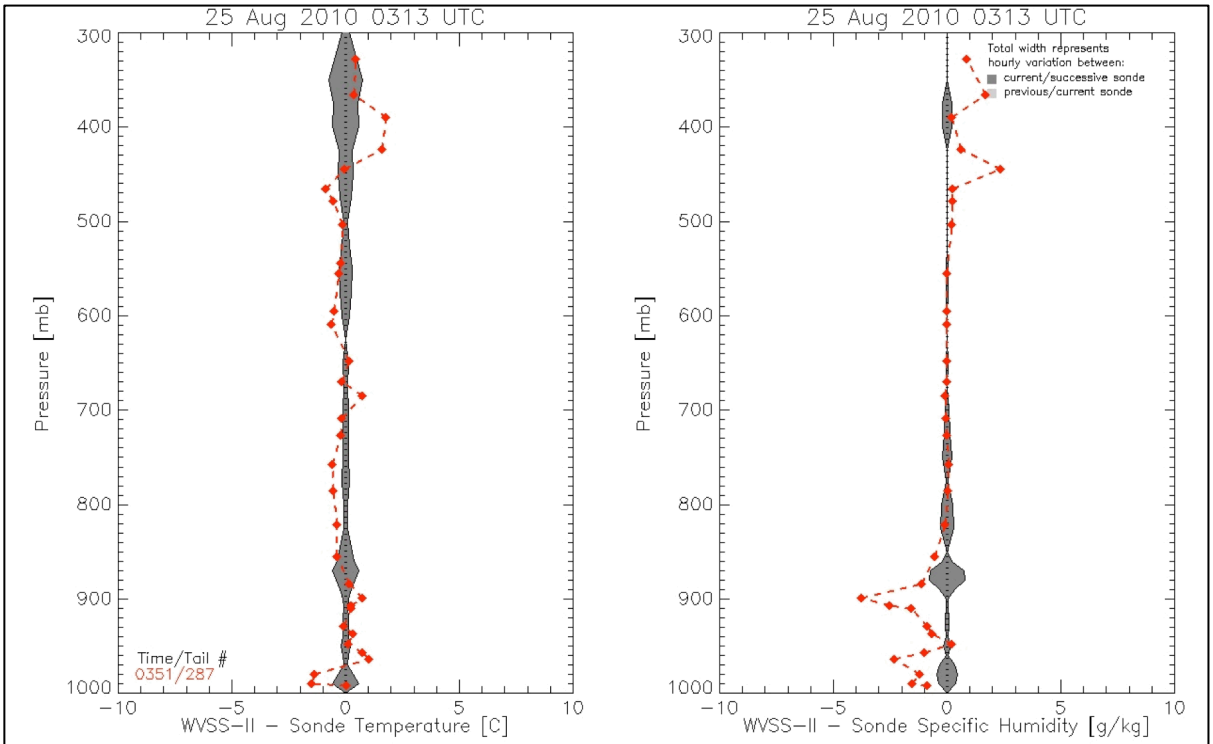

Figure B-31: Differences between RAOB and aircraft temperature and moisture profiles from within one hour of RAOB launch time of 0313 UTC on 25 Aug. 2010 at Rockford Illinois. Gray shaded indicate change between successive RAOB launches

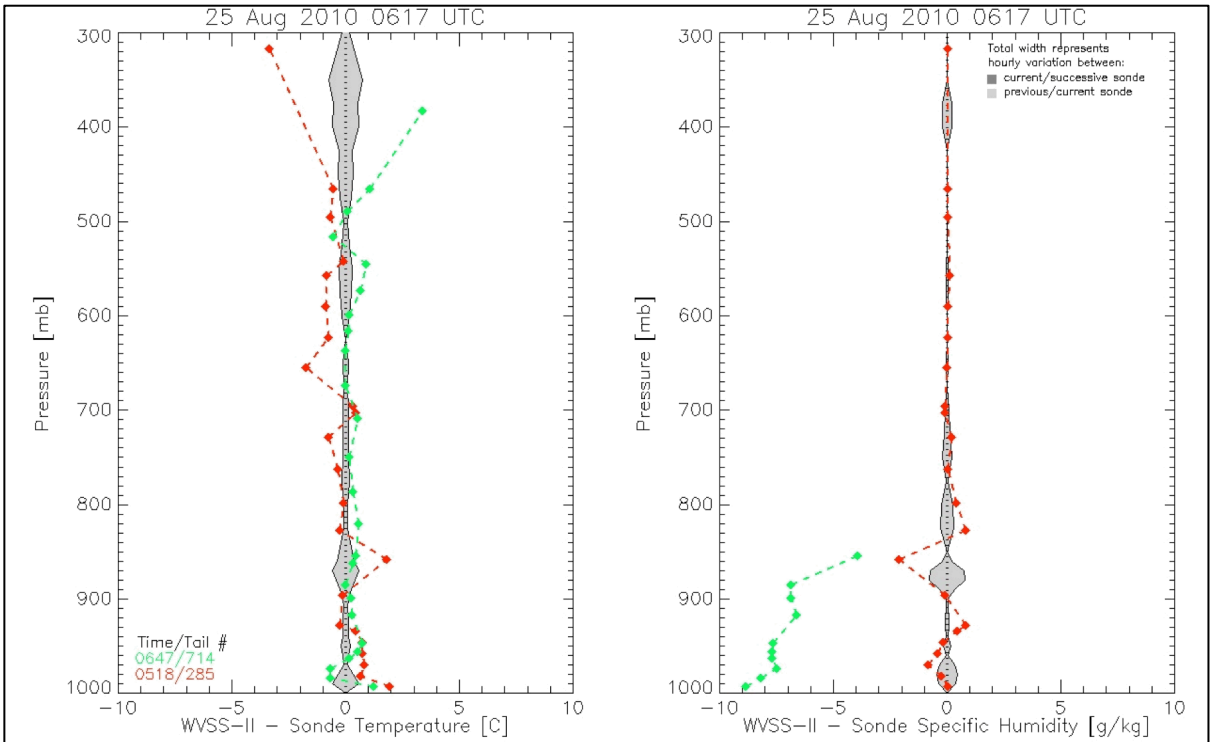

Figure B-32: Differences between RAOB and aircraft temperature and moisture profiles from within one hour of RAOB launch time of 0617 UTC on 24 Aug. 2010 at Rockford Illinois. Gray shaded indicate change between successive RAOB launches

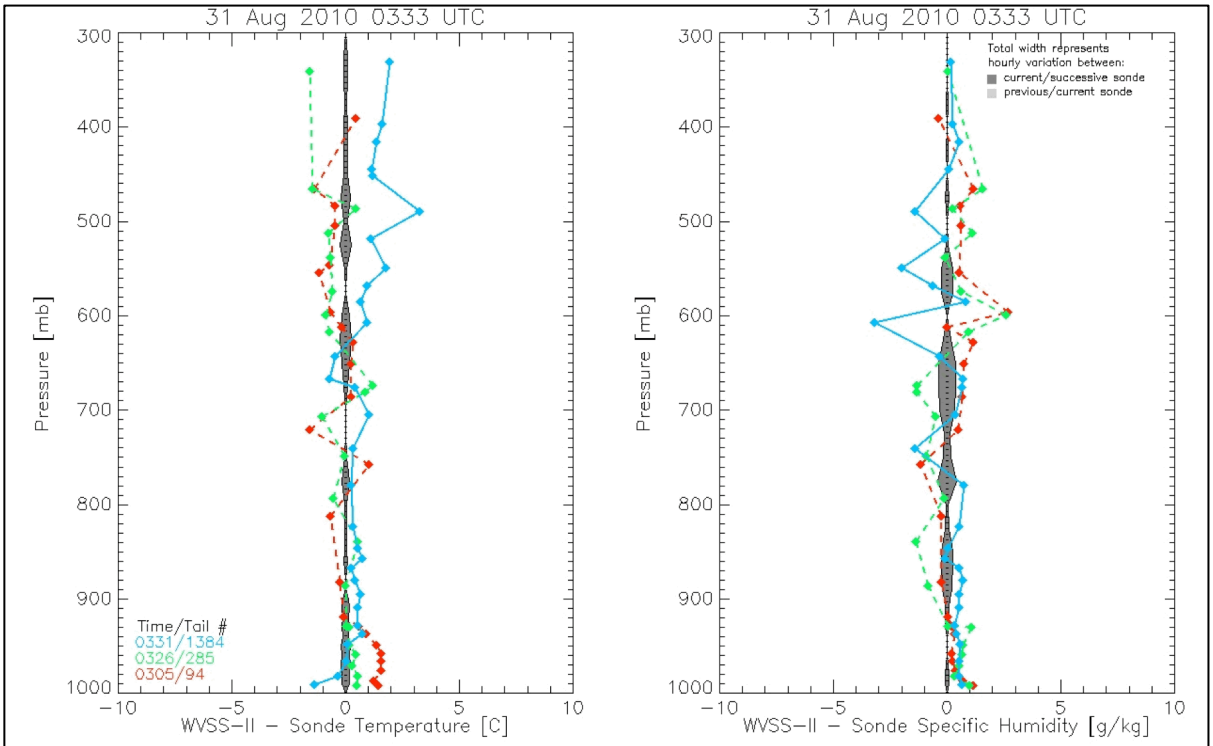

Figure B-33: Differences between RAOB and aircraft temperature and moisture profiles from within one hour of RAOB launch time of 0333 UTC on 31 Aug. 2010 at Rockford Illinois. Gray shaded indicate change between successive RAOB launches

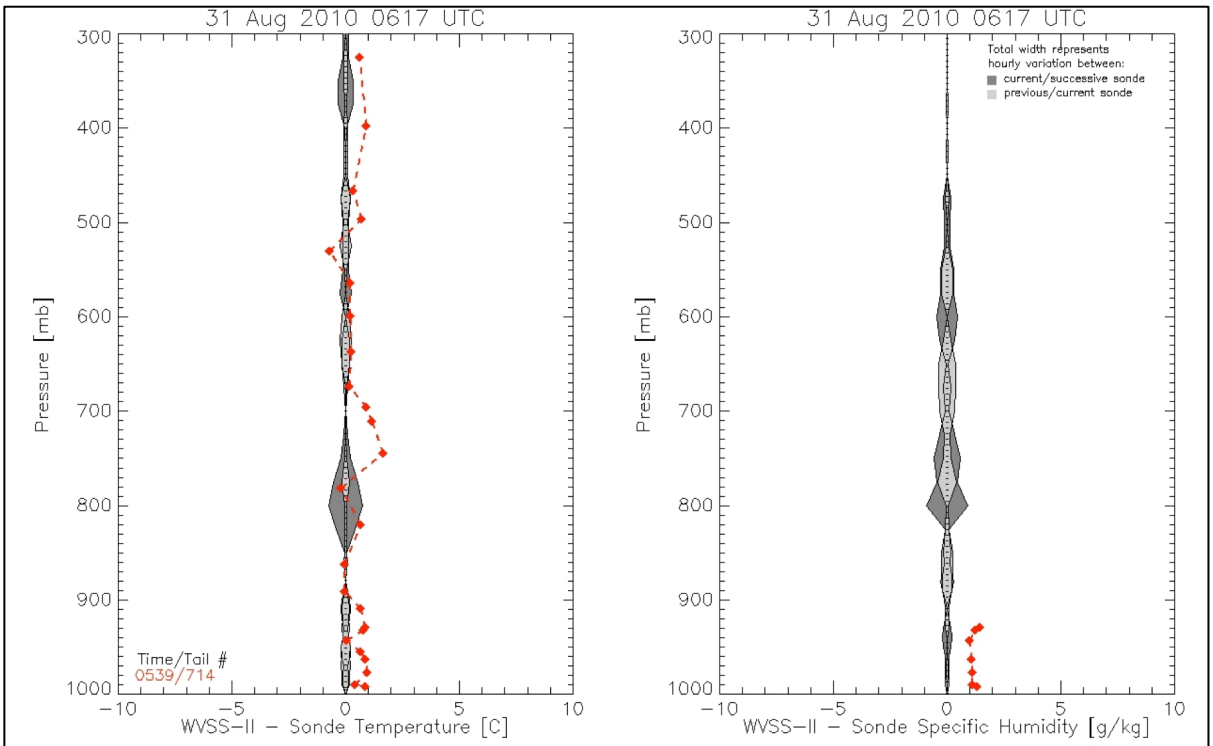

Figure B-34: Differences between RAOB and aircraft temperature and moisture profiles from within one hour of RAOB launch time of 0617 UTC on 31 Aug. 2010 at Rockford Illinois. Gray shaded indicate change between successive RAOB launches

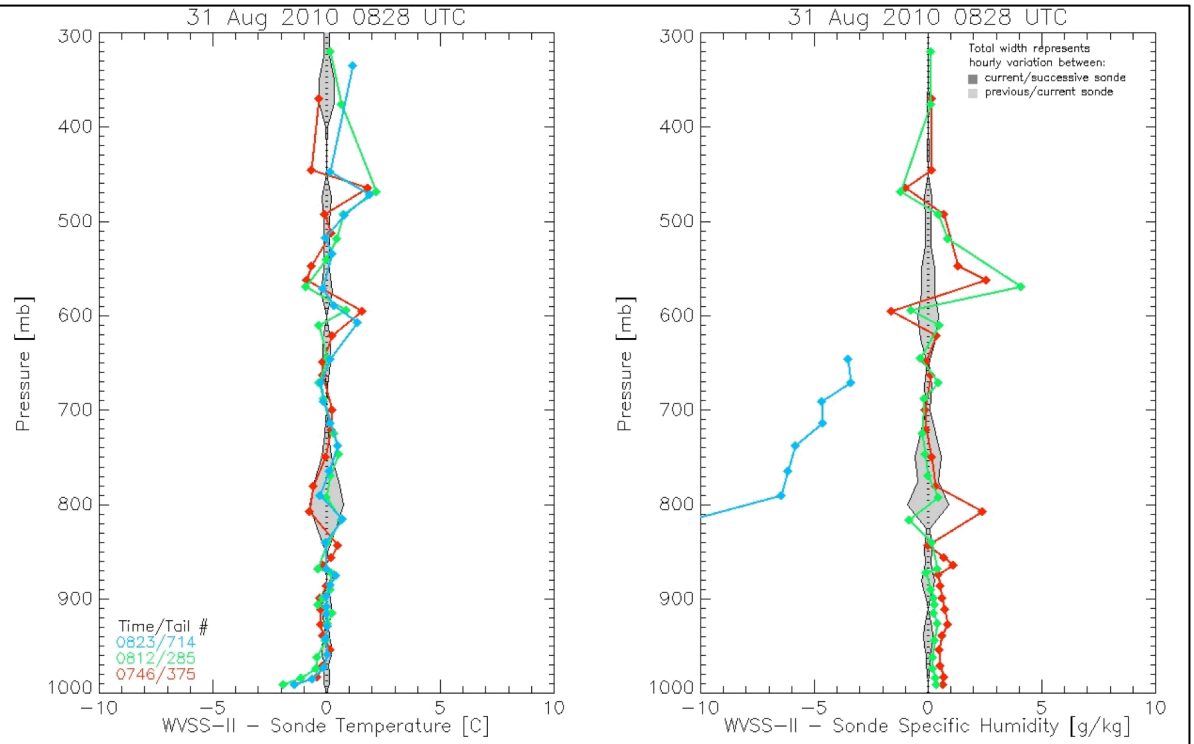

Figure B-35: Differences between RAOB and aircraft temperature and moisture profiles from within one hour of RAOB launch time of 0828 UTC on 31 Aug. 2010 at Rockford Illinois. Gray shaded indicate change between successive RAOB launches

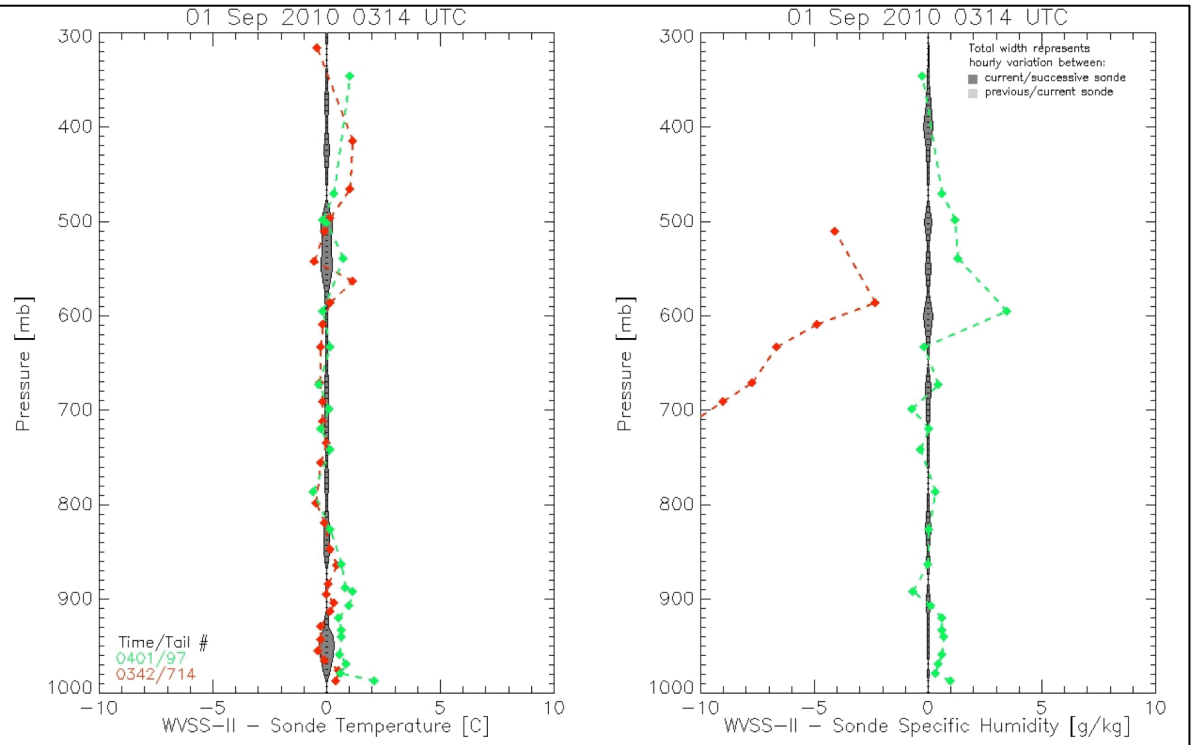

Figure B-36: Differences between RAOB and aircraft temperature and moisture profiles from within one hour of RAOB launch time of 0314 UTC on 01 Sept. 2010 at Rockford Illinois. Gray shaded indicate change between successive RAOB launches

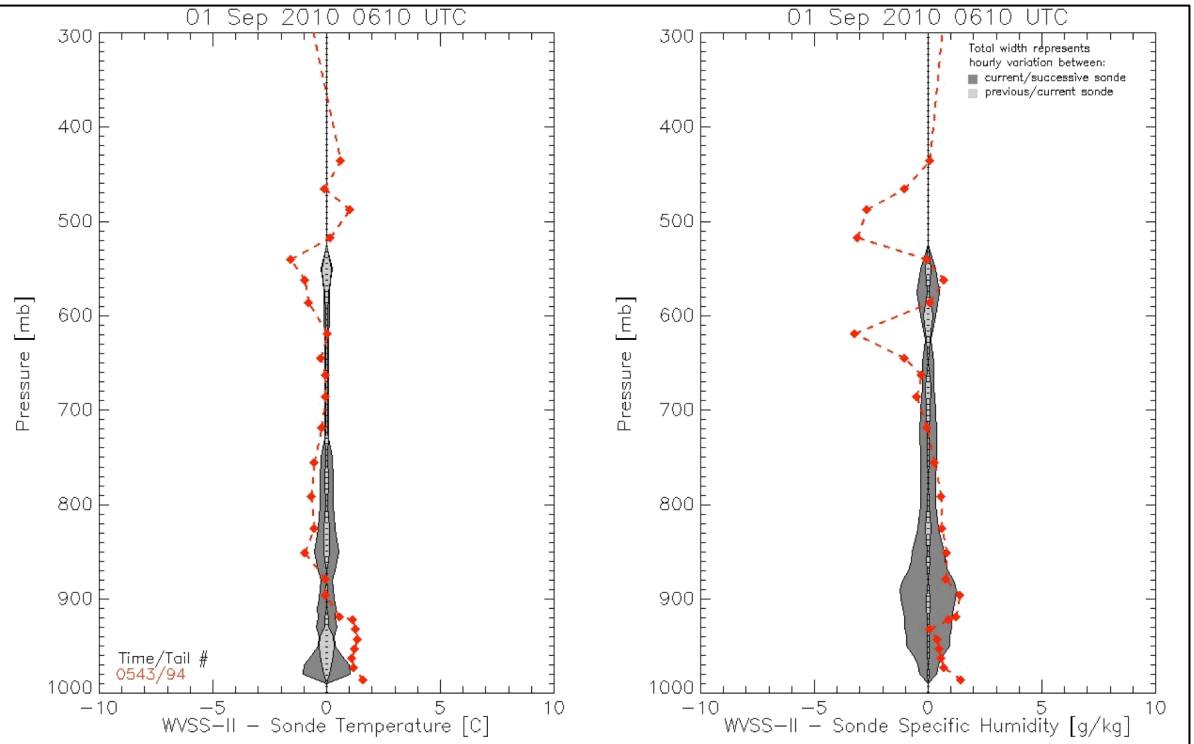

Figure B-37: Differences between RAOB and aircraft temperature and moisture profiles from within one hour of RAOB launch time of 0610 UTC on 01 Sept. 2010 at Rockford Illinois. Gray shaded indicate change between successive RAOB launches

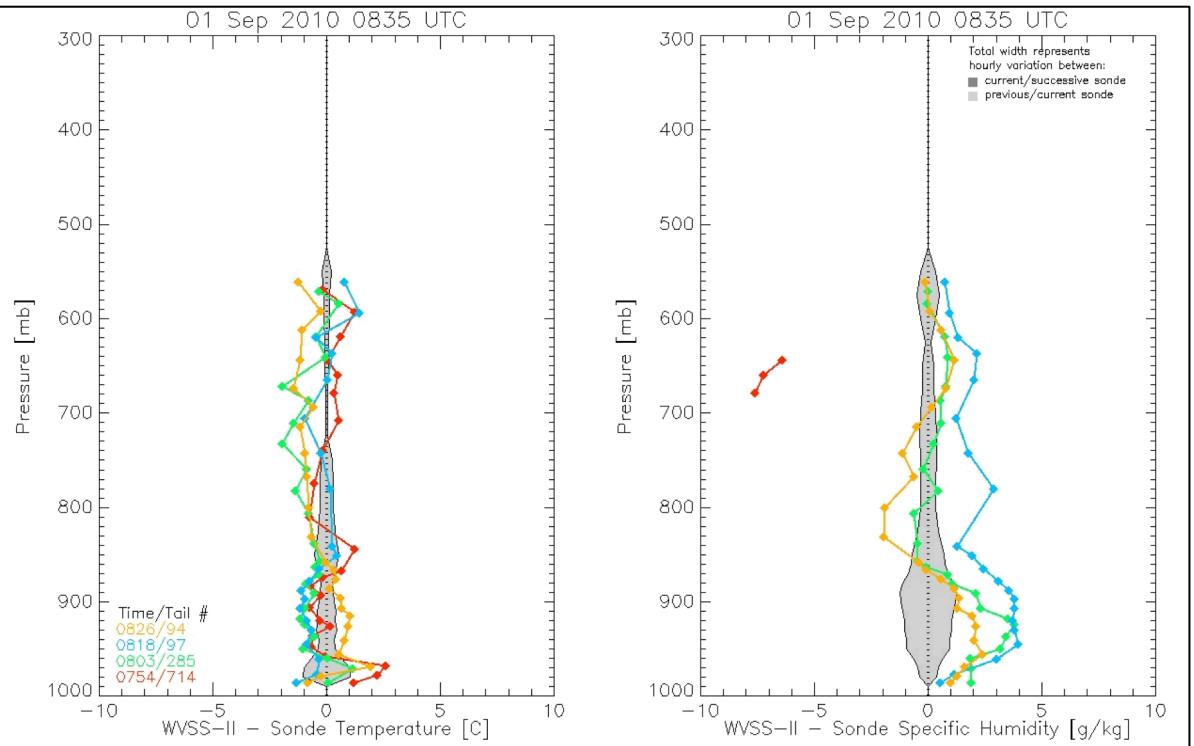

Figure B-38: Differences between RAOB and aircraft temperature and moisture profiles from within one hour of RAOB launch time of 0835 UTC on 01 Sept. 2010 at Rockford Illinois. Gray shaded indicate change between successive RAOB launches

Appendix C: Evaluations of fits of WVSS-II observations to ROABs using various temporal and vertical matching criteria.

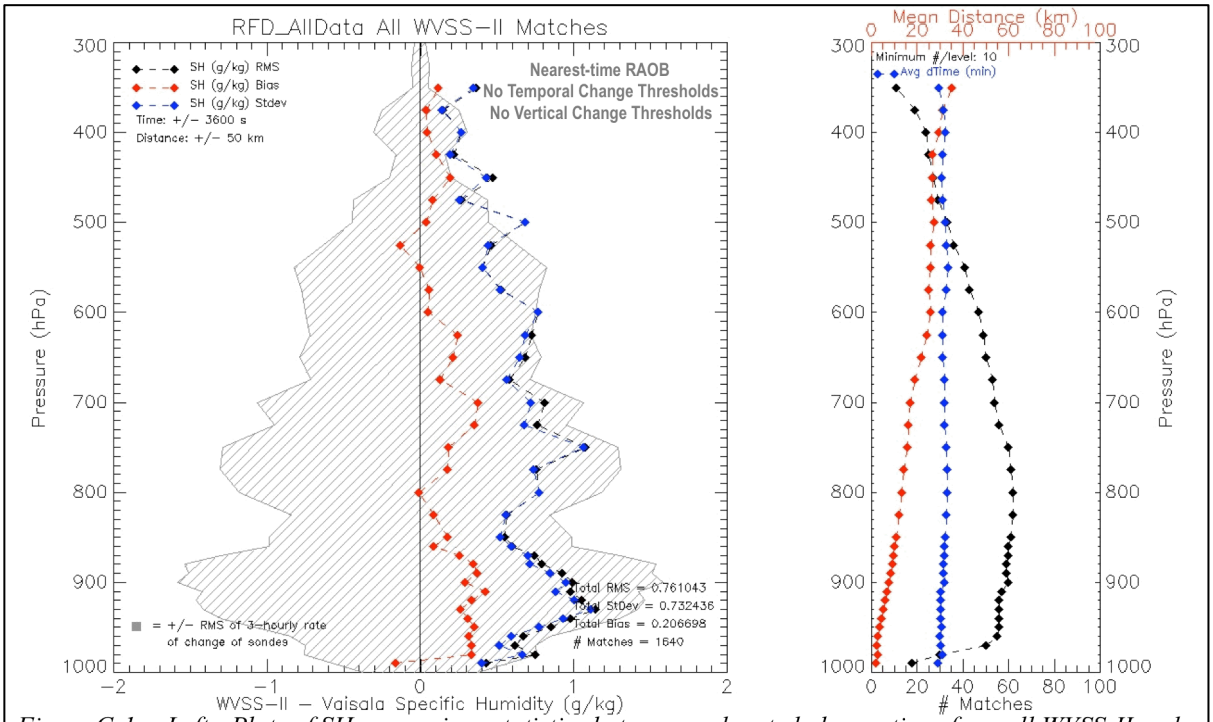

Figure C-1: - Left - Plots of SH comparison statistics between co-located observations from all WVSS-II and nearest-time RAOB report taken for all 2009-2010 inter-comparison periods at Rockford, IL (Bias, g/kg, red; RMS, g/kg, black; StDev, g/kg, blue). No temporal/vertical quality assurance applied. Hatching indicates RMS of change between successive ROAB observations throughout test period, normalized to 3-hourly rates. Right - Number of observations inter-comparisons used (black), mean distance between reports (km, red) and mean time difference between reports (minutes, blue).

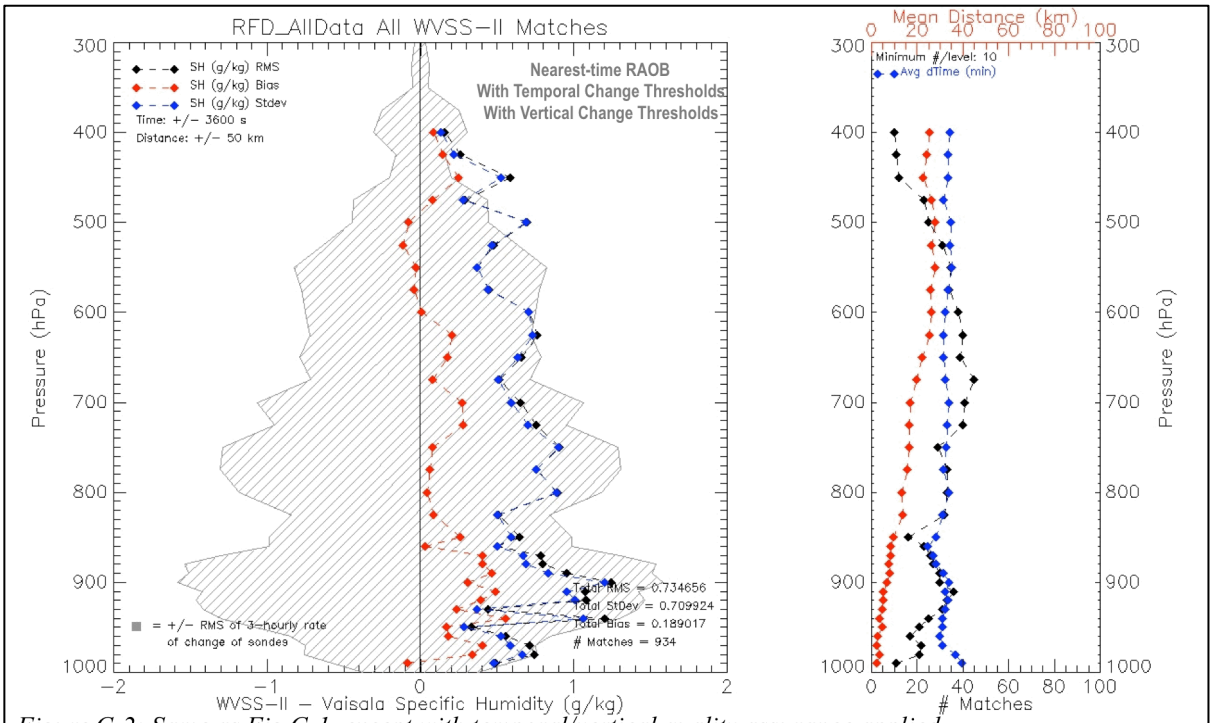

Figure C-2: Same as Fig C-1, except with temporal/vertical quality assurance applied.

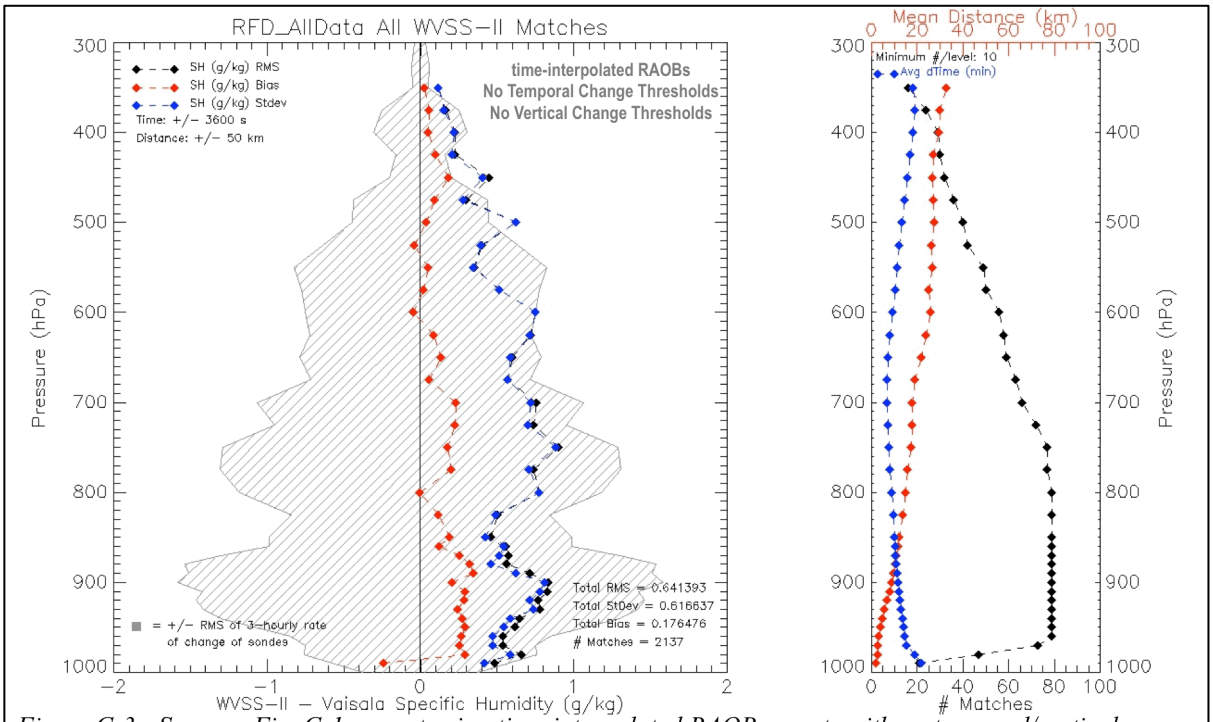

Figure C-3: Same as Fig. C-1, except using time-interpolated RAOB reports with no temporal/vertical quality assurance applied.

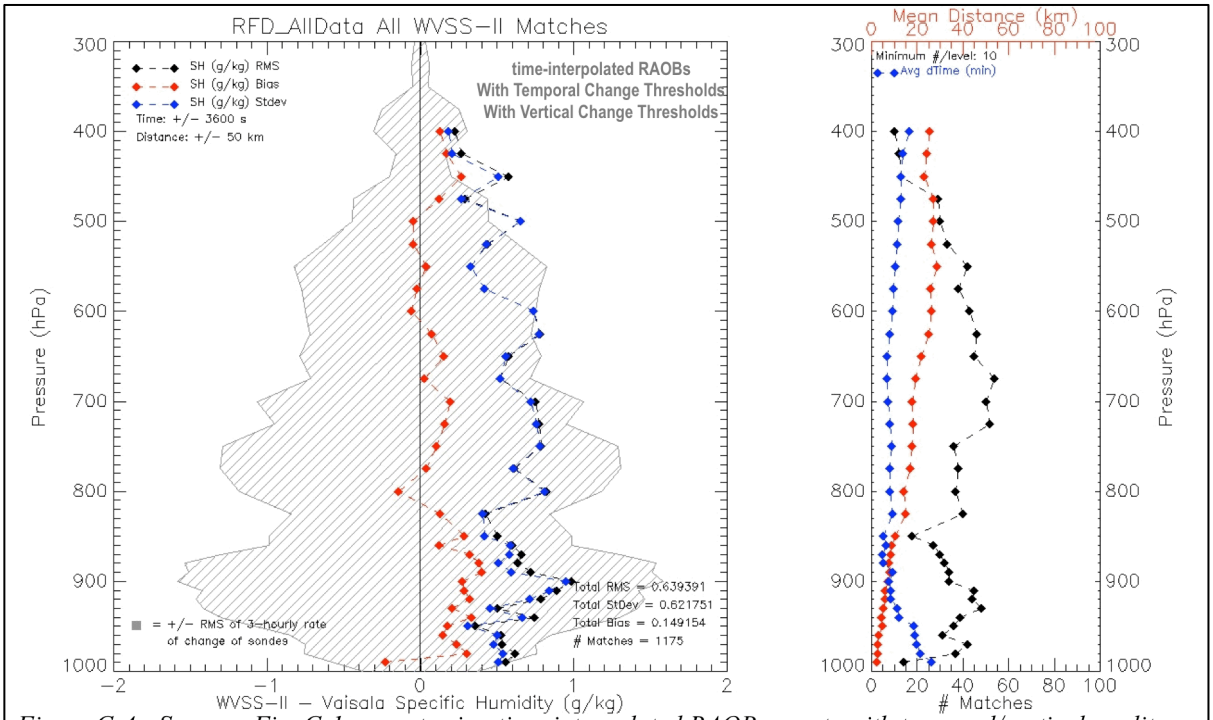

Figure C-4: Same as Fig. C-1, except using time-interpolated RAOB reports with temporal/vertical quality assurance applied.

SH RMS		Vertical/Time	Change Thresholds
	(g/kg)	No	Yes
Time	No	0.761	0.735
Interpolation	Yes	0.641	**0.639**

# SH Matches		Vertical/Time	Change Thresholds
		No	Yes
Time	No	1640	934
Interpolation	Yes	2137	**1175**

Figure C-5: Contingency Table of SH RMS and number of WVSS-II to RAOB matchups with/without Time Interpolation and Vertical/Temporal Tendency Limits. Selected method highlighted in bold.

Appendix D: Fits of individual-level WVSS-II reports to ROABs by time and distance (total and separated by ascent/descent)

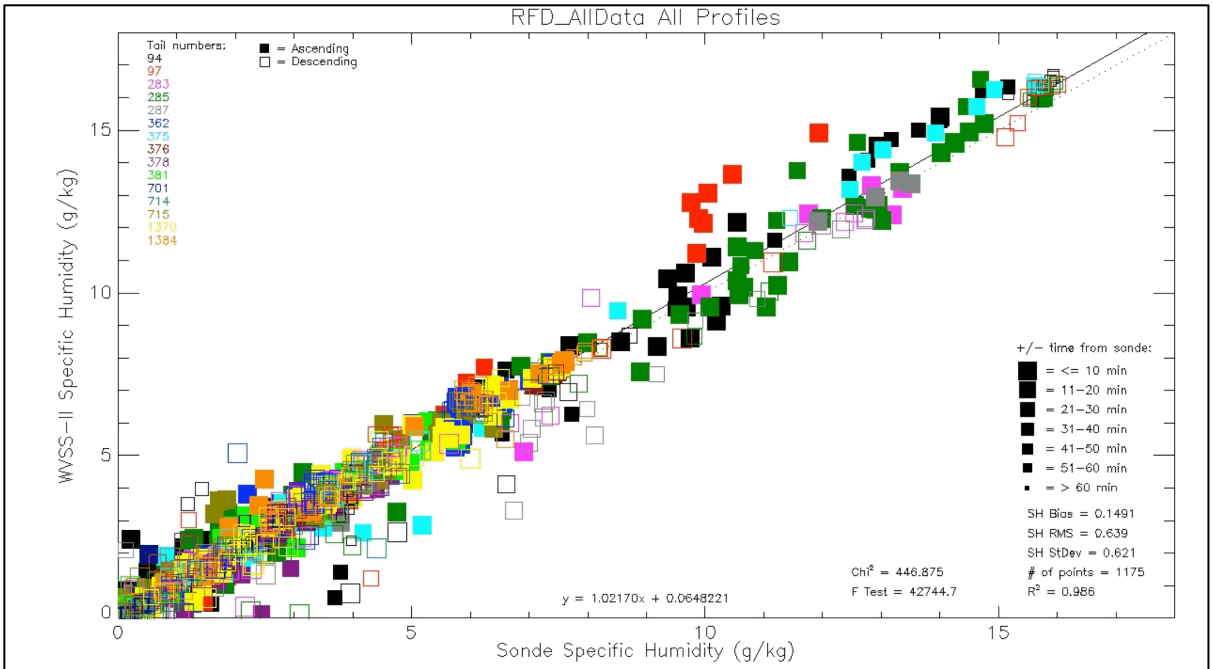

Figure D-1: Scatter plot of co-located WVSS-II and RAOB SH reports for all levels and all separation distances for all observation inter-comparison periods (left) and period from 27 April-10 May 2010 at Rockford, IL. Markers color coded by aircraft. Marker size indicates time spread between WVSS-II and RAOB observations – larger markers indicate matchups that are closer in time. Ascents presented as solid squares, descents by open squares. Fit statistics included in lower right.

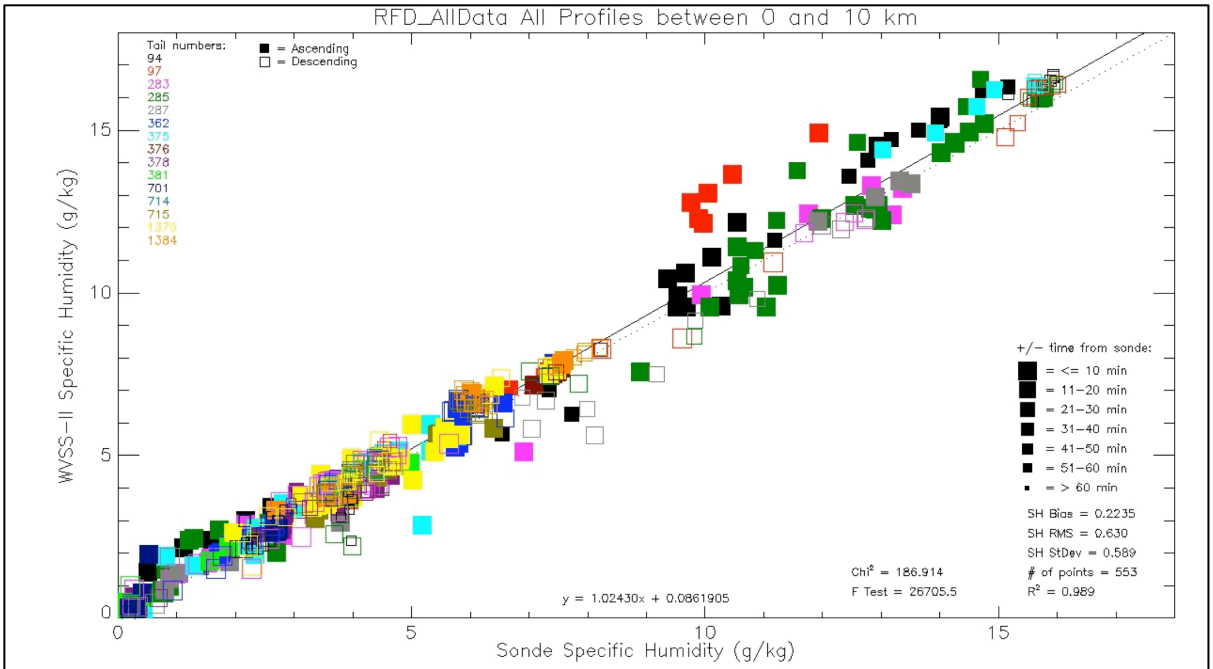

Figure D-2: Scatter plot of co-located WVSS-II and RAOB SH reports for all levels and 0-10 km separation distances for all observation inter-comparison periods (left) and period from 27 April-10 May 2010 at Rockford, IL. Markers color coded by aircraft. Marker size indicates time spread between WVSS-II and RAOB observations – larger markers indicate matchups that are closer in time. Ascents presented as solid squares, descents by open squares. Fit statistics included in lower right.

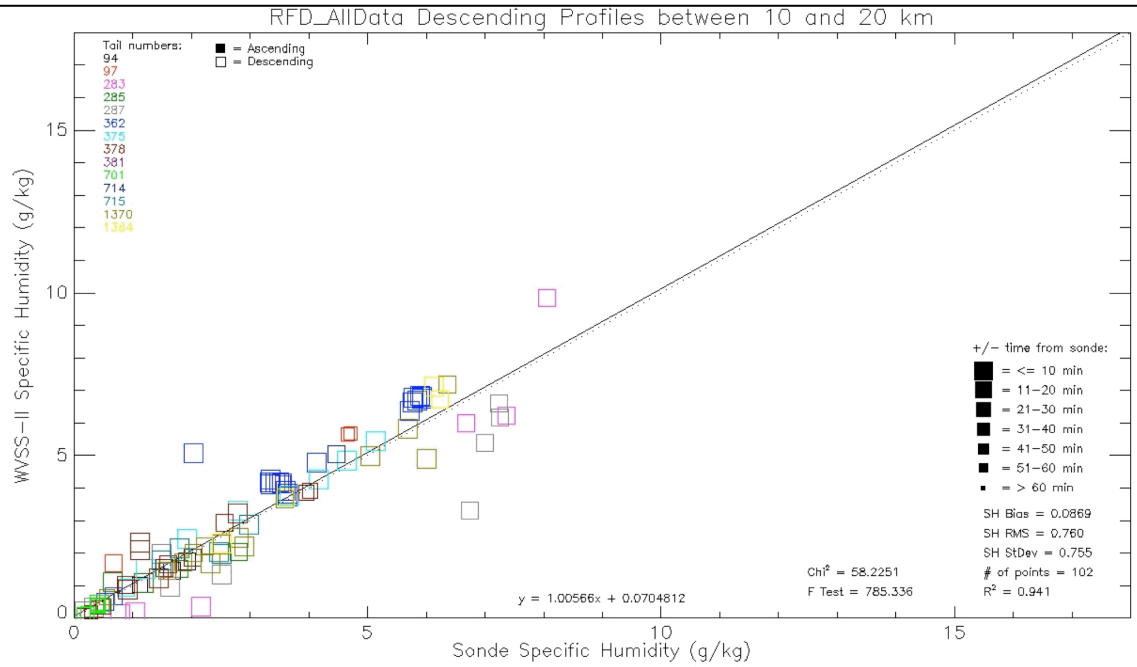

Figure D-3: Scatter plot of co-located WVSS-II and RAOB SH reports for all levels and 10-20 km separation distances for all observation inter-comparison periods (left) and period from 27 April-10 May 2010 at Rockford, IL. Markers color coded by aircraft. Marker size indicates time spread between WVSS-II and RAOB observations – larger markers indicate matchups that are closer in time. Ascents presented as solid squares, descents by open squares. Fit statistics included in lower right.

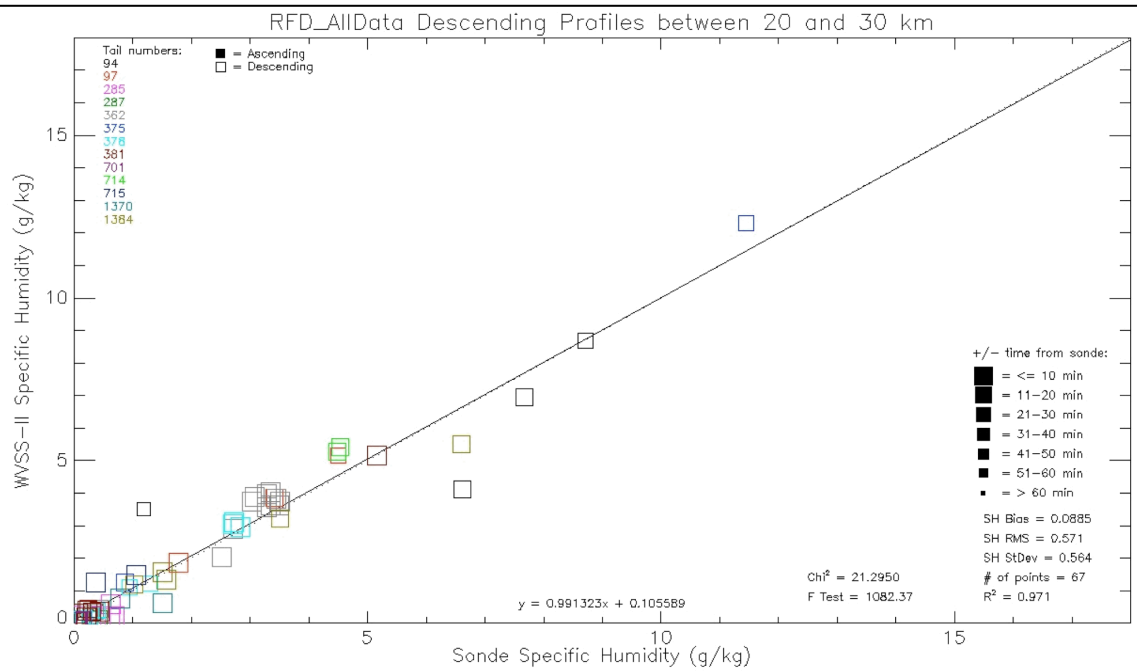

Figure D-4: Scatter plot of co-located WVSS-II and RAOB SH reports for all levels and 20-30 km separation distances for all observation inter-comparison periods (left) and period from 27 April-10 May 2010 at Rockford, IL. Markers color coded by aircraft. Marker size indicates time spread between WVSS-II and RAOB observations – larger markers indicate matchups that are closer in time. Ascents presented as solid squares, descents by open squares. Fit statistics included in lower right.

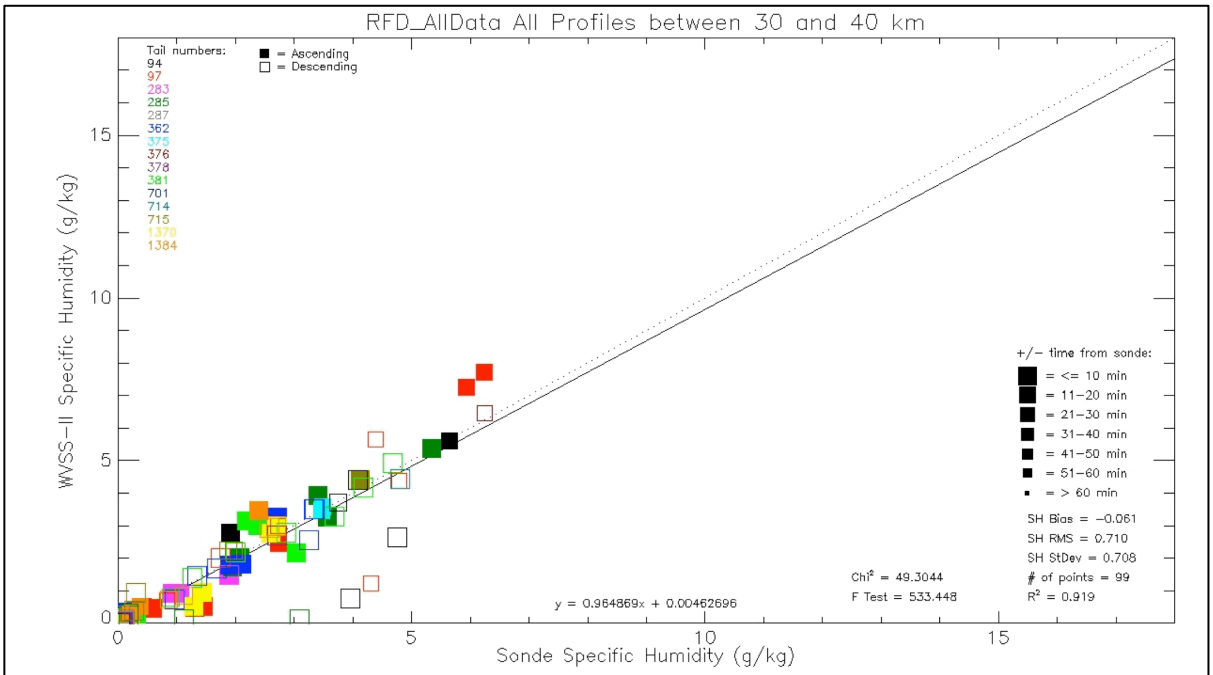

Figure D-5: Scatter plot of co-located WVSS-II and RAOB SH reports for all levels and 30-40 km separation distances for all observation inter-comparison periods (left) and period from 27 April-10 May 2010 at Rockford, IL. Markers color coded by aircraft. Marker size indicates time spread between WVSS-II and RAOB observations – larger markers indicate matchups that are closer in time. Ascents presented as solid squares, descents by open squares. Fit statistics included in lower right.

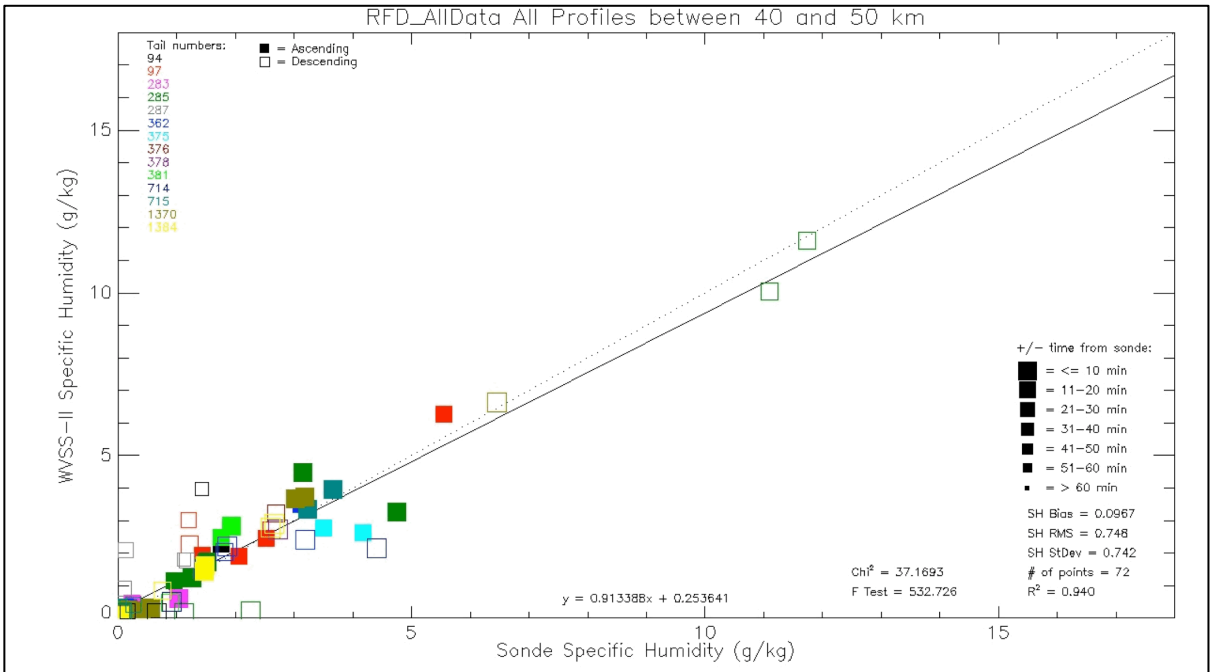

Figure D-6: Scatter plot of co-located WVSS-II and RAOB SH reports for all levels and 40-50 km separation distances for all observation inter-comparison periods (left) and period from 27 April-10 May 2010 at Rockford, IL. Markers color coded by aircraft. Marker size indicates time spread between WVSS-II and RAOB observations – larger markers indicate matchups that are closer in time. Ascents presented as solid squares, descents by open squares. Fit statistics included in lower right.

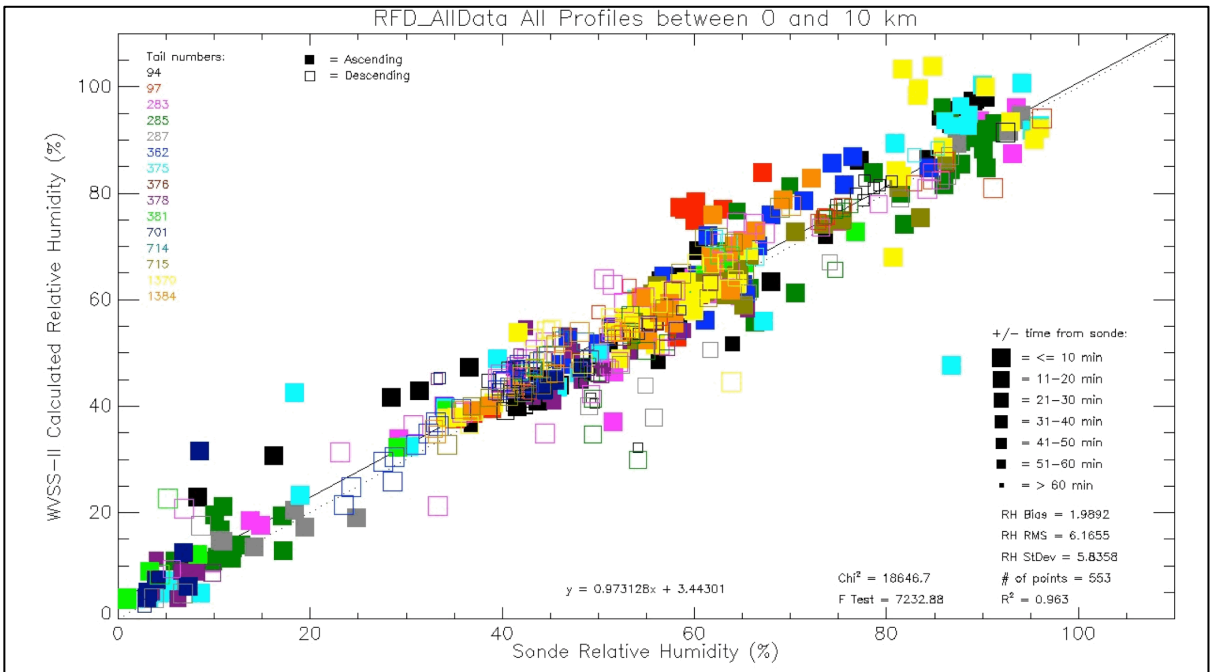

Figure D-7: Scatter plot of co-located WVSS-II and RAOB RH reports for all levels and 0-10 km separation distances for all observation inter-comparison periods (left) and period from 27 April-10 May 2010 at Rockford, IL. (RAOB temperatures used in both RH calculations) Markers color coded by aircraft. Marker size indicates time spread between WVSS-II and RAOB observations – larger markers indicate matchups that are closer in time. Ascents presented as solid squares, descents by open squares. Fit statistics included in lower right.

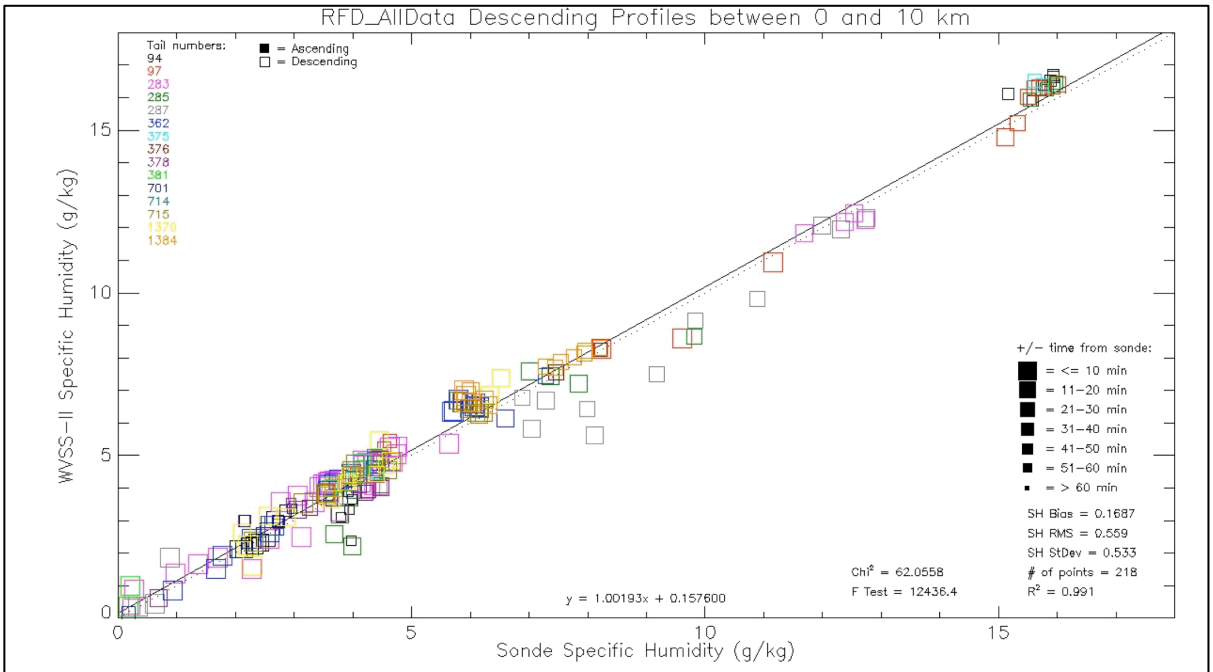

Figure D-8: Scatter plot of co-located WVSS-II and RAOB RH reports for all levels and 0-10 km separation distances for descending observation inter-comparison periods (left) and period from 27 April-10 May 2010 at Rockford, IL. (RAOB temperatures used in both RH calculations) Markers color coded by aircraft. Marker size indicates time spread between WVSS-II and RAOB observations – larger markers indicate matchups that are closer in time. Ascents presented as solid squares, descents by open squares. Fit statistics included in lower right.

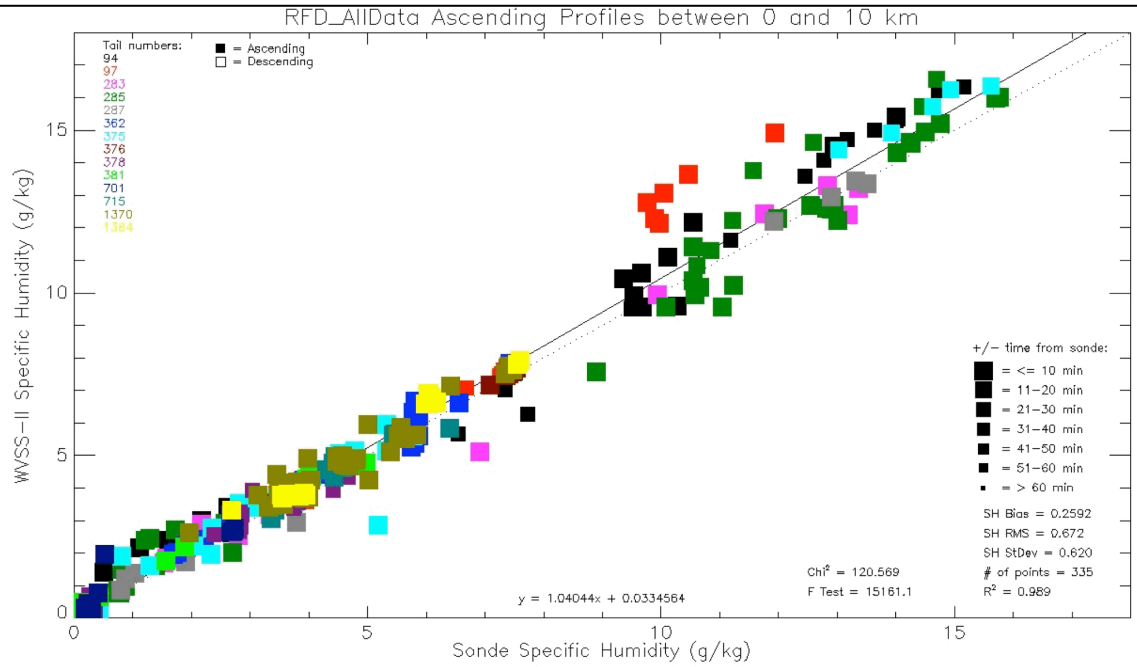

Figure D-9: Scatter plot of co-located WVSS-II and RAOB RH reports for all levels and 0-10 km separation distances for ascending observation inter-comparison periods (left) and period from 27 April-10 May 2010 at Rockford, IL. (RAOB temperatures used in both RH calculations) Markers color coded by aircraft. Marker size indicates time spread between WVSS-II and RAOB observations – larger markers indicate matchups that are closer in time. Ascents presented as solid squares, descents by open squares. Fit statistics included in lower right.

Appendix E: Evaluations of fits of AMDAR observation components to co-located ROABs (total and separated by ascent/descent)

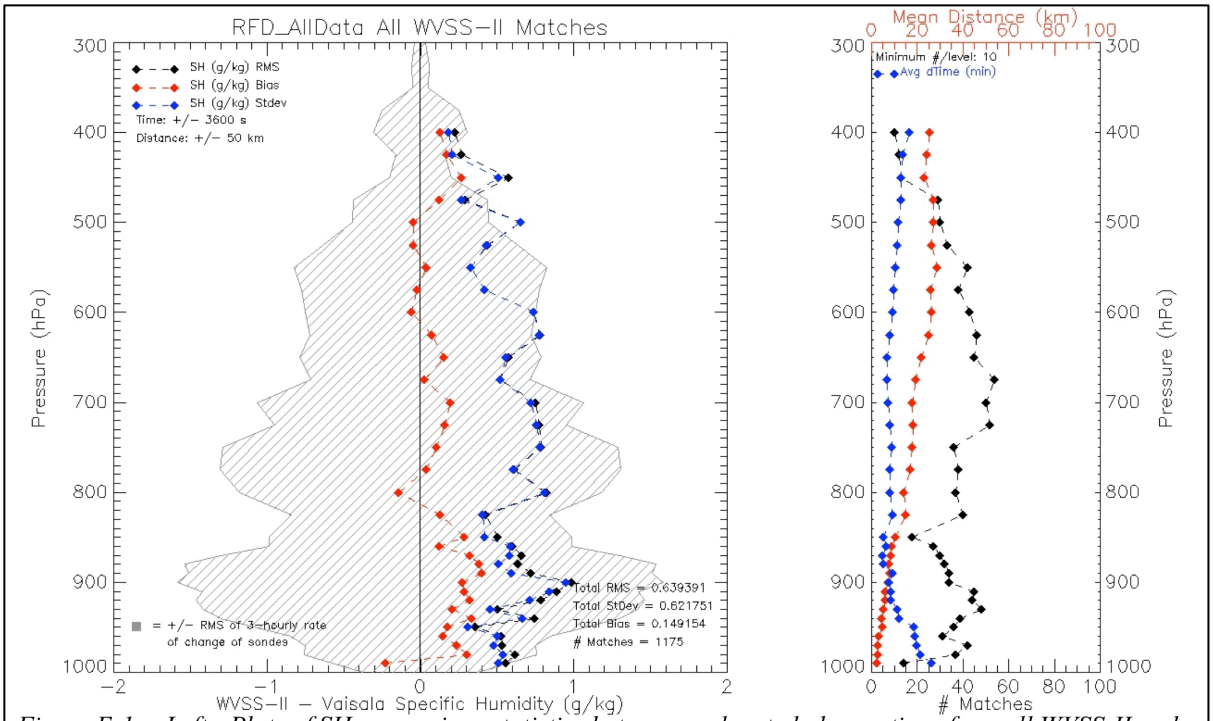

Figure E-1: - Left - Plots of SH comparison statistics between co-located observations from all WVSS-II and time-interpolated RAOB reports taken for all 2009-2010 inter-comparison periods at Rockford, IL (Bias, g/kg, red; RMS, g/kg, black; StDev, g/kg, blue). Hatching indicates RMS of change between successive ROAB observations throughout test period, normalized to 3-hourly rates. Right - Number of observations inter-comparisons used (black), mean distance between reports (km, red) and mean time difference between reports (minutes, blue).

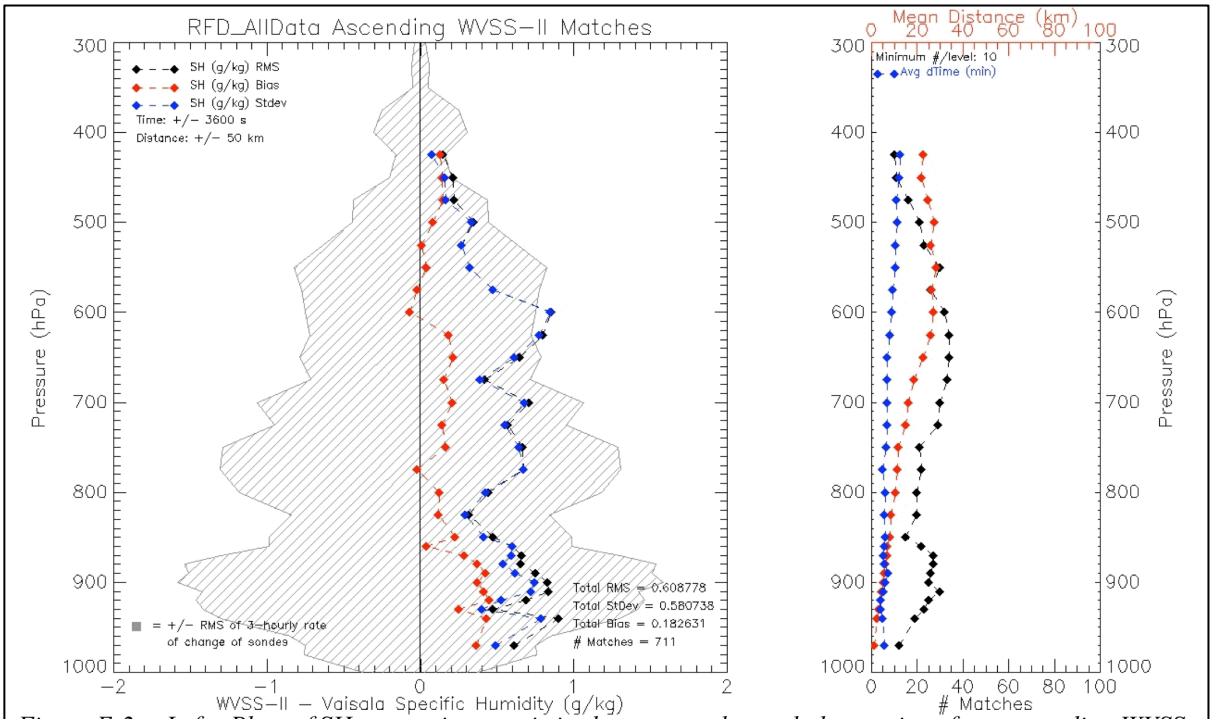

Figure E-2: - Left - Plots of SH comparison statistics between co-located observations from ascending WVSS-II and time-interpolated RAOB reports taken for all 2009-2010 inter-comparison periods at Rockford, IL (Bias, g/kg, red; RMS, g/kg, black; StDev, g/kg, blue). Hatching indicates RMS of change between successive ROAB observations throughout test period, normalized to 3-hourly rates. Right - Number of observations inter-comparisons used (black), mean distance between reports (km, red) and mean time difference between reports (minutes, blue).

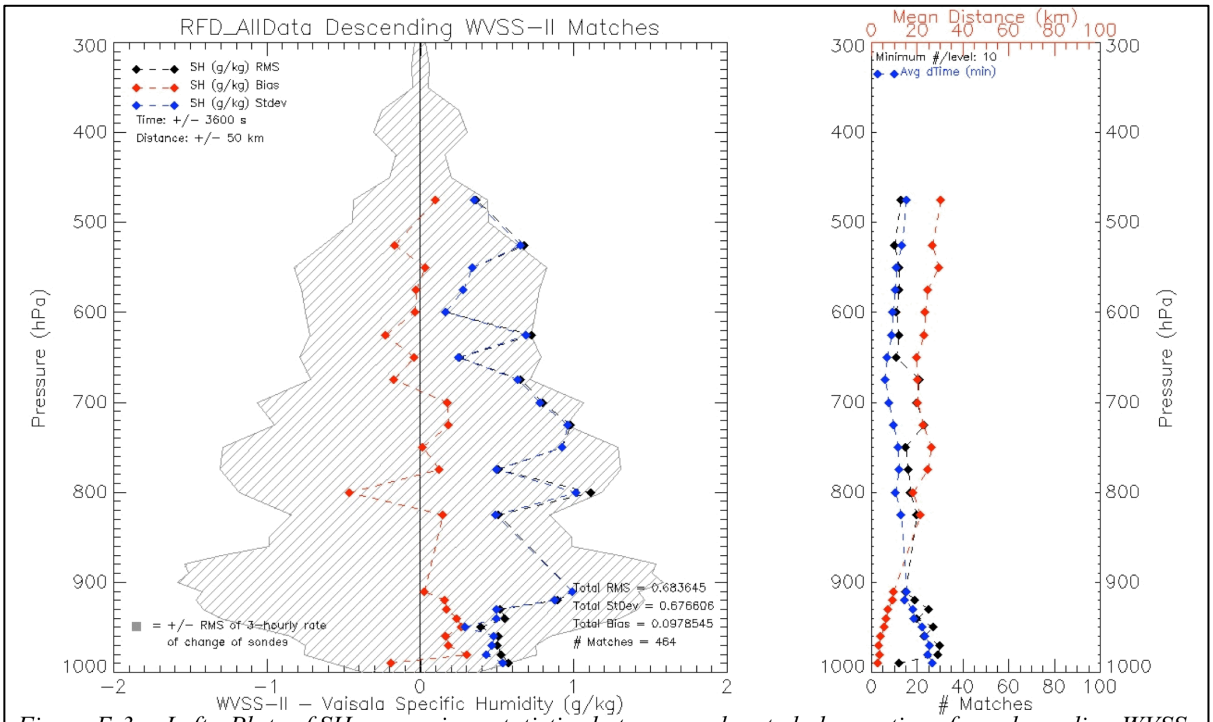

Figure E-3: - Left - Plots of SH comparison statistics between co-located observations from decending WVSS-II and time-interpolated RAOB reports taken for all 2009-2010 inter-comparison periods at Rockford, IL (Bias, g/kg, red; RMS, g/kg, black; StDev, g/kg, blue). Hatching indicates RMS of change between successive ROAB observations throughout test period, normalized to 3-hourly rates. Right - Number of observations inter-comparisons used (black), mean distance between reports (km, red) and mean time difference between reports (minutes, blue).

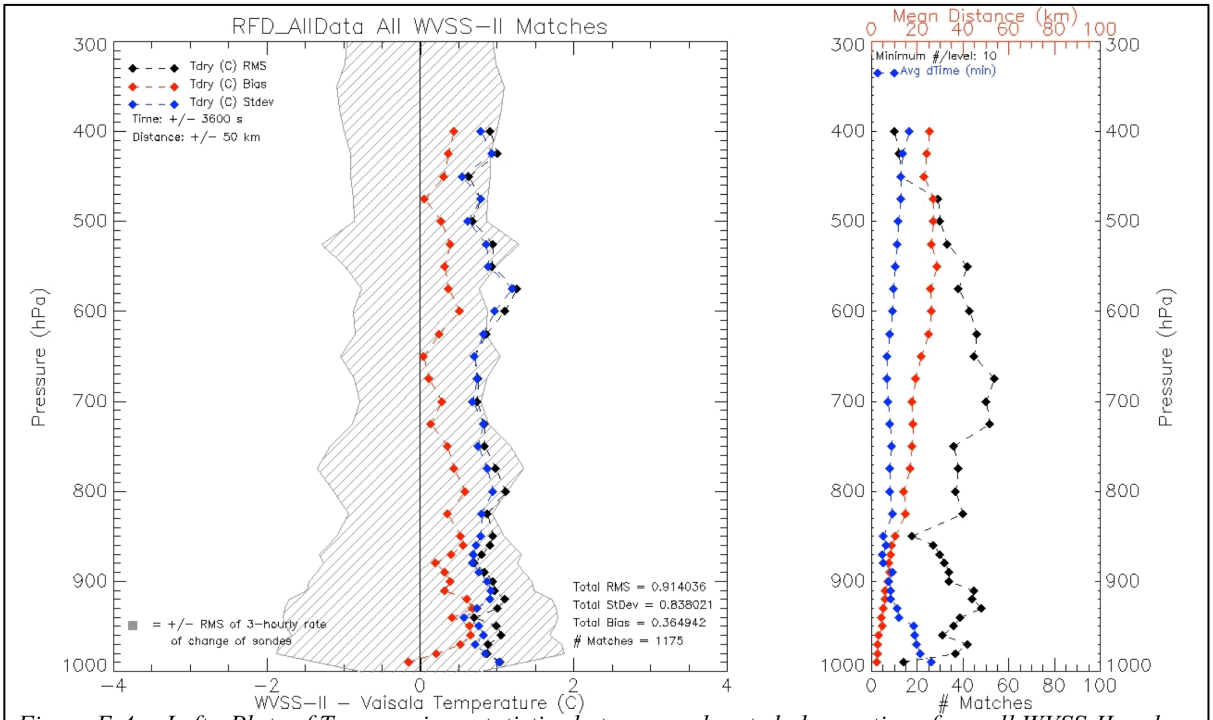

Figure E-4: - Left - Plots of T comparison statistics between co-located observations from all WVSS-II and time-interpolated RAOB reports taken for all 2009-2010 inter-comparison periods at Rockford, IL (Bias, g/kg, red; RMS, g/kg, black; StDev, g/kg, blue). Hatching indicates RMS of change between successive ROAB observations throughout test period, normalized to 3-hourly rates. Right - Number of observations inter-comparisons used (black), mean distance between reports (km, red) and mean time difference between reports (minutes, blue).

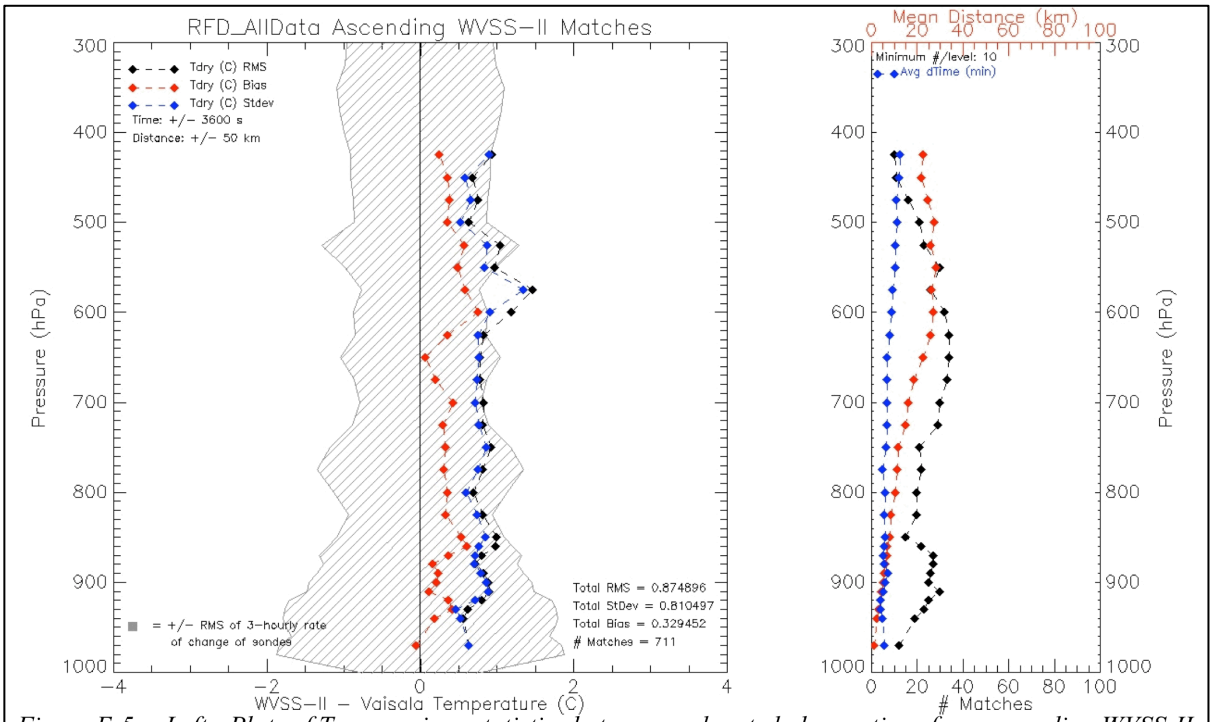

Figure E-5: - Left - Plots of T comparison statistics between co-located observations from ascending WVSS-II and time-interpolated RAOB reports taken for all 2009-2010 inter-comparison periods at Rockford, IL (Bias, g/kg, red; RMS, g/kg, black; StDev, g/kg, blue). Hatching indicates RMS of change between successive ROAB observations throughout test period, normalized to 3-hourly rates. Right - Number of observations inter-comparisons used (black), mean distance between reports (km, red) and mean time difference between reports (minutes, blue).

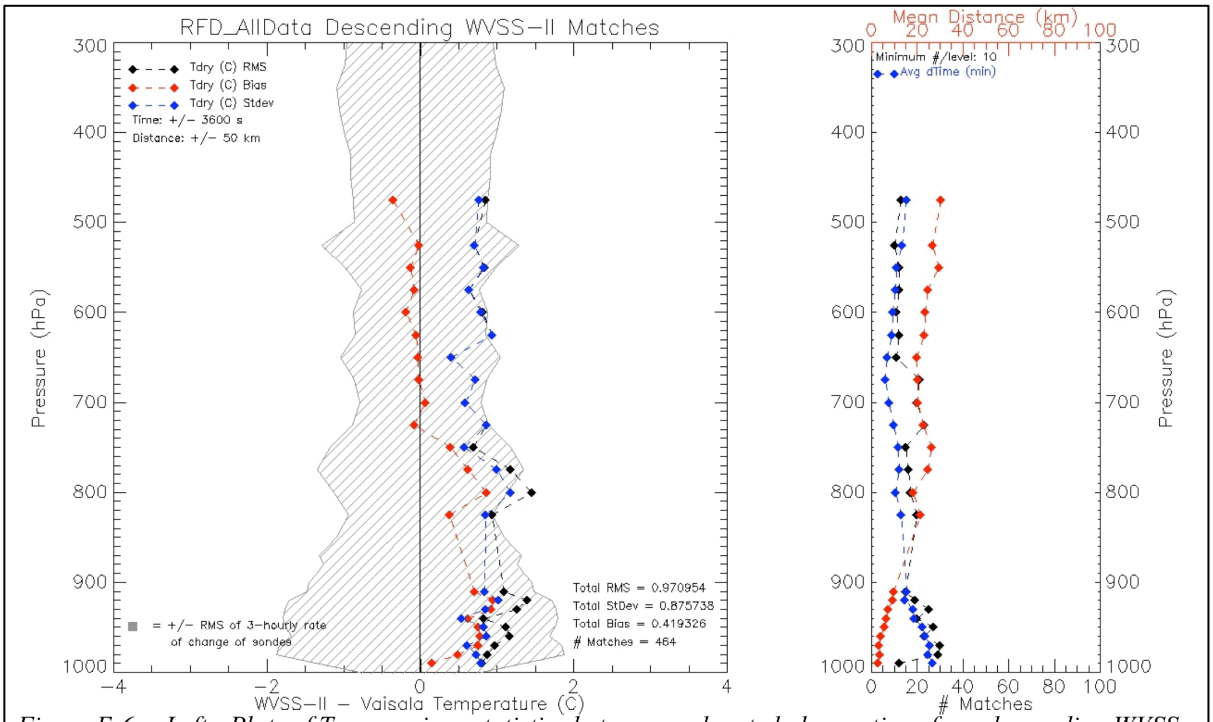

Figure E-6: - Left - Plots of T comparison statistics between co-located observations from descending WVSS-II and time-interpolated RAOB reports taken for all 2009-2010 inter-comparison periods at Rockford, IL (Bias, g/kg, red; RMS, g/kg, black; StDev, g/kg, blue). Hatching indicates RMS of change between successive ROAB observations throughout test period, normalized to 3-hourly rates. Right - Number of observations inter-comparisons used (black), mean distance between reports (km, red) and mean time difference between reports (minutes, blue).

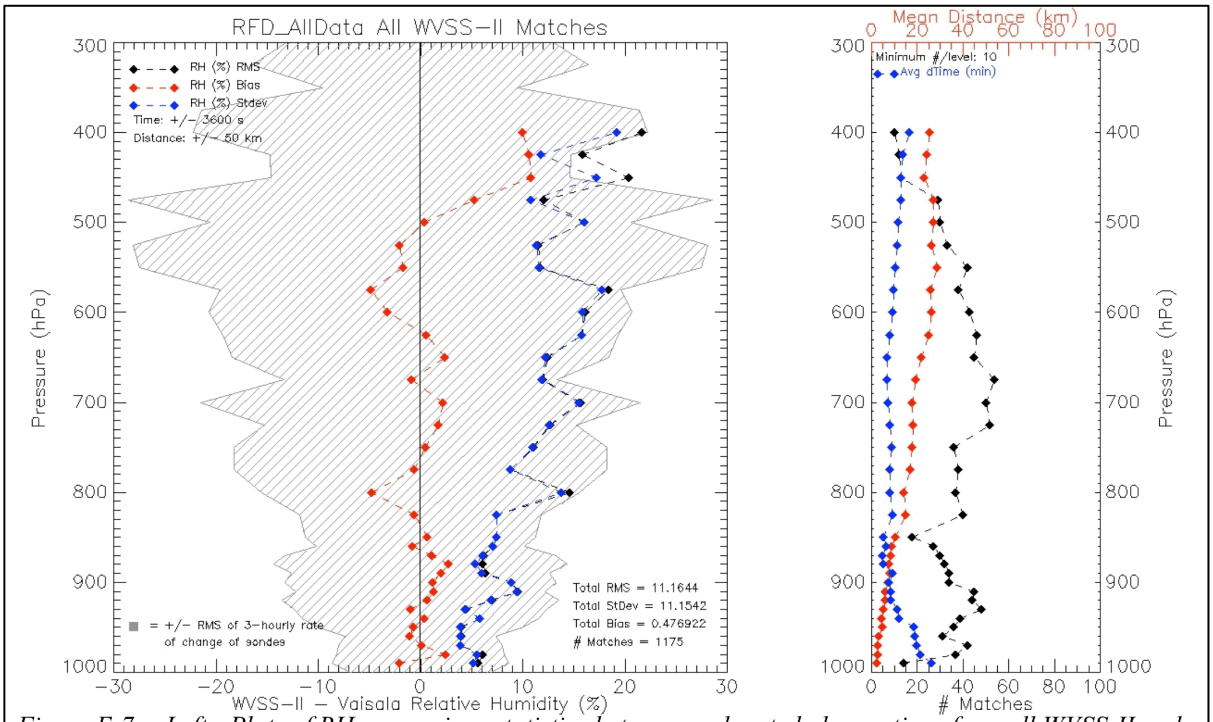

Figure E-7: - Left - Plots of RH comparison statistics between co-located observations from all WVSS-II and time-interpolated RAOB reports taken for all 2009-2010 inter-comparison periods at Rockford, IL (Bias, g/kg, red; RMS, g/kg, black; StDev, g/kg, blue). Hatching indicates RMS of change between successive ROAB observations throughout test period, normalized to 3-hourly rates. Right - Number of observations inter-comparisons used (black), mean distance between reports (km, red) and mean time difference between reports (minutes, blue).

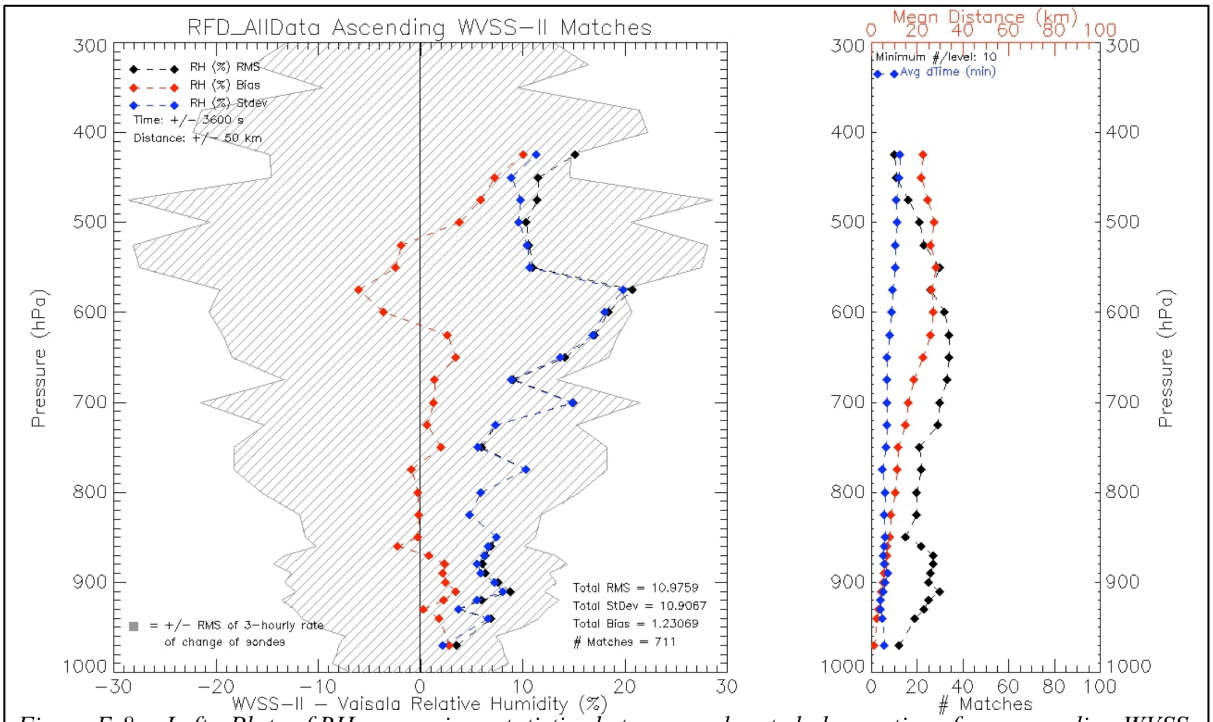

Figure E-8: - Left - Plots of RH comparison statistics between co-located observations from ascending WVSS-II and time-interpolated RAOB reports taken for all 2009-2010 inter-comparison periods at Rockford, IL (Bias, g/kg, red; RMS, g/kg, black; StDev, g/kg, blue). Hatching indicates RMS of change between successive ROAB observations throughout test period, normalized to 3-hourly rates. Right - Number of observations inter-comparisons used (black), mean distance between reports (km, red) and mean time difference between reports (minutes, blue).

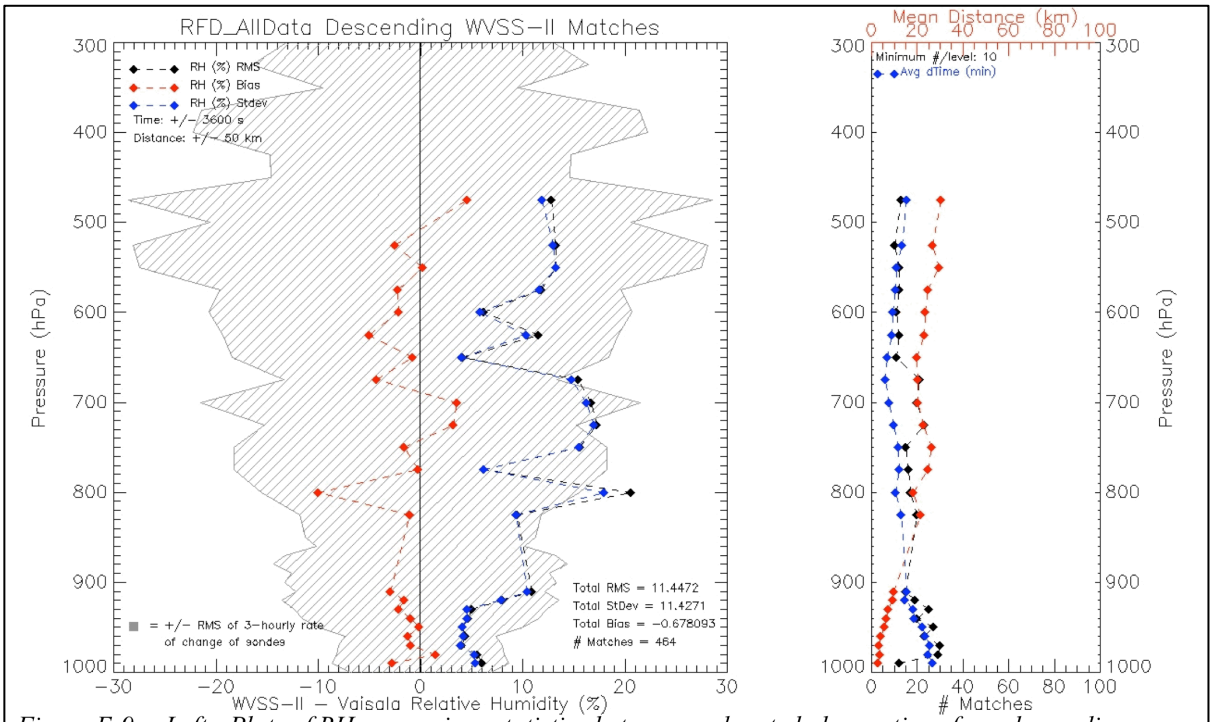

Figure E-9: - Left - Plots of RH comparison statistics between co-located observations from descending WVSS-II and time-interpolated RAOB reports taken for all 2009-2010 inter-comparison periods at Rockford, IL (Bias, g/kg, red; RMS, g/kg, black; StDev, g/kg, blue). Hatching indicates RMS of change between successive ROAB observations throughout test period, normalized to 3-hourly rates. Right - Number of observations inter-comparisons used (black), mean distance between reports (km, red) and mean time difference between reports (minutes, blue).

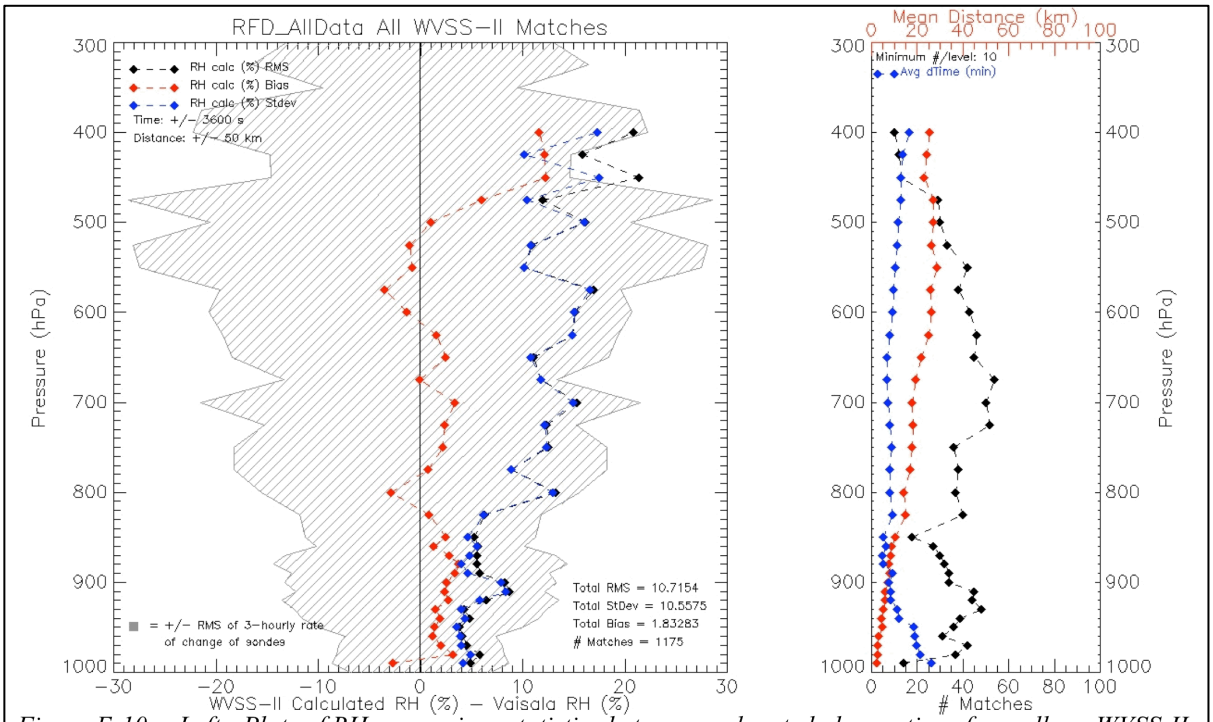

Figure E-10: - Left - Plots of RH comparison statistics between co-located observations from all WVSS-II and time-interpolated RAOB reports taken for all 2009-2010 inter-comparison periods at Rockford, IL (Bias, g/kg, red; RMS, g/kg, black; StDev, g/kg, blue). RAOB T data used in both all calculations. Hatching indicates RMS of change between successive ROAB observations throughout test period, normalized to 3-hourly rates. Right - Number of observations inter-comparisons used (black), mean distance between reports (km, red) and mean time difference between reports (minutes, blue).

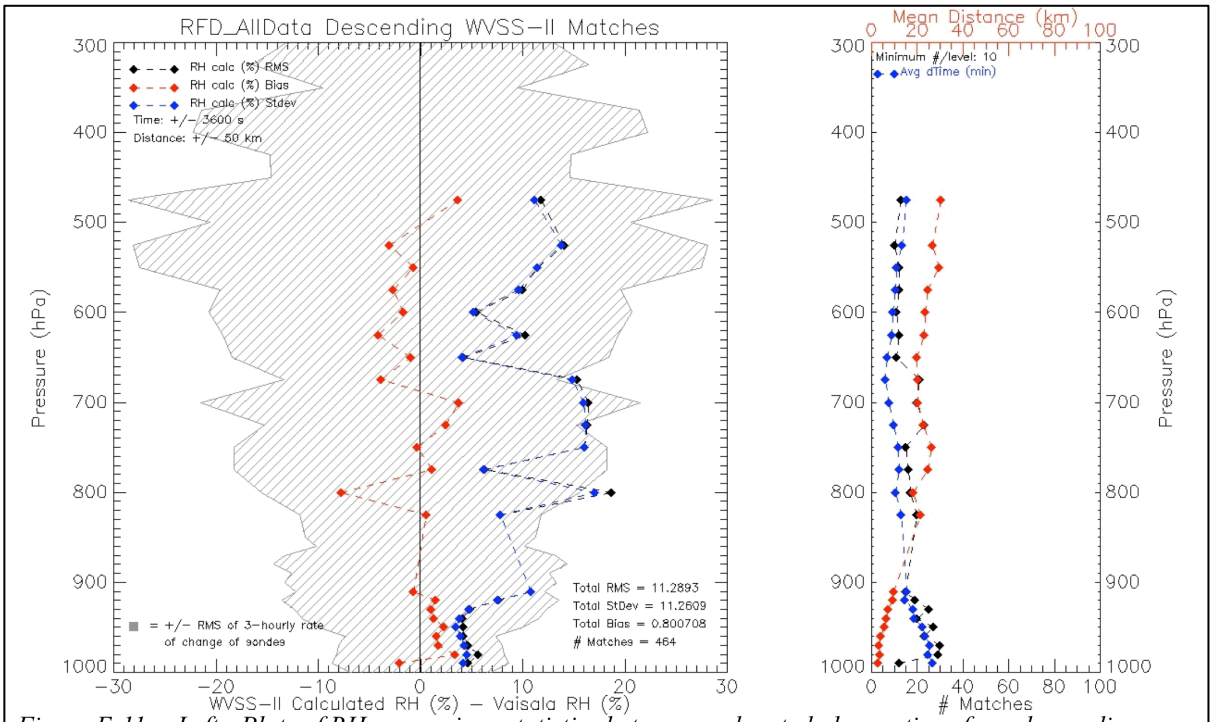

Figure E-11: - Left - Plots of RH comparison statistics between co-located observations from descending WVSS-II and time-interpolated RAOB reports taken for all 2009-2010 inter-comparison periods at Rockford, IL (Bias, g/kg, red; RMS, g/kg, black; StDev, g/kg, blue). RAOB T data used in both all calculations. Hatching indicates RMS of change between successive ROAB observations throughout test period, normalized to 3-hourly rates. Right - Number of observations inter-comparisons used (black), mean distance between reports (km, red) and mean time difference between reports (minutes, blue).

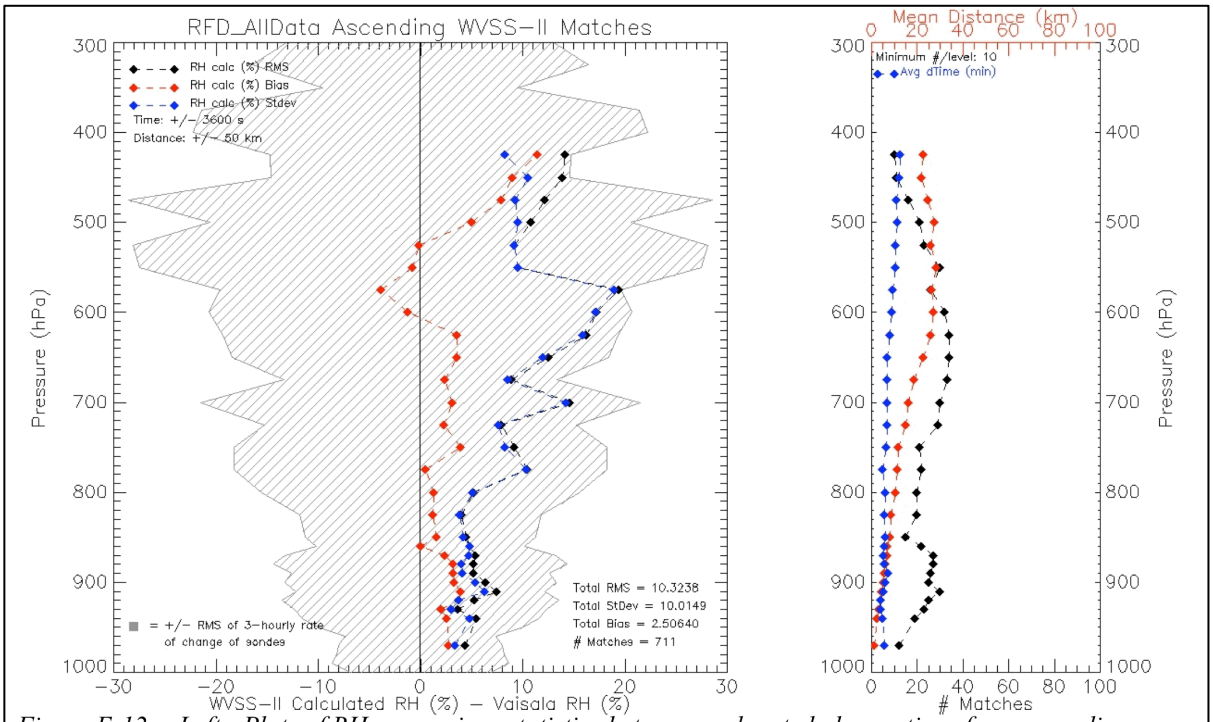

Figure E-12: - Left - Plots of RH comparison statistics between co-located observations from ascending WVSS-II and time-interpolated RAOB reports taken for all 2009-2010 inter-comparison periods at Rockford, IL (Bias, g/kg, red; RMS, g/kg, black; StDev, g/kg, blue). RAOB T data used in both all calculations. Hatching indicates RMS of change between successive ROAB observations throughout test period, normalized to 3-hourly rates. Right - Number of observations inter-comparisons used (black), mean distance between reports (km, red) and mean time difference between reports (minutes, blue).

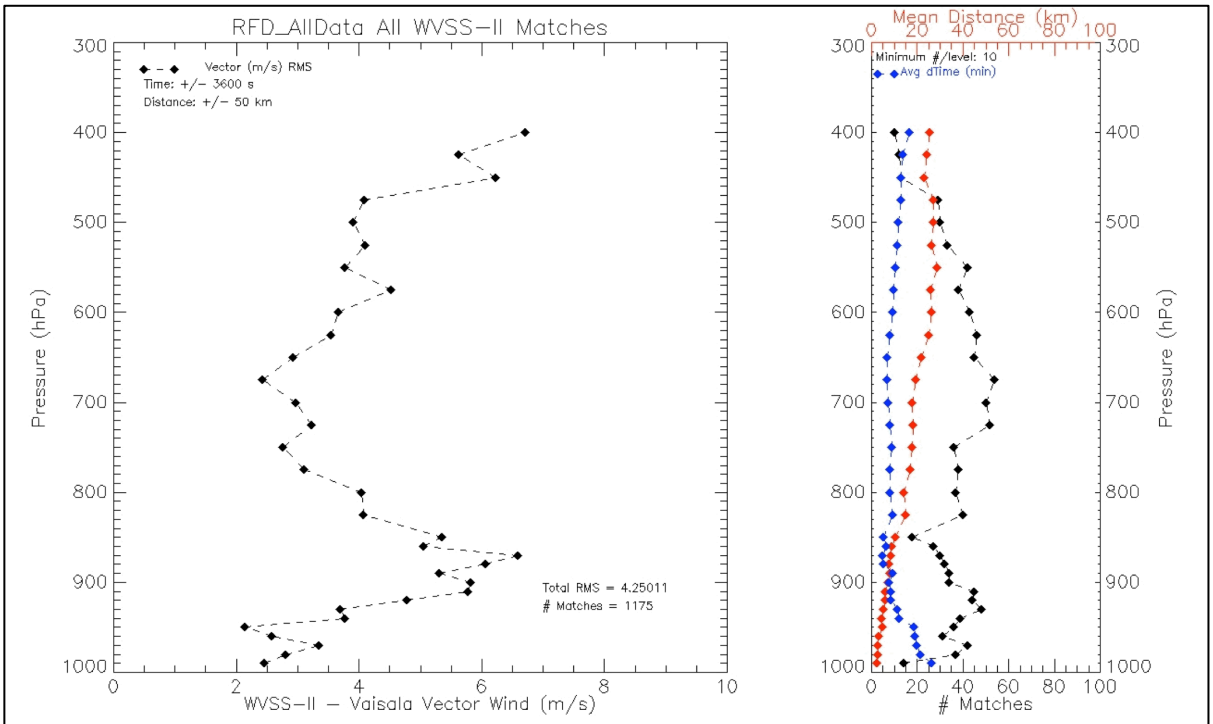

Figure E-13: - Left - Plots of moisture Wind comparison statistics between co-located observations from all WVSS-II and time-interpolated RAOB reports taken for all 2009-2010 inter-comparison periods at Rockford, IL. [RMS Vector difference, (m/s).] Right - Number of observations inter-comparisons used (black), mean distance between reports (km, red) and mean time difference between reports (minutes, blue).

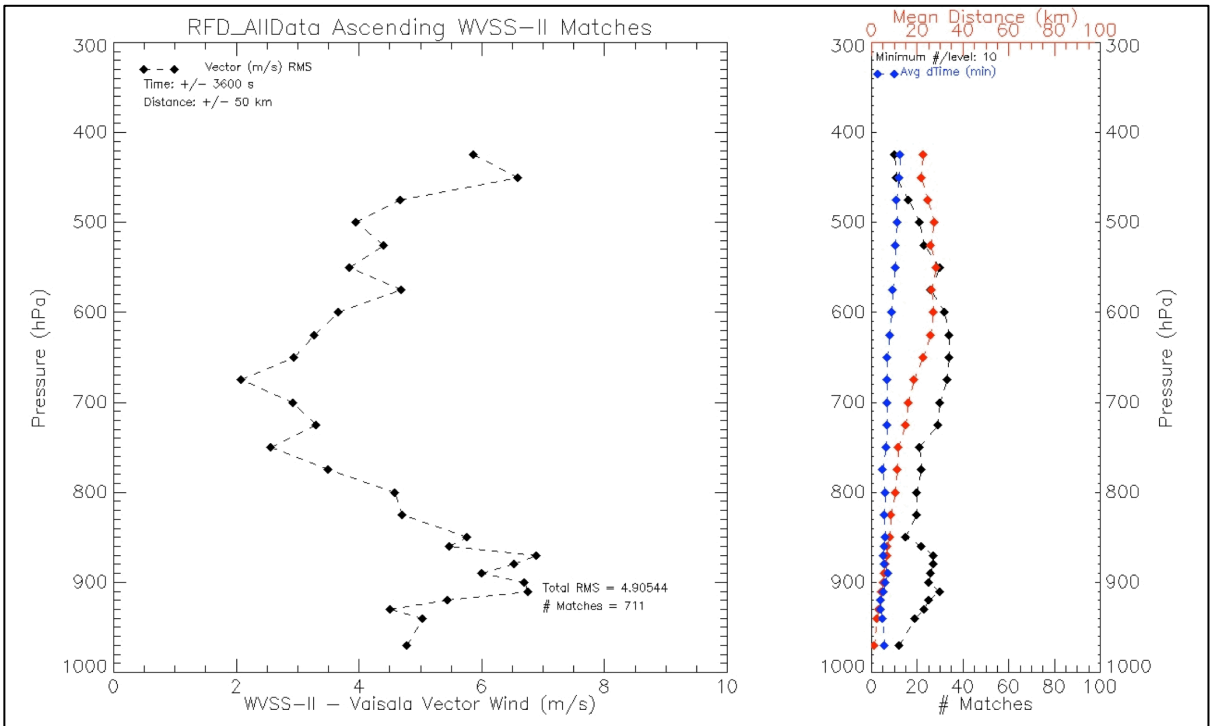

Figure E-14: - Left - Plots of moisture Wind comparison statistics between co-located observations from ascending WVSS-II and time-interpolated RAOB reports taken for all 2009-2010 inter-comparison periods at Rockford, IL. [RMS Vector difference, (m/s).] Right - Number of observations inter-comparisons used (black), mean distance between reports (km, red) and mean time difference between reports (minutes, blue).

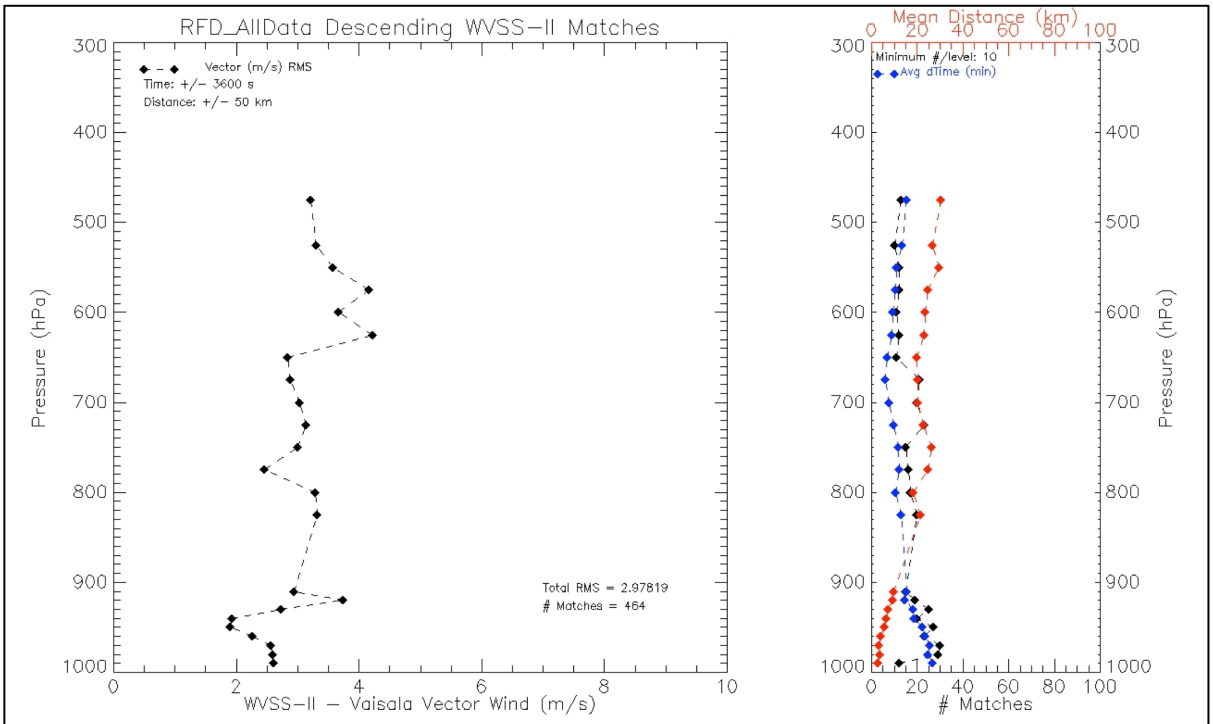

Figure E-15: - Left - Plots of moisture Wind comparison statistics between co-located observations from descending WVSS-II and time-interpolated RAOB reports taken for all 2009-2010 inter-comparison periods at Rockford, IL. [RMS Vector difference, (m/s).] Right - Number of observations inter-comparisons used (black), mean distance between reports (km, red) and mean time difference between reports (minutes, blue).

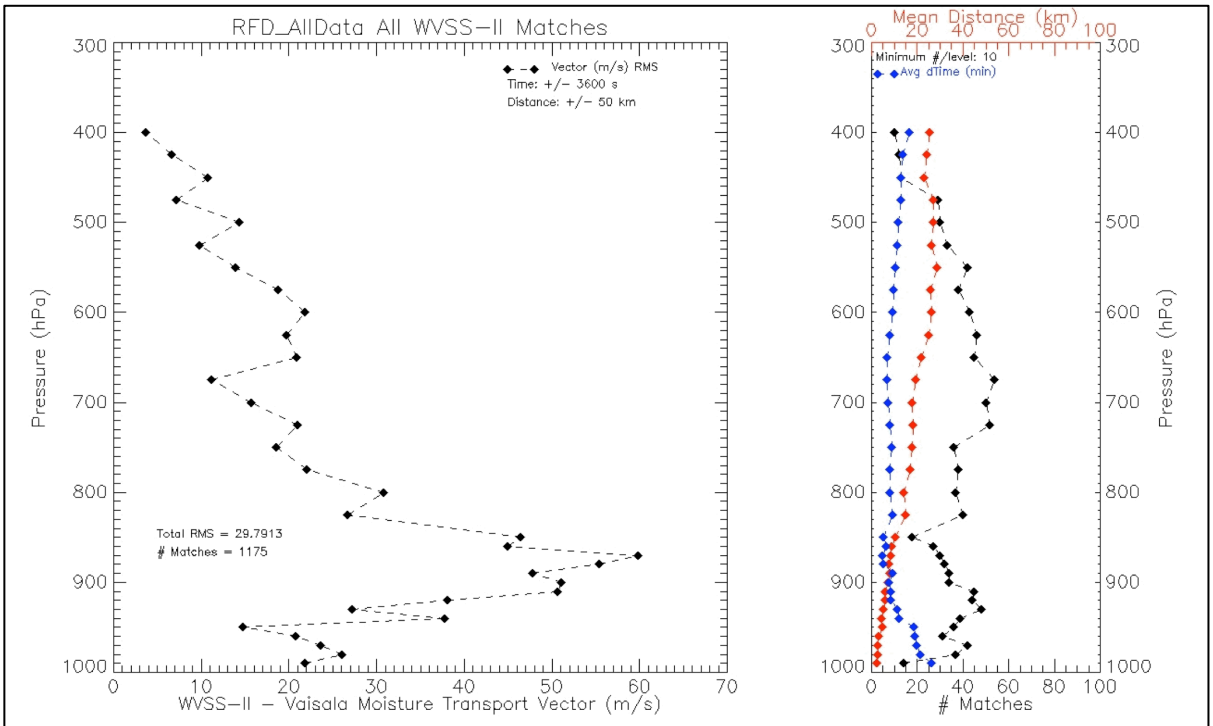

*Figure E-16: - Left - Plots of moisture transport (SH*Wind) comparison statistics between co-located observations from all WVSS-II and time-interpolated RAOB reports taken for all 2009-2010 inter-comparison periods at Rockford, IL. (RMS Vector difference, (g/kg)*(m/s). Right - Number of observations inter-comparisons used (black), mean distance between reports (km, red) and mean time difference between reports (minutes, blue).*

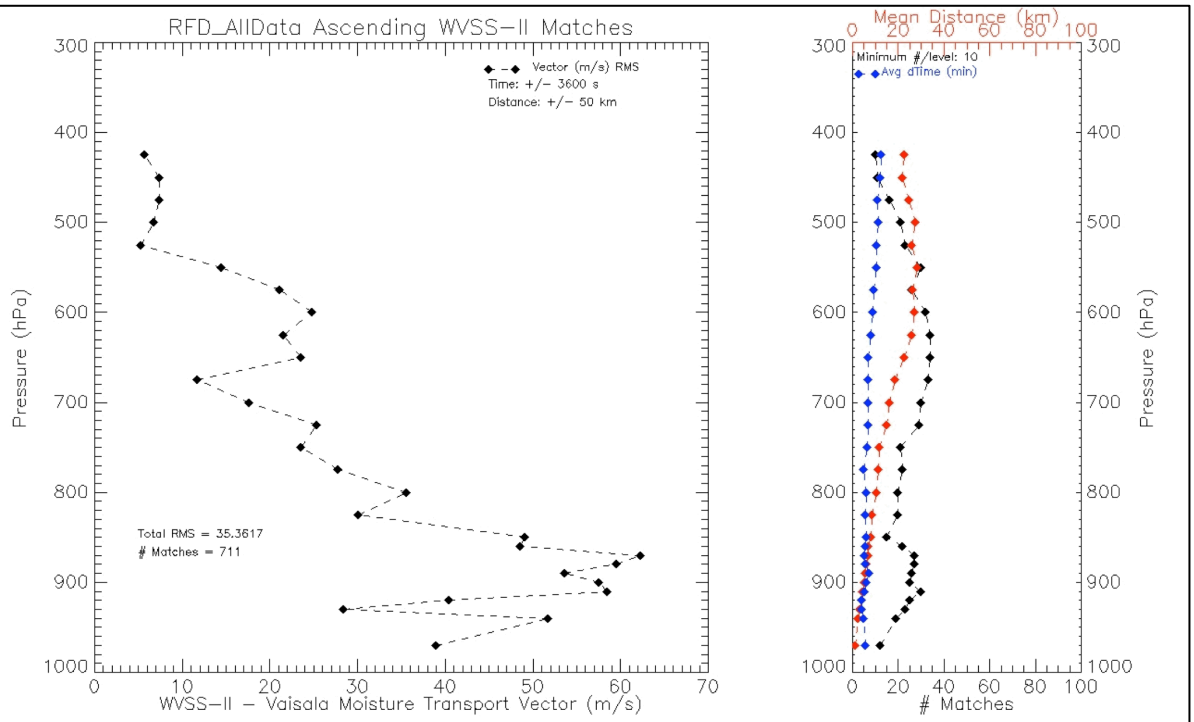

*Figure E-17: - Left - Plots of moisture transport (SH*Wind) comparison statistics between co-located observations from aascending WVSS-II and time-interpolated RAOB reports taken for all 2009-2010 inter-comparison periods at Rockford, IL. (RMS Vector difference, (g/kg)*(m/s). Right - Number of observations inter-comparisons used (black), mean distance between reports (km, red) and mean time difference between reports (minutes, blue).*

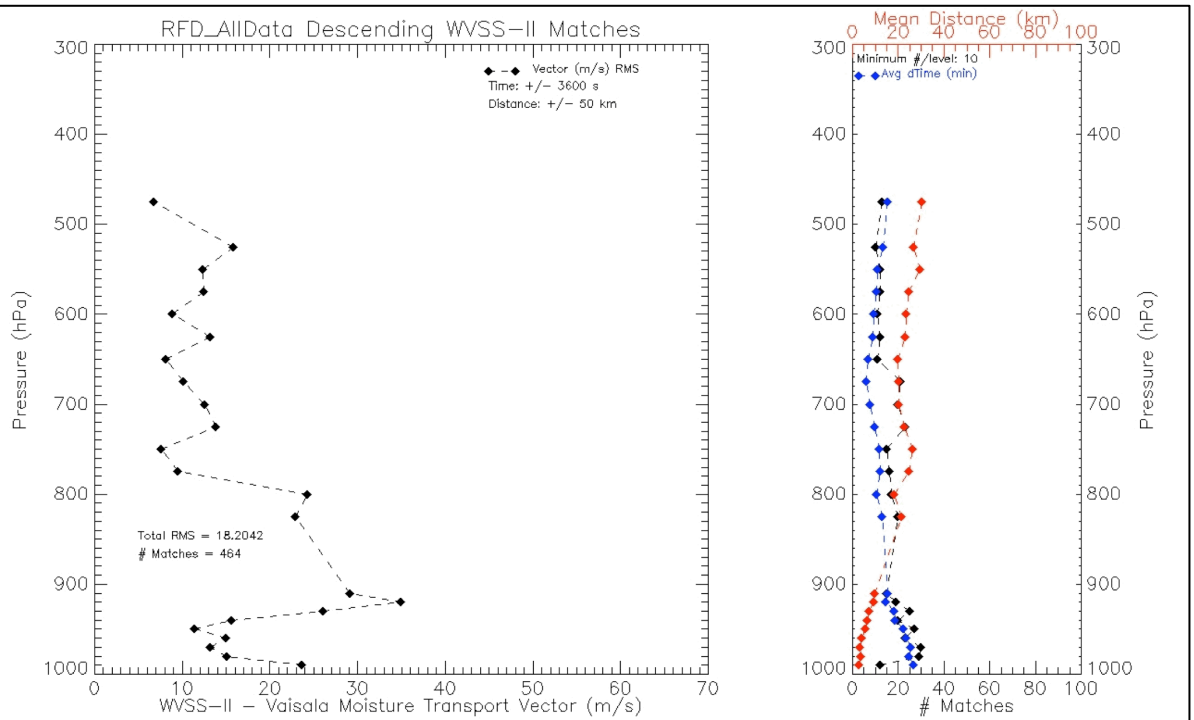

*Figure E-18: - Left - Plots of moisture transport (SH*Wind) comparison statistics between co-located observations from descending WVSS-II and time-interpolated RAOB reports taken for all 2009-2010 inter-comparison periods at Rockford, IL. (RMS Vector difference, (g/kg)*(m/s). Right - Number of observations inter-comparisons used (black), mean distance between reports (km, red) and mean time difference between reports (minutes, blue).*

Appendix F: Intercomparison of Winds and Moisture Transport observations derived from co-located AMDAR and RAOBs reports (total and separated by ascent/desent)

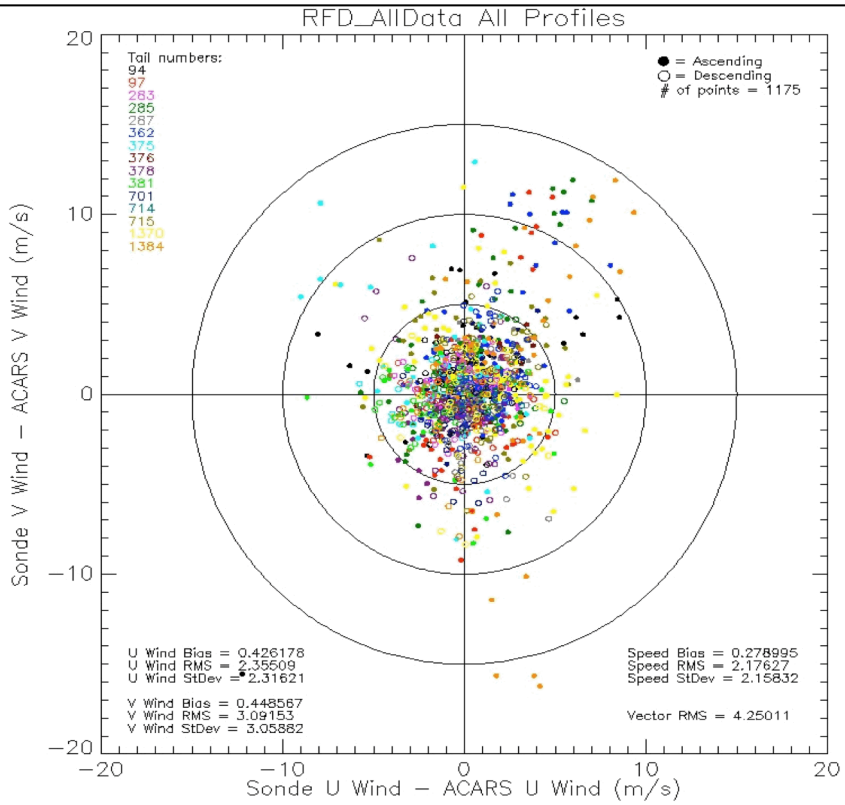

Figure F-1: Plot of Wind comparisons between co-located observations from all WVSS-II equipped aircraft and time-interpolated RAOB reports taken for all 2009-2010 inter-comparison periods at Rockford, IL. Color coded by aircraft. Statistics in lower-left and -right.

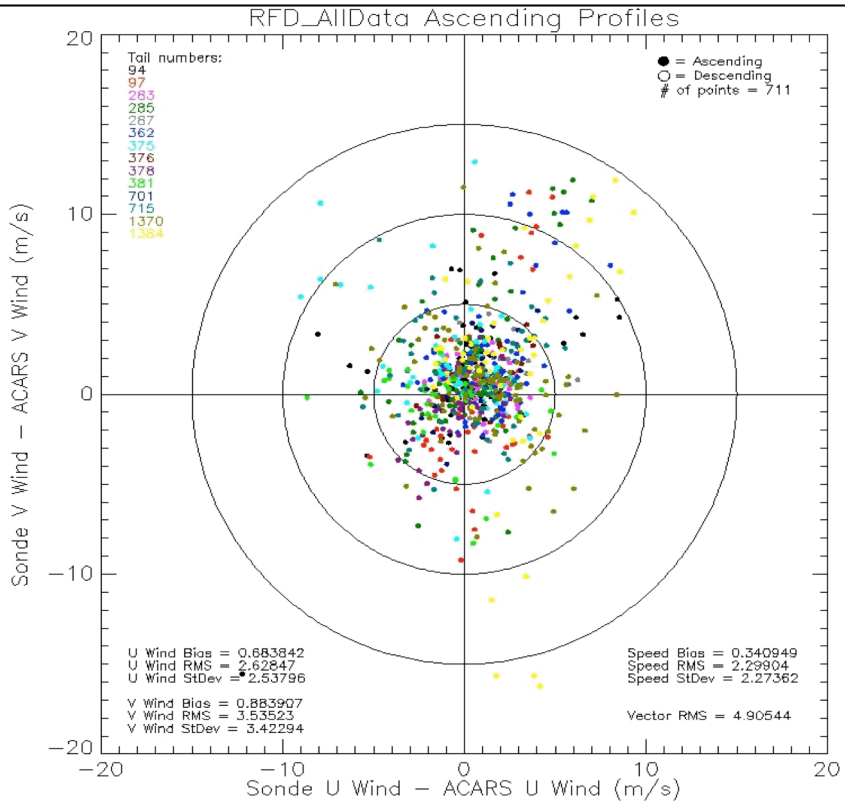

Figure F-2: Plot of Wind comparisons between co-located observations from ascending WVSS-II equipped aircraft and time-interpolated RAOB reports taken for all 2009-2010 inter-comparison periods at Rockford, IL. Color coded by aircraft. Statistics in lower-left and -right.

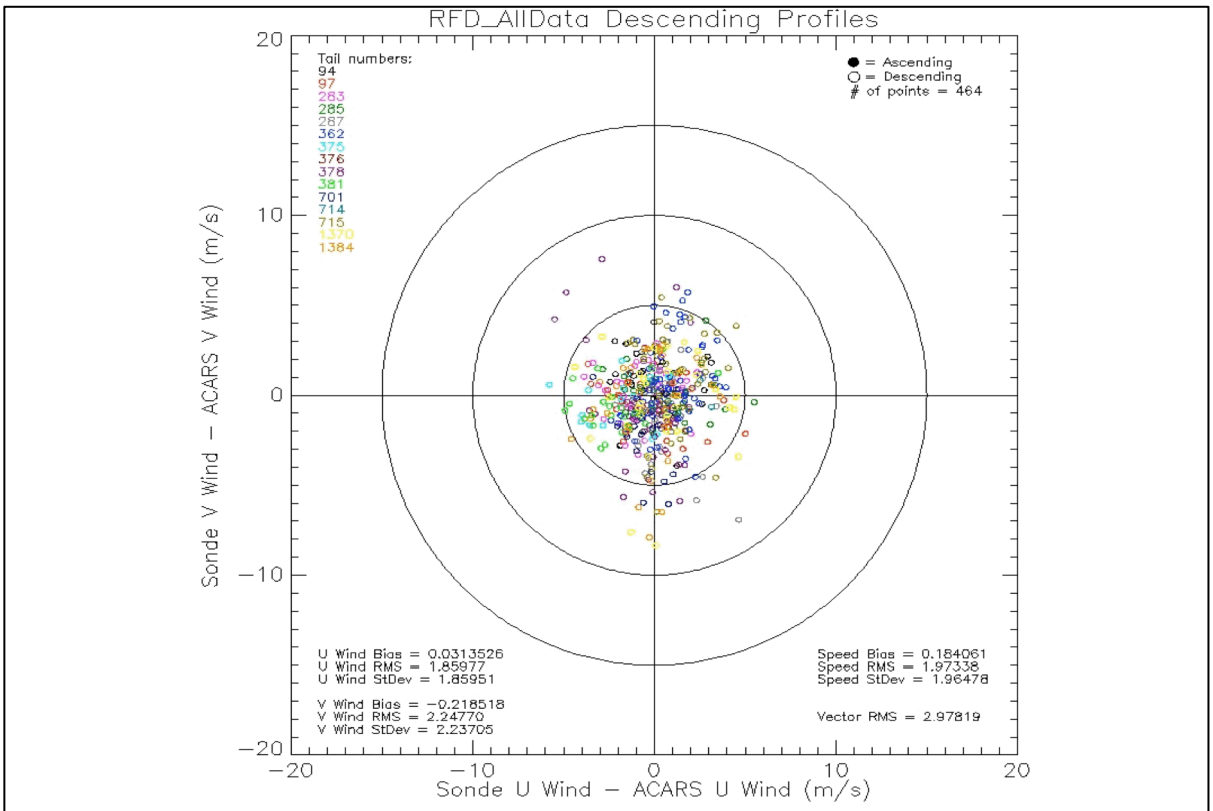

Figure F-3: Plot of Wind comparisons between co-located observations from descending WVSS-II equipped aircraft and time-interpolated RAOB reports taken for all 2009-2010 inter-comparison periods at Rockford, IL. Color coded by aircraft. Statistics in lower-left and -right.

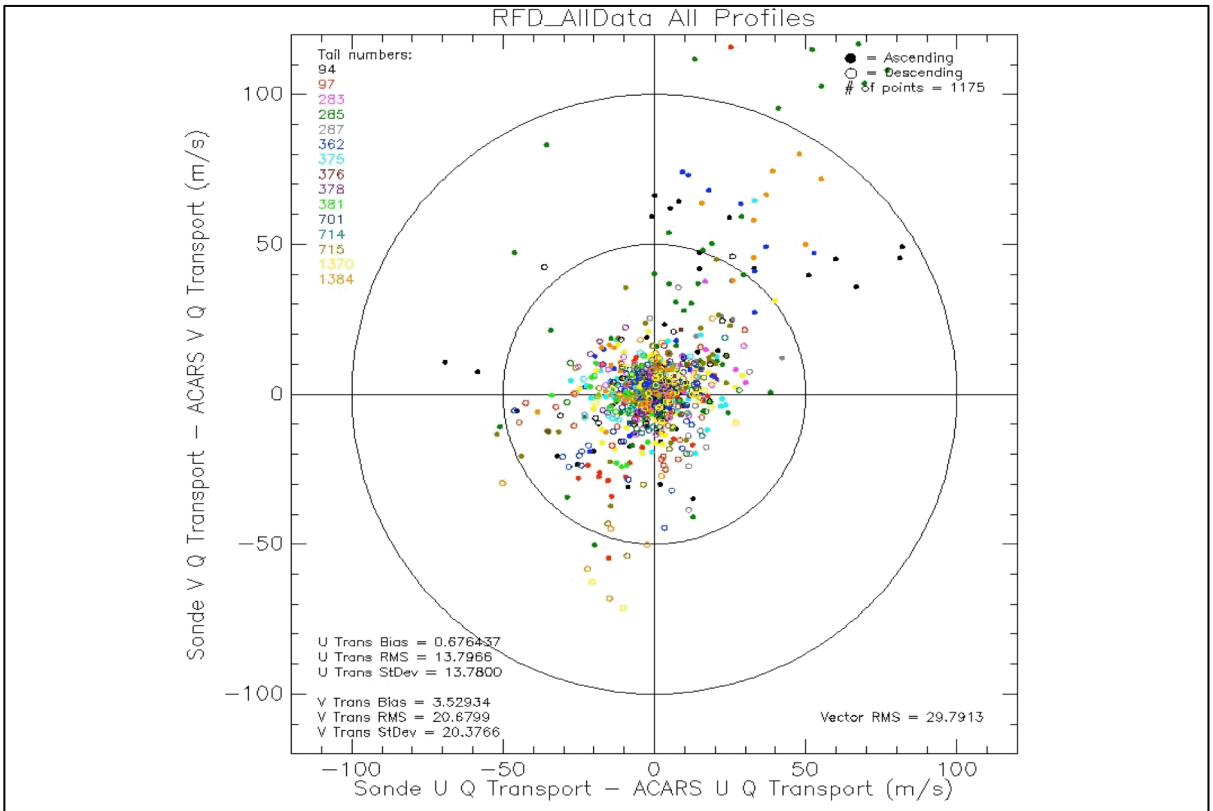

Figure F-4: Plot of Moisture Transport (SH weighted Wind, g/kg m/sec) comparisons between co-located observations from all WVSS-II equipped aircraft and time-interpolated RAOB reports taken for all 2009-2010 inter-comparison periods at Rockford, IL. Color coded by aircraft. Statistics in lower-left and -right.

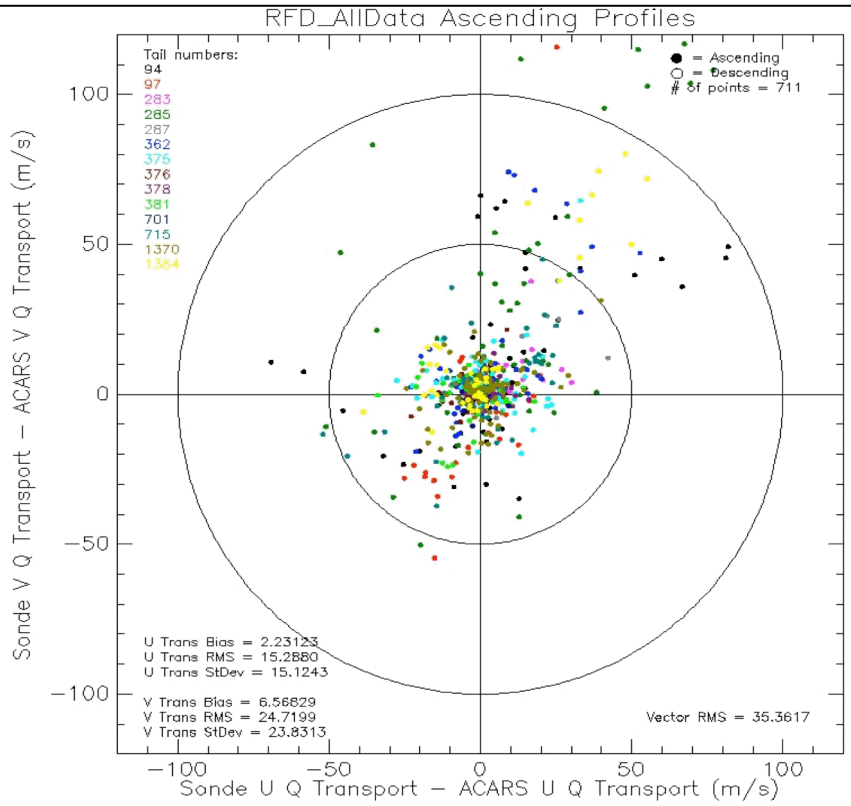

Figure F-5: Plot of Moisture Transport (SH weighted Wind, g/kg m/sec) comparisons between co-located observations from ascending WVSS-II equipped aircraft and time-interpolated RAOB reports taken for all 2009-2010 inter-comparison periods at Rockford, IL. Color coded by aircraft. Statistics lower-left and -right.

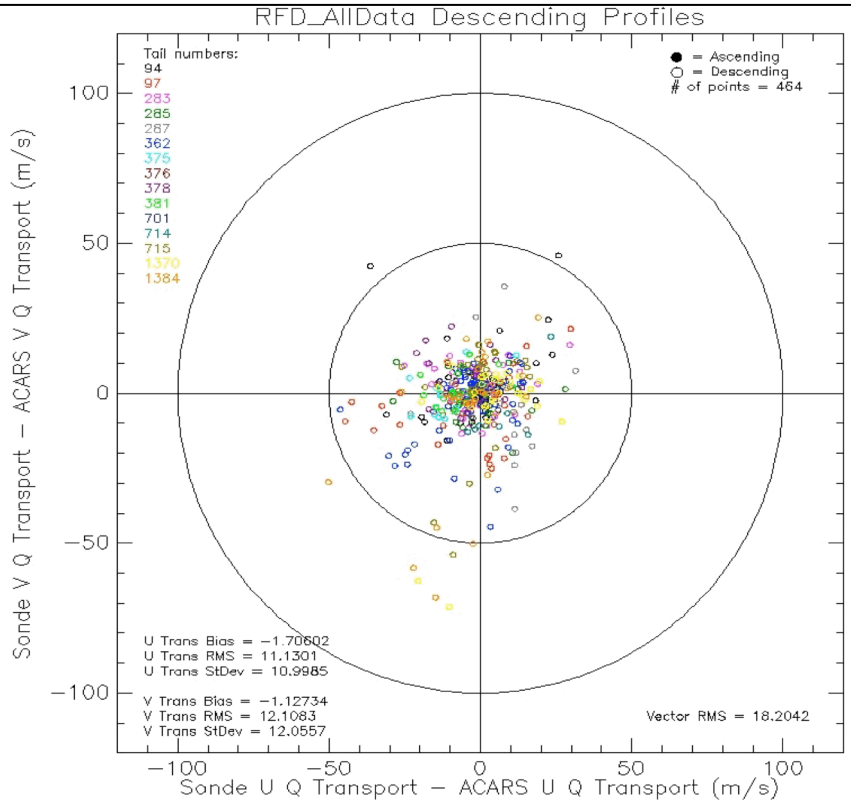

Figure F-6: Plot of Moisture Transport (SH weighted Wind, g/kg m/sec) comparisons between co-located observations from descending WVSS-II equipped aircraft and time-interpolated RAOB reports taken for all 2009-2010 inter-comparison periods at Rockford, IL. Color coded by aircraft. Statistics lower-left and -right.

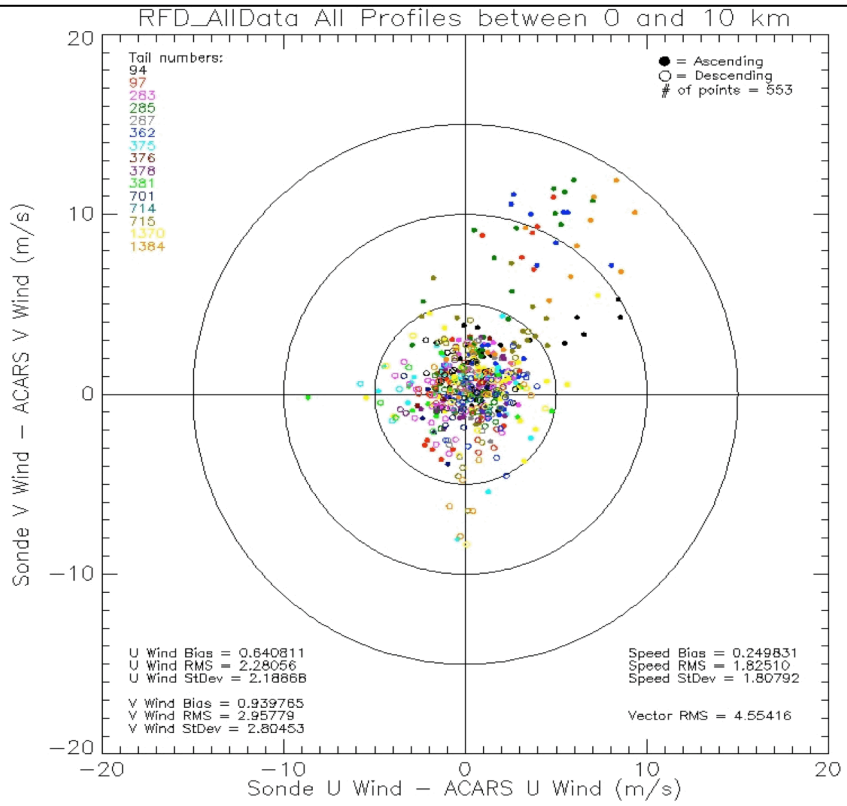

Figure F-7: Same as Fig. F-1, expect for aircraft-RAOB matchups with less than 10 km separations.

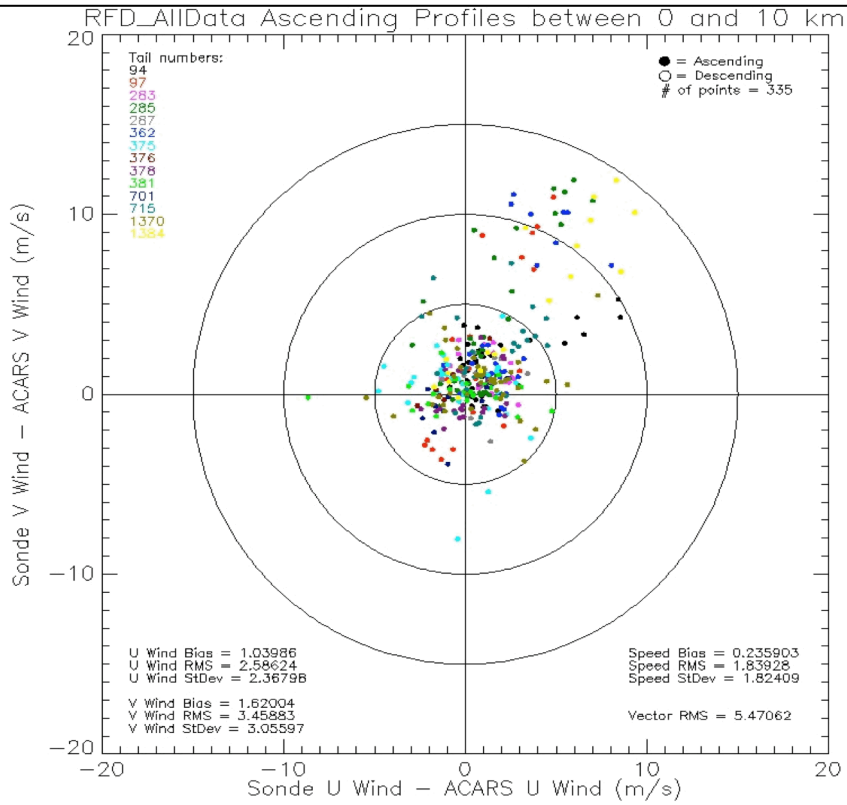

Figure F-8: Same as Fig. F-2, expect for aircraft-RAOB matchups with less than 10 km separations.

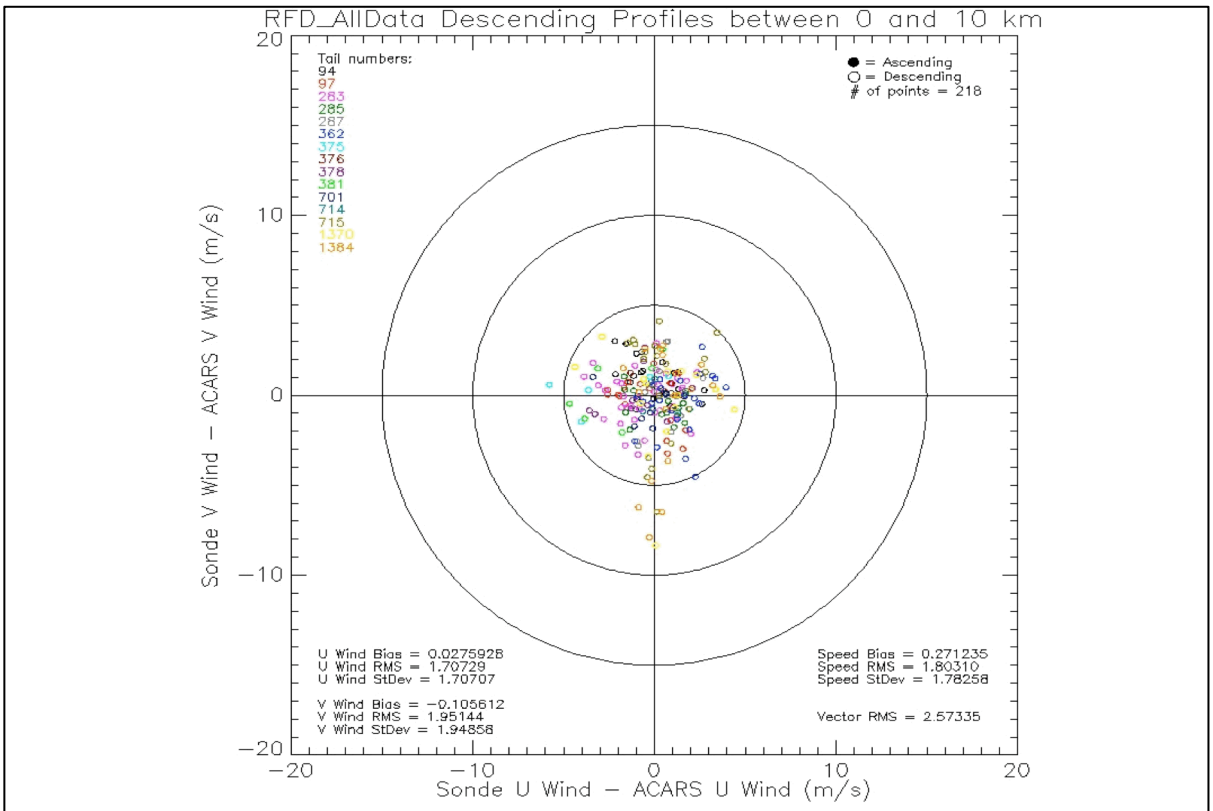

Figure F-9: Same as Fig. F-3, expect for aircraft-RAOB matchups with less than 10 km separations.

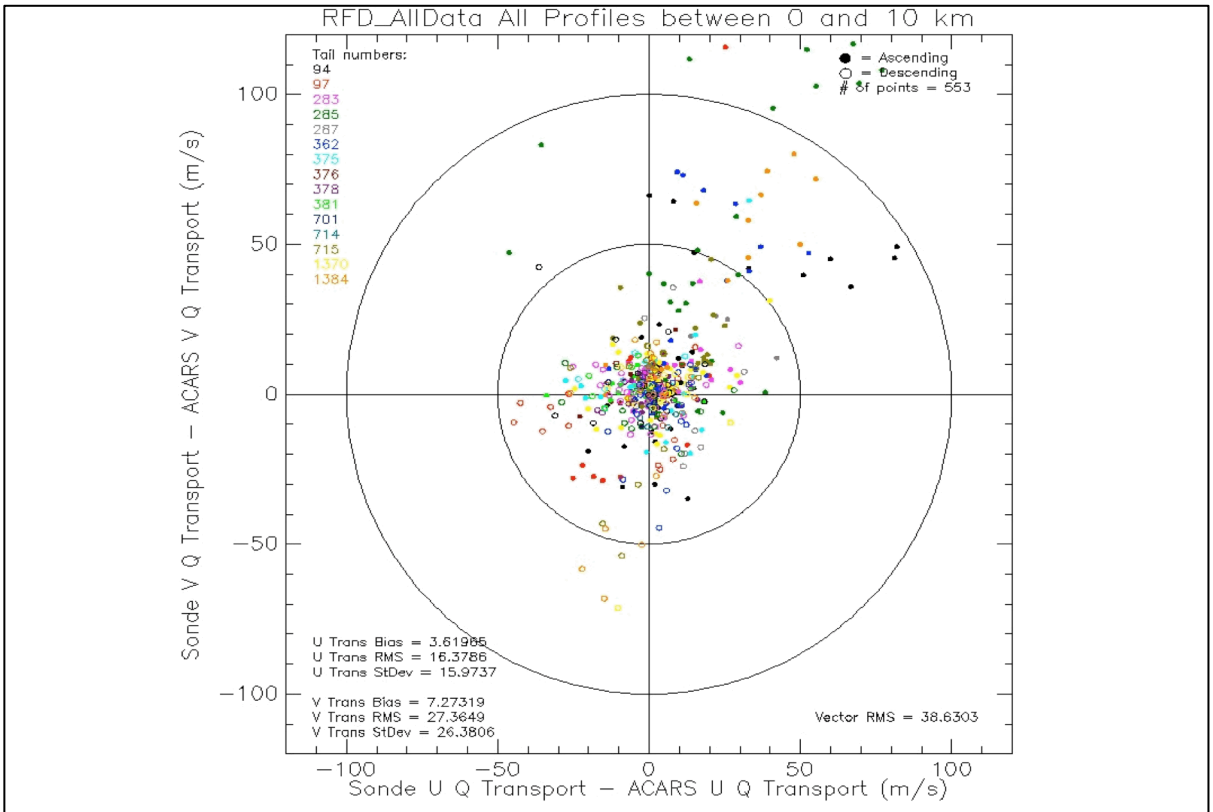

Figure F-10: Same as Fig. F-4, expect for aircraft-RAOB matchups with less than 10 km separations.

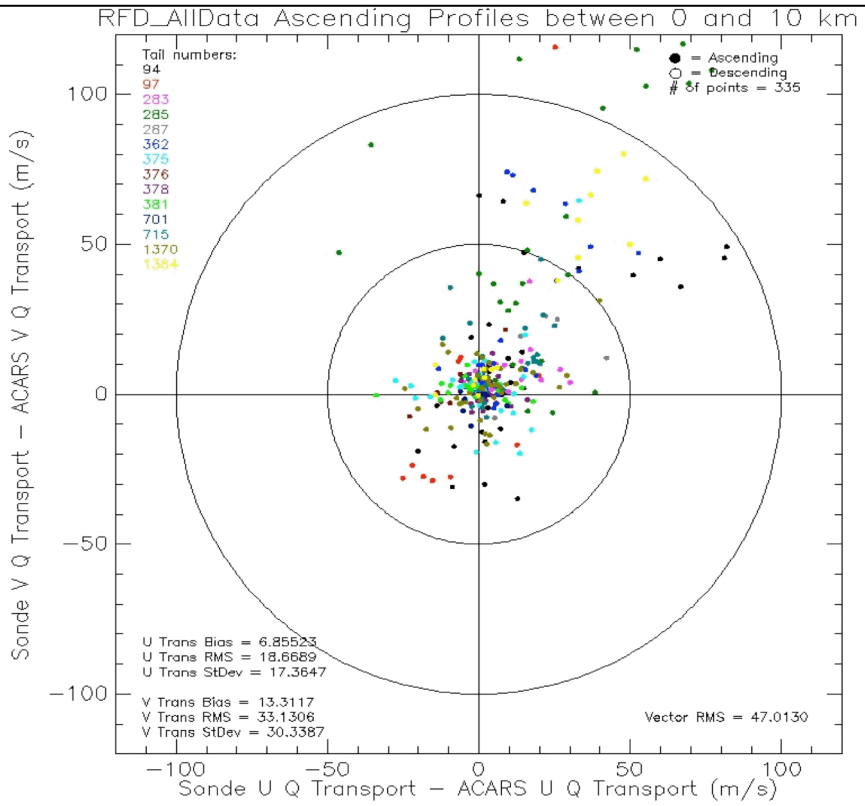

Figure F-11: Same as Fig. F-5, expect for aircraft-RAOB matchups with less than 10 km separations.

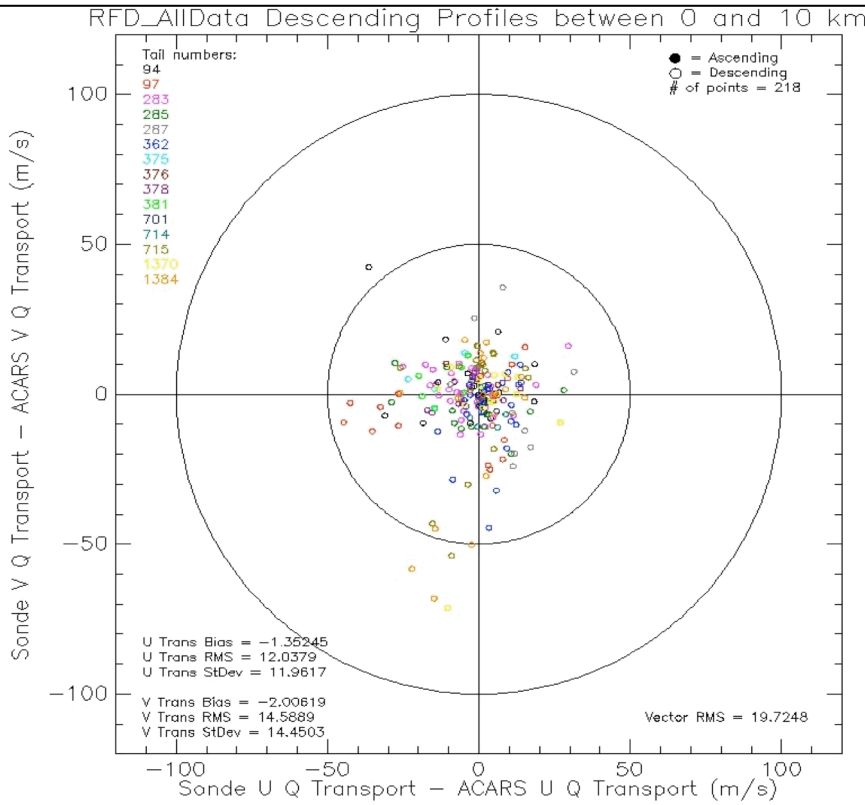

Figure F-12: Same as Fig. F-6, expect for aircraft-RAOB matchups with less than 10 km separations.

Acknowledgments: This report was commissioned by the World Meteorological Organization, Geneva, Switzerland. Particular thanks go to Dean Lockett and Frank Grooters in supporting this work. The contributions and efforts of Sarah Bedka in the early stages of the WVSS evaluations were invaluable, as were those of Erik Olson and the multiple other CIMSS personnel involved in the field tests in Rockford, IL and Louisville, KY. The efforts of David Helms of NOAA were instrumental in the formative and testing stages of the WVSS-II program deserve to be recognized, as do the reviewers for their helpful suggestions. Finally, the roles of Kenneth Macleod, Charles Sprinkle and Jeff Stickland in developing the AMDAR program through WMO need to be acknowledged.

References:

Alexander, C., S. G. Benjamin, S. Weygandt, D. Dowell, M. Hu, T. Smirnova, J. Olson, J. Brown, E. James, and H. Lin, 2014: The High-Resolution Rapid Refresh (HRRR): A maturation of frequently updating convection-allowing numerical weather prediction. Presented at World Weather Open Science Conference, Montreal, 16-21 August 2014. Available at: http://ruc.noaa.gov/ppt_pres/WWOSC2014_Alexander_Final.pdf.

Andersson, E., C. Cardinali, B. Truscott and T. Hovberg, 2005: High frequency AMDAR data – a European aircraft data collection trial and impact assessment. ECMWF Technical Memorandum # 457, 15 pp.

Andersson, E. and G. Radnóti, 2012: Impact of satellite and conventional observations on the performance of the ECMWF data assimilation system by OSEs. Presented at the Proc. 5th WMO Workshop on The Impact of Various Observing Systems on Numerical Weather Prediction, Sedona, AZ, 14-17 May 2012. Available at: http://www.wmo.int/pages/prog/www/OSY/Reports/NWP-5_Sedona2012.html

Baker, R.; Curtis, R.; Helms, D.; Homans, A.; Ford, B., 2011: Studies of the Effectiveness of the Water Vapor Sensing System, WVSS-II, in Supporting Airline Operations and Improving Air Traffic Capacity. Second AMS Aviation, Range and Aerospace Meteorology Special Symposium on Weather-Air Traffic Management Integration, Seattle, WA.

Ballish, B. A. and V. K. Kumar, 2008: Systematic differences in aircraft and radiosonde temperatures – Implications for NWP and Climate Studies. *Bull. Amer. Meteor. Soc.*, 89, 1689-1707.

Benjamin, S. G., 1989: An isentropic meso-alpha scale analysis system and its sensitivity to aircraft and surface observations. *Mon. Wea. Rev.*, 117, 1586-1605.

Benjamin, S. G., K. A. Brewster, R. Brümmer, B. F. Jewett, T. W. Schlatter, T. L. Smith, and P. A. Stamus, 1991: An isentropic three-hourly data assimilation system using ACARS aircraft observations. *Mon. Wea. Rev.*, 119, 888-906.

Benjamin, S. G., D. Dévényi, S. S. Weygandt, K. J. Brundage, J. M. Brown, G.A. Grell, D. Kim, B. E. Schwartz, T. G. Smirnova, T. L. Smith, G. S. Manikin, 2004: An hourly assimilation–forecast cycle: The RUC. *Mon. Wea. Rev.*, 132, 495–518.

Benjamin, S.G., B.E. Schwartz, and R.E. Cole, 1999: Accuracy of ACARS wind and temperature observations determined by collocation. *Wea. Forecasting*, **14**, 1032-1038.

Benjamin, S. G., J. M. Brown, K. J. Brundage, D. Devenyi, G. A. Grell, D. Kim, B. E. Schwartz, T. G. Smirnova, T. L. Smith, S. Weygandt, and G. S. Manikin, 2002: RUC20 - The 20-km version of the Rapid Update Cycle. NOAA Technical Memorandum OAR FSL-28, 30pp.

Benjamin, S. G, B. D. Jamison, W. R. Moninger, S. R. Sahm, B. E. Schwartz, T. W. Schlatter, 2010: Relative Short-Range Forecast Impact from Aircraft, Profiler, Radiosonde, VAD, GPS-PW, METAR, and Mesonet Observations via the RUC Hourly Assimilation Cycle. *Mon. Wea. Rev.*, 138, 1319-1343.

Benjamin, S. G., H. Lin, S. Weygandt, S. R. Sahm and W. Moninger, 2012: Impact of upper-air and near-surface observations on short-range forecasts from NOAA hourly assimilation cycles (RUC and Rapid Refresh), Presented at the Proc. 5th WMO Workshop on The Impact of Various Observing Systems on Numerical Weather Prediction, Sedona, AZ, 14-17 May 2012. Available at: http://www.wmo.int/pages/prog/www/OSY/Reports/NWP-5_Sedona2012.html

Benjamin, S. G., E. James, W. Moninger, B. Jamison, S. Weygandt, C. Alexander, 2014: Impact of aircraft observations on short-range aviation weather forecasts from NOAA regional models. Presented at NOAA Aircraft Data Workshop, Annapolis, MD, 29-30 April 2014. Available at: http://www.arinc.com/resources/customers/meetings/NOAA/NOAA_Aircraft_Data_Workshop_2014/.

Cardinali, C., 2009: Monitoring the observation impact on the short-range Forecast. *Q.J.R M S.*, 135, 239–250.

Cardinali, C., L. Isaksen, and E. Andersson, 2003: Use and Impact of Automated Aircraft Data in a Global 4DVAR Data Assimilation System. *Mon. Wea. Rev*., 131, 1865-1877.

Cardinali, C., L. Rukhovets, and J. Tenenbaum, 2004: Jet Stream Analysis and Forecast Errors Using GADS Aircraft Observations in the DAO, ECMWF, and NCEP Models. *Mon. Wea. Rev.*, 132, 764-779.

Cress A., H. Anlauf, H. W. Bitzer, A. Rhodin, C. Schraff, K. Helmert and K. Stephan, 2012: Global and regional impact studies at the German Weather Service (DWD). Presented at the Proc. 5th WMO Workshop on The Impact of Various Observing Systems on Numerical Weather Prediction, Sedona, AZ, 14-17 May 2012. Available at: http://www.wmo.int/pages/prog/www/OSY/Reports/NWP-5_Sedona2012.html.

Daniels, T. S., W. R. Moninger, R. D. Mamrosh, 2006: Tropospheric Airborne Meteorological Data Reporting (TAMDAR) Overview. 10th Symposium on Integrated Observing and Assimilation Systems for Atmosphere, Oceans, and Land Surface (IOAS-AOLS), Atlanta, GA, Amer. Meteor. Soc.

Dee, D., and S. Uppala, 2009: Variational Bias Correction of Satellite Radiance Data in the ERA Interim Reanalysis. *Q.J.R.M.S.,* 135, 1830–1841.

Derber, J. C. and A. Collard, 2011: Current Status and Future of Satellite Data Assimilation. Presentation at the EMCWF Annual Seminar on Data Assimilation for Atmosphere and Ocean, Proc. 11th Annual ECMWF Seminar, Reading, UK, 6-9 September 2011, 81-93.

Eyre, J. and R. Reid, 2014: Cost-benefit studies of observing systems. Forecasting Research Technical Report No: 593. Met Office, Exeter, UK, 11pp.

Fleming, R. J., 1996: The use of commercial aircraft as platforms for environmental measurements. *Bull. Amer. Meteor. Soc.*, 2229-2242.

Fleming, R., J., T. M. Kaneshige and W. E. McGovern, 1979: The global Weather Experiment 1. The observational phase through the first special observing period. *Bull. Amer. Meteor. Soc*., 60, 649-661.

Fleming, R. J.; D. R. Gallant; W. F. Feltz; J. G. Meitin; W. R. Moninger; S. F. Williams, and R. T. Baker, 2002: Water vapor profiles from commercial aircraft. UCAR, Boulder, CO. 37pp.

Gao, F., X. Zhang, N. Jacobs, X.-Y. Huang, Xin Zhang, P. Childs, 2012: Estimation of TAMDAR Observational Error and Assimilation Experiments. *Wea. Forecasting*, 27, 4, 856-877.

Hartung, D. C., J. A. Otkin, R. A. Petersen, D. D. Turner, W. F. Feltz, 2011: Assimilation of Surface-Based Boundary Layer Profiler Observations during a Cool-Season Weather Event Using an Observing System Simulation Experiment. Part II: Forecast Assessment. *Mon. Wea. Rev,* 139, 2327-2346.

Helms, D., K. Johnston, G. Sanger, B. Taubvurtzel, R. Petersen, A. Homans and A. Hoff, 2009: Testing and Deployment of the Water Vapor Sensing System II. 25th AMS Conference on International Interactive Information and Processing Systems (IIPS), Phoenix, AZ

Hoff, A., 2009: WVSS-II Assessment at the DWD. Available from Deutsche WetterDienst, Offenbach am Main, Germany.

Hoover, B., C. Velden and R. Langland, 2014: Adjoint-based analysis of observational impact on tropical cyclone forecasts. Presented at the National Hurricane Workshop, 14-17 Apr 2014, Orlando, FL. Available at: http://aurora.aos.wisc.edu/~hoover/7A.3_abstract.pdf.

Huang, X.-Y., F. Gao, N. Jacobs, and H. Wang, 2013: Assimilation of wind speed and direction observations: a new formulation and results from idealized experiments. *Tellus* A, 65, 19936.

Isaksen, L., 2014: Data Assimilation overview - Why aircraft observations are valuable for NWP. Presented at NOAA Aircraft Data Workshop, Annapolis, MD, 29-30 April 2014. Available at: http://www.arinc.com/resources/customers/meetings/NOAA/NOAA_Aircraft_Data_Workshop_2014/.

Isaksen, L., D. Vasiljevic , R. Dee and S. Healy, 2011: Bias correction of aircraft data. *ECMWF Newsletter*, 131, 6.

Jacobs, N. A., D. J. Mulally and A. K. Anderson, 2014: Correction of Flux Valve–Based Heading for Improvement of Aircraft Wind Observations. *J. Atmos. Oceanic Technol.*, **31**, 1733–1747.

Julian, P. R. and R. Steinberg, 1975: Commercial aircraft as a source of automated meteorological data for GATE and DST. *Bull Amer. Meteor. Soc.,* 56, 243-251.

Kalnay, E., 2003: *Atmospheric modeling, data assimilation and predictability.* Cambridge University Press, Cambridge, United Kingdom, 364pp.

Kang, J-S., B-J. Jung, Y. Jo and Y. Oto, 2014: Estimation of Forecast Sensitivity to Observations within KIAPS. Presentation at The Sixth EnKF Workshop, Buffalo, N.Y., 18-22 May 2014. Available at: http://hfip.psu.edu/fuz4/EnKF2014/Day3/Kang_EnKF2014_EFSO_diff_loc.pdf.

Kelly, G., 2004: Personal Communication, Following presentation made at the 3rd WMO Workshop on The Impact of Various Observing Systems on Numerical Weather Prediction, Alpbach, Austria.

Kelly, G., T. McNally, J.-N. Thépaut and M. Szyndel, 2004: OSEs on all main data types in the ECMWF operation system. Proc. 3rd WMO Workshop on The Impact of Various Observing Systems on Numerical Weather Prediction, Alpbach, Austria, 9-12 March 2004, Eds. H. Böttger, P. Menzel and J. Pailleux. WMO/TD No. 1228, 63-94.

Kelly, G. and J.-N. Thépaut, 2007: Evaluation of the impact of the space component of the Global Observing System through Observing System Experiments. Proc. 7th Annual ECMWF Seminar, Reading, UK, 3-7 September 2007, 327-348.

Langland, R. H. and N. Baker, 2004: Estimation of observation impact using the NRL atmospheric variational data assimilation adjoint system. *Tellus*, 56A , pp 189–201.

Laroche, S. and R. Sarrazin, 2010: Impact study with observations assimilated over North America and the North Pacific Ocean on the MSC global forecast system. Part ii: Sensitivity experiments. *Atmosphere-Ocean* 48:1, 26-38.

Lockett, D., 2015: Aircraft-based Observations Contributing to WMO Global Observing Systems. Presented at NOAA Aircraft Data Workshop, Annapolis, MD, 29-30 April 2014. Available at: http://www.arinc.com/resources/customers/meetings/NOAA/NOAA_Aircraft_Data_Workshop_2014.

Lupu, C., P. Gauthier, and S. Laroche, 2011: Evaluation of the Impact of Observations on Analyses in 3D- and 4D-Var Based on Information Content. *Mon. Wea. Rev.,* 139, 726-737.

Lupu C., P. Gauthier, and S. Laroche, 2012: Assessment of the Impact of Observations on Analyses Derived from Observing System Experiments. *Mon. Wea. Rev.,* 140, 245–257.

Martin, R. C., M. M. Wolfson, and R. G. Hallowell, 1993: MDCRS: Aircraft observations collection and uses. *Fifth Conf. on Aviation Weather Systems*, Vienna, VA, Amer. Meteor. Soc., 317-321.

Miller, E. R., J. Wang, and H. L. Cole, 1999: Correction for Dry Bias in Vaisala Radiosonde RH Data. Proceedings of the 9th ARM Science Team Meeting Proceedings, San Antonio, Texas. Available at: https://www.arm.gov/publications/proceedings/conf09/extended_abs/miller_er.pdf

Moninger, W. R., R. D. Mamrosh, and P. M. Pauley, 2003: Automated meteorological reports from commercial aircraft. *Bull. Amer. Meteor. Soc.,* 84, 203-216.

Moninger, W. R., S. G. Benjamin, B. D. Jamison, T. W. Schlatter, T. L. Smith, E. J. Szoke, 2007: TAMDAR and its impact on Rapid Update Cycle (RUC) forecasts. 22nd Conference on Weather Analysis and Forecasting and 18th Conference on Numerical Weather Prediction, Park City, UT, Amer. Meteor. Soc.

NCAR, 1986: Final report, Aviation Weather Forecasting Task Force. NCAR, Boulder, CO., 87pp.

NOAA, 2009: Retest and evaluation report for the SpectraSensors Water Vapor Sensing System II (WVSS-II) - October, 2009. Available at: http://amdar.noaa.gov/docs/WVSS300_test_results.pdf .

Ota, Y., J. C. Derber, E. Kalnay and T. Miyoshi, 2013: Ensemble-based observation impact estimates using the NCEP GFS. *Tellus* A 2013, **65**, 20038. Available at: http://dx.doi.org/10.3402/tellusa.v65i0.20038

Otkin, J. A., D. C. Hartung, D. D. Turner, R. A. Petersen, W. F. Feltz, E. Janzon, 2011: Assimilation of Surface-Based Boundary Layer Profiler Observations during a Cool-Season Weather Event Using an Observing System Simulation Experiment. Part I: Analysis Impact. *Mon. Wea. Rev,* 139, 2309-2326.

Pauley, P. M., A. Anderson, B. Ballish, H. Bénichou, X-Y. Huang, B. Ingleby, L., N. Jacobs, T. Kleinert, W. Moninger, C. Parrett, S. Taylor, G. Verner, Y. Zaitseva, 2014: Quality Control for Aircraft Data in Numerical Weather Prediction Systems. Presented at NOAA Aircraft Data Workshop, Annapolis, MD, 29-30 April 2014. Available at: http://www.arinc.com/resources/customers/meetings/NOAA/NOAA_Aircraft_Data_Workshop_2014/.

Pauley, P. and N. Baker, 2014: Assimilating MDCRS Humidity in NAVGEM. Presented at NOAA Aircraft Data Workshop, Annapolis, MD, 29-30 April 2014. Available at: http://www.arinc.com/resources/customers/meetings/NOAA/NOAA_Aircraft_Data_Workshop_2014/

Petersen, R. A., 2004: "Do automated meteorological data reports from commercial aircraft improve forecasts?" *ICAO Magazine*, 6 pp.

Petersen, R. A., 2015a: On the impact and future benefits of AMDAR observations in operational forecasts – Part 1 – A review of the impact of automated aircraft wind and temperature reports. Accepted by *Bull. Amer. Meteor. Soc.*

Petersen, R. A., L. Cronce, R. Mamrosh and R. Baker, 2015b: On the current impact and future benefits of AMDAR observations in Operational Forecasting – Part 2 – Water Vapor Observations. Submitted to *Bull Amer. Meteor. Soc.*

Petersen, R. A., 2004: Impact of AMDAR data on Numerical Prediction Models. Proc. 3rd WMO Workshop on The Impact of Various Observing Systems on Numerical Weather Prediction, Alpbach, Austria, 9-12 March 2004, Eds. H. Böttger, P. Menzel and J. Pailleux. World Meteorological Organization, Geneva, WMO/TD No. 1228, 298-307.

Petersen, R. A., W. Feltz, and S. Bedka, 2005: Final report of results of the June 2005 WVSS-II – Rawinsonde Intercomparison Study. Submitted to NOAA/NWS/OST by the University of Wisconsin – Madison, Cooperative Institute for Meteorological Satellite Studies (CIMSS). Copies available upon request.

Petersen, R. A., W. Feltz, E. Olson and S. Bedka, 2006a: Evaluation of the WVSS-II moisture sensor using co-located in-situ and remotely sensed observations. 10th AMS Symposium on Integrated Observing and Assimilation Systems for the Atmosphere, Oceans, and Land Surface (IOAS-AOLS), Atlanta, GA.

Petersen, R. A., W. Feltz, E. Olson and S. Bedka, 2006b: Final report of results of the November 2006 WVSS-II – Rawinsonde Intercomparison Study. Submitted to NOAA/NWS/OST by the University of Wisconsin – Madison, Cooperative Institute for Meteorological Satellite Studies (CIMSS). Copies available upon request.

Petersen, R. A., S. Bedka, W. Feltz, E. Olson and D. Helms, 2009: WVSS-II Moisture Observations: A low-cost tool for validating and monitoring asynoptic satellite data. Bath, United Kingdom, 21-25 Sept. 2009. Available at: http://www.eumetsat.int/website/home/News/ConferencesandEvents/DAT_2042712.html

Petterssen, S., 1956*: Weather Analysis and Forecasting.* Vol. 2, McGraw-Hill, 266 pp.

Schwartz, B. E., S. G. Benjamin, S. M. Green, and M. R. Jardin, 2000: Accuracy of RUC-1 and RUC-2 Wind and Aircraft Trajectory Forecasts by Comparison with ACARS Observations. *Wea. Forecasting*, **15**, 313–326.

Sparkman, J. K., and J. Giraytys, 1981: ASDAR: A FGGE real-time data collection system. *Bull. Amer. Meteor. Soc.,* 62, 394-400.

Spectra Sensors, 2015: Atmospheric Water Vapor Sensing System (WVSS-II) Technical Specifications. Available at: http://www.spectrasensors.com/media/files/user/3ad985de/WVSS-II_Spec_Sheet_-_Feb_2015.pdf.

U.S. Coast Guard, 1962: The Loran-C system of navigation. Jansky & Bailey, A Division of Atlantic Research Corporation, Washington, D. C., 135pp.

Viasala, 2015: Vaisala Radiosonde RS92-SGP. Available at: http://www.vaisala.com/Vaisala%20Documents/Brochures%20and%20Datasheets/RS92SGP-Datasheet-B210358EN-F-LOW.pdf

WAFC-Washington, 2011: The Worlds Area Forecast System (WAFS) Internet Service (WIFS) Users Guide – Version 4.1. U.S. National Weather Service, Silver Spring, MD, 32 pp.

Wendisch, M., and J.-L. Brenguier, ed., 2013: Airborne Measurements for Environmental Research, Wiley-VCH, 655pp.

Woodman, O., J., 2007: An introduction to inertial navigation. University of Cambridge Computer Lab, Technical Report 696, 37pp.

WMO, 2003a: Aircraft Meteorological Data Relay (AMDAR) Reference Manual. World Meteorological Organization, Geneva, 84 pp.

WMO, 2003b: Manual on the Global Observing System (WMO-No. 544 - Part II, Requirements for observational data). Available from World Meteorological Organization, Geneva, Switzerland, 50 pp.

WMO, 2011: WMO intercomparison of high quality radiosonde systems (WMO/TD No. 1580). Available from World Meteorological Organization, Geneva, Switzerland, 238 pp.

WMO, 2012: Final Report of the Fifth WMO Workshop on the Impact of Various Observing Systems on Numerical Weather Prediction, Sedona, Arizona, USA, 22-25 May 2012, Eds. E. Andersson and Y. Sato., WMO/TR No. 2012-1, 25 pp.

WMO, 2014a: WIGOS - WMO Integrated Global Observing System: Requirements for the Implementation and Operation of an AMDAR Programme. WMO/TR No. 2014-2, 31 pp.

WMO, 2014b: Aircraft Observations Workshop held April 2014 in Annapolis, USA. AMDAR Observing System Newsletter*, No. 8, World Meteorological Organization, Geneva.*

Zhu, Y., J. Derber, R. J. Purser, J. Whiting, and B. R. Ballish, 2015: Variational correction of aircraft temperature bias in the NCEP's GSI analysis system. Accepted by *Mon. Wea. Rev.*